CHEMICAL ENGINEERING
June 2012
www.che.com

SHOW PREVIEW
ACHEMA 2012
PAGE 321-1

Draining Process Vessels

PAGE 34

ISOTHERMAL PIPE FLOW
CFD ANALYSIS OF HEAT TRANSFER FROM FLARES
DISTILLATION STARTUP
CHE EDUCATION
STEAM SYSTEM CONTROL
SPRAY DRYING PARAMETERS
EXPLOSION PROTECTION EQUIPMENT
FOCUS ON SOFTWARE

Access Intelligence

Fill one bulk bag per week or 20 per hour at the lowest cost per bag

Flexicon's extra-broad model range, patented innovations and performance enhancements let you exact-match a filler to your specific cost and capacity requirements

FILLER FOR PALLET JACK BAG REMOVAL
Low profile version of patented TWIN-CENTERPOST™ filler allows removal of filled bags using a pallet jack, eliminating the need for a forklift or roller conveyor. Low cost standard models offered with many performance options.

BULK BAG FILLER USES PLANT SCALE
Full length forklifting tubes allow positioning of this TWIN-CENTERPOST™ filler model on a plant scale as needed, allowing you to fill by weight without investing in load cells and automated controls.

FILLERS WITH AUTOMATED FEEDING SYSTEMS
Every Flexicon filler is offered with pneumatic (shown) or mechanical (bottom right) feeding/weighing systems, as well as inlet adapters to interface with optional overhead storage vessels.

COMBINATION BULK BAG/DRUM FILLER
Patented SWING-DOWN® filler features a fill head that lowers and pivots down for safe, easy bag spout connections at floor level, and a swing-arm-mounted chute for automated filling and indexing of drums.

PATENTED SWING-DOWN® FILLER
Fill head lowers, pivots and stops in a vertically-oriented position, allowing operator to safely and quickly connect empty bags at floor level and resume automated filling and spout-cinching operations.

CANTILEVERED REAR-POST FILLER
Offered with performance options including: powered fill head height adjustment, pneumatically retractable bag hooks, inflatable bag spout seal, dust containment vent, roller conveyor, and vibratory bag densification/deaeration system.

BASIC FILLER FOR TIGHTEST BUDGETS
A lighter-duty version of the economical TWIN-CENTERPOST™ filler, the BASIC FILLER reduces cost further still, yet has an inflatable bag spout seal and feed chute dust vent as standard, and a limited list of performance options.

PATENTED TWIN-CENTERPOST™ FILLER
Two heavy-gauge, on-center posts boost strength and access to bag hooks while reducing cost. Standard manual fill head height adjustment, and feed chute vent for displaced dust. Numerous performance options. First filler to receive USDA acceptance.

Flexicon®.com

See the full range of fast-payback equipment at flexicon.com: Flexible Screw Conveyors, Pneumatic Conveying Systems, Bulk Bag Unloaders, Bulk Bag Conditioners, Bulk Bag Fillers, Bag Dump Stations, Drum/Box/Container Dumpers, Weigh Batching and Blending Systems, and Automated Plant-Wide Bulk Handling Systems

USA
sales@flexicon.com
1 888 FLEXICON

CHILE +56 2 415 1286
UK +44 (0)1227 374710
AUSTRALIA +61 (0)7 3879 4180
SOUTH AFRICA +27 (0)41 453 1871

AA-0658

Circle 21 on p. 76 or go to adlinks.che.com/40268-21

Proven Process Solutions for You

CT.39e-1

SULZER

- You get the best from our innovative range of technologies: distillation - evaporation - liquid-liquid extraction - crystallization - membrane separation - hybrid solutions - polymer production.
- Jointly we fully develop your process solution from first concept and pilot testing to an installed plant with guaranteed performance.

Whether you are active in the chemical, pharmaceutical, biofuels or food & beverage industry, we are here to support you.

We invite you to come and visit us at ACHEMA Hall 4.0 Booth D48.

Sulzer Chemtech Ltd
Process Technology
4123 Allschwil, Switzerland
Phone +41 61 486 3737
contactpt@sulzer.com
www.sulzerchemtech.com

Sulzer Chemtech USA, Inc.
Tulsa, OK 74131, USA
Phone +1 918 446 6672

Sulzer Chemtech Pte. Ltd.
Singapore 629845
Phone +65 6515 5500

Circle 51 on p. 76 or go to adlinks.che.com/40268-51

Solutia

WHEN THE HEAT IS ON, PUT THE THERMINOL® PERFORMANCE CREW TO WORK FOR YOU.

In the heat transfer fluid race the competition can get pretty heated. That's why you need the Therminol® Heat Transfer Fluid Performance Crew working for you. From start to finish, the Therminol TLC Total Lifecycle Care® team of seasoned professionals is ready to support you with everything you need to win. For your people, we provide start-up assistance, operational training and a technical service hotline. For your facility, we offer system design, quality Therminol products, sample analysis, flush fluid & refill and a fluid trade-in program*. We provide everything you need to keep your heat transfer system at peak performance throughout its lifecycle. So join the winning team. In North America call 1-800-426-2463 or in Europe 32.10.48.12.11. You'll see no other heat transfer fluid delivers more proven comprehensive performance than Therminol.

www.therminol.com

THERMINOL®
Heat Transfer Fluids
by Solutia

THERMINOL TLC TOTAL LIFECYCLE CARE®

FOR YOUR PEOPLE
- Start-Up Assistance
- Operational Training
- Technical Service Hotline

FOR YOUR FACILITY
- System Design
- Quality Therminol Products
- Sample Analysis
- Flush Fluid & Refill
- Fluid Trade-In Program*

Therminol TLC Total Lifecycle Care is a complete program of products and services from Solutia designed to keep your heat transfer system in top operating condition through its entire lifecycle.

Circle 48 on p. 76 or go to adlinks.che.com/40268-48

CHEMICAL ENGINEERING
www.che.com

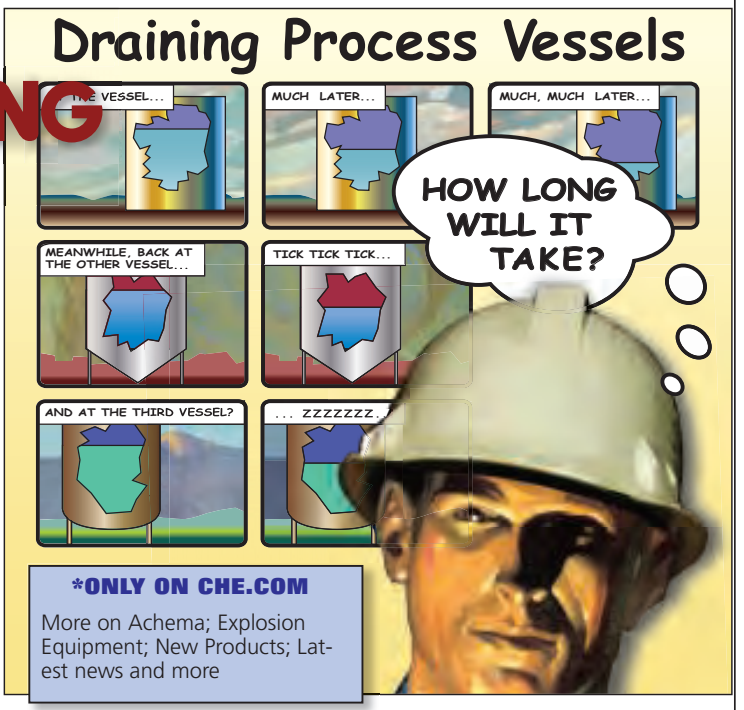

***ONLY ON CHE.COM**

More on Achema; Explosion Equipment; New Products; Latest news and more

COVER STORY

34 Cover Story **Draining Vessels** Determine how long it will take to drain flat-, cone- or dish-shaped units

NEWS

11 Chementator Convert wastewater and carbon dioxide into chemicals with this technology; A non-crop-based sugar feedstock for bio-based chemicals and biofuels; and more

20 Newsbriefs GE and Shenhua open cleaner-coal-technology JV in China; CSB releases new safety video on Dupont hot work explosion; Cybersecurity bill to ease information sharing passes House; and more

22 Newsfront **Education Evolution** To prepare students for globalized industries, chemical engineering departments are incorporating new requirements, utilizing IT and connecting with CPI companies

26 Equipment News Roundup **Explosions: Are You Prepared?*** Explosion protection equipment can minimize damage, but process understanding is key to optimized solutions

ENGINEERING

33 Facts at Your Fingertips **Spray Drying Parameters** This one-page reference guide outlines the main considerations involved in spray drying

42 Feature Report **Dynamic Modeling for Steam System Control** Dynamic modeling fills in the gaps of steady-state modeling and provides a more complete, reliable and efficient analysis

48 Engineering Practice **Distillation: Avoid Problems During Tower Startup** Practical procedures for both effective startup and problem analysis are discussed here for a depropanizer that experienced downcomer seal loss

60 Engineering Practice **CFD Analysis of Heat Transfer From Flares** A way to obtain conservative estimates for the temperatures at the support structures of a flare system

66 Engineering Practice **A Novel Equation for Isothermal Pipe Flow** A newly derived equation for isothermal gas flow in pipes yields improved mass-flux predictions

EQUIPMENT & SERVICES

30 Focus on Software Plant-management software for increased integration, and more; Track equipment health at large operations; Enhancements for simulation of batch reactors; and more

32D-1 Show Preview **Achema 2012** Held once every three years, Achema will take place June 18–22 in Frankfurt, Germany. A small portion of the products that will be exhibited on the show floor are discussed here

32I-1 Show Preview II **Achema 2012*** More of the products and services to be exhibited at Achema are included: Tube-in-tube design augments safety in these heat exchangers; A wear-resistant rotary valve for abrasive bulk solids; and much more

COMMENTARY

5 Editor's Page **Achema expected to exceed previous years' results** Attendance at the largest exhibition congress for the chemical process industries is expected to outpace that of the previous (2009) event, which recorded 3,767 exhibitors and over 173,000 visitors

72 The Fractionation Column **A very confined space** This real-life experience reminds us of how dangerous confined spaces can be

DEPARTMENTS

Letters 6
Calendar. 8–9
Who's Who. 78
Reader Service 76
Economic Indicators 79–80

ADVERTISERS

Literature Review . . 69
Product Showcase. . 73
Classified Advertising 74–75
Advertiser Index . . . 77

COMING IN JULY

Look for: **Feature Reports** on Mixing; and Corrosion; an **Engineering Practice article** on Evaluating Green Projects; a **You and Your Job article** on Working with the CSB after an accident; **Environmental Manager articles** on Guidelines for Safe Process Vacuum Systems; and Overpressure Protection; **News articles** on Biogas; and Catalysts; and more

Cover: David Whitcher

Circle 52 on p. 76 or go to adlinks.che.com/40268-52

Winner of Eight Jesse H. Neal Awards for Editorial Excellence

CHEMICAL ENGINEERING

Published since 1902
An Access Intelligence Publication

HEADQUARTERS

88 Pine Street, 5th Floor, New York, NY 10005, U.S.
Tel: 212-621-4900 Fax: 212-621-4694

EUROPEAN EDITORIAL OFFICES

Zeilweg 44, D-60439 Frankfurt am Main, Germany
Tel: 49-69-9573-8296 Fax: 49-69-5700-2484

CIRCULATION REQUESTS:

Tel: 847-564-9290 Fax: 847-564-9453
Fullfillment Manager; P.O. Box 3588,
Northbrook, IL 60065-3588 email: clientservices@che.com

ADVERTISING REQUESTS: see p. 76

For photocopy or reuse requests: 800-772-3350 or info@copyright.com
For reprints: Wright's Media, 1-877-652-5295, sales@wrightsmedia.com

ACCESS INTELLIGENCE, LLC

Access Intelligence
4 Choke Cherry Road, Second Floor
Rockville, MD 20850 • www.accessintel.com

BPA

Editor's Page

Achema expected to exceed previous years' results

This month, individuals from across the chemical process industries (CPI) and the globe will gather together for the 30th time at Achema, the world's largest exhibition congress on chemical engineering, environmental protection and biotechnology (June 18–22; Frankfurt am Main, Germany). Organizers at Dechema e.V. (Frankfurt; www.dechema.de) are optimistic that the attendance and exhibitor totals will outpace those of the previous (2009) event, which recorded a total of 3,767 exhibitors and over 173,000 visitors.

Held once every three years, Achema is an event truly like no other. Starting several months before the event itself, Achema begins to take center stage on the schedule of every *Chemical Engineering* editor. The first reason reflects the sheer number and impact of innovative technologies that are unveiled there. Examples of these technologies are scattered throughout this issue, including our Chementator department (starting on p. 11), our Focus on Software (pp. 30–31) and the second installment of our Achema Preview, which begins on p. 32 (and continues on our website at www.che.com/new_products_and_services/). The second reason drawing our attention stems from over 900 lectures in the conference lineup that provide a fruitful ground for good technical manuscripts that we are always seeking for the magazine.

The pinnacle, however, of a *Chemical Engineering* editor's preoccupation with Achema is in our production of the *Achema Daily*, a 64-page newspaper that is produced onsite every day of the show. Even with so many pages to fill, we are only able to hit the highlights. Consider for a moment that if a person spent eight hours from Monday to Friday touring only the exhibit halls and ignoring conference sessions, meals, walking time and interaction with other attendees, he or she would have less than 40 seconds to spend at each exhibitor booth.

The typical booth visit, of course, is much longer than that. Visitors come to have meaningful discussions with suppliers, often getting into the specification stages. After all, Achema has proven its ability to provide virtually every type of technology needed to build, operate and maintain a chemical process plant, from suppliers across the globe. And, Thomas Scheuring, CEO of Dechema, says "With a proportion of around 50% of exhibitors from abroad, Achema 2012 will be even more international than all of its predecessors."

Of all the Achema exhibition groups, Scheuring says that two particularly stand out: "Instrumentation, Control and Automation Techniques" and "Pharmaceutical, Packaging and Storage Techniques" have achieved impressive growth rates. Due to the completion of a new hall at the Frankfurt Messe, Achema was able to offer both of these exhibition groups more scope for expansion, which he says was promptly snapped up. He adds that demand in the two largest exhibition groups, "Pumps, Compressors, Valves and Fittings" and "Laboratory and Analytical Techniques", also remains gratifyingly stable. In fact, the record total of 996 exhibitors (and growing) makes Achema the largest pump exhibition in the world.

For those of you who cannot make it to Achema this time, we will be offering the *Achema Daily* in a digital format. Meanwhile, our July and August issues will certainly contain more of the groundbreaking news that we find there. ■

Rebekkah Marshall

Letters

Call for corrosion papers

The 2013 Corrosion Solutions Conference has issued a call for papers for an event to be held September 15–18, 2013 in San Diego, Calif. The conference will address the specific needs and interests of professionals in materials, application and equipment fabrication for chemical processing, oil and gas, nuclear and other corrosion-related industries.

This conference is sponsored by ATI (Albany, Ore.; www.atimetals.com), a producer of specialty metals, and has been held every second year since 1997. The most recent conference (2011) attracted over 225 attendees from 13 countries.

Potential topics and areas of interest include, but are not limited to, case histories, advances and other valuable information focused on corrosion in these applications:

- Organics
- Ethanol
- Biofuels
- Urea
- Acetic acid
- Hydrocarbon processing
- Formic acid
- Nitric acid
- Sulfuric acid
- Hydrochloric acid
- Nuclear
- Alternative energy

Other topics of interest include:

- Preventative maintenance and repairs
- Alloy development
- Design and engineering
- Fabrication advancements
- Failure analysis
- Equipment advances

Interested authors should submit an abstract with the subject title, author name, position title and company name, along with any coauthor names, position titles, and company names by November 1, 2012. Abstracts can be uploaded to the conference website at:

www.aticorrosionconference.com/presenters

Each abstract will be reviewed and, if accepted, authors will receive a notice of acceptance by February 1, 2013. Upon acceptance, authors will receive further information regarding paper and presentation formatting. The conference registration fee for presenters will be waived. For more information or to discuss a potential topic, contact Mr. Richard Sutherlin at (541) 967-6924 or richard.sutherlin@atimetals.com.

Every abstract received will be considered for inclusion based on the technical content and relevance to the chosen session topics. Abstracts that are promotional in nature will not be considered. Final manuscripts will be due no later than July 1, 2013.

Postscripts, corrections

May 2012 (p. 14), Chementator: In the article, A new catalyst enables room-temperature interconversion of CO_2 and formic acid, Brookhaven National Laboratory (BNL) was referred to as Brookhaven National Institute. The corrected, online version of the article can be found at www.che.com. ■

Calendar

NORTH AMERICA

Semicon West. SEMI (San Jose, Calif.). Phone: 408-943-6945; Web: semiconwest.org
San Francisco, Calif. **July 10–12**

Energy Training & Electric Power Classroom Seminars. PGS Energy Training (Hilton Head Island, S.C.). Phone: 412-521-4737; Web: psgenergy.com
Seattle, Wash. **July 19–20**

16th AFPM Cat Cracker Seminar. American Fuel and Petrochemical Manufacturers (AFPM; formerly the National Petrochemical and Refiners Assn.; Washington, D.C.). Phone: 202-457-0480; Web: afpm.org
Houston, Tex. **August 21–22**

2012 ACEEE Summer Study on Energy Efficiency in Buildings. American Council for an Energy-Efficient Economy (Washington, D.C.). Phone: 202-507-4000; Web: aceee.org
Bloomington, Minn. **August 12–17**

57th Annual Safety in Ammonia Plants and Related Facilities Symposium. AIChE (New York, N.Y.). Phone: 646-495-1300; Web: aiche.org
Chicago, Ill. **September 9–13**

Auditing Management Systems — ISO19011. BW Marguglio LLC (Cold Spring, N.Y.). Phone: 845-265-0123; Web: hightechnologyseminars.com
Memphis, Tenn. **September 24–25**

2012 SOCMA Leadership Conference 2012. SOCMA (Washington, D.C.). Phone: 202-741-4100; Web: socma.com/leadership
Cambridge, Md. **September 25–27**

WEFTEC. Water Environment Federation (Alexandria, Va.). Phone: 703-684-24920; Web: weftec.org
New Orleans, La. **September 29–October 3**

4th Regional Process Technology Conference. AIChE (New York, N.Y.). Phone: 646-495-1300; Web: aiche.org
League City, Tex. **October 4–5**

ASME/STLE 2012 International Joint Tribology Conference. American Society of Mechanical Engineers (ASME) and the Society of Tribologists and Lubrication Engineers (STLE; New York, N.Y.). Phone: 800-843-2763 (U.S.); 973-882-1170 (outside the U.S.); Web: asme.org
Denver, Colo. **October 7–10**

AIChE 2012 Annual Meeting. AIChE (New York, N.Y.). Phone: 646-495-1300; Web: aiche.org
Pittsburgh, Pa. **October 28–November 2**

Continues

3rd Annual ChemInnovations Conference & Exhibition, co-located with Clean Gulf/ Industrial Fire, Safety and Security, and Shale EnviroSafe Conference & Exhibitions. The TradeFair Group (Houston). Phone: 713-343-1891; Web: cpievent.com
New Orleans, La. **November 14–15**

EUROPE

The Scaleup of Chemical Processes. Scientific Update (East Sussex, U.K.). Phone: +44-1435-873062; Web: scientificupdate.co.uk
Milan, Italy **July 9–12**

International Symposium on Chemical Reaction Engineering (ISCRE22). European Federation of Chemical Engineering (Frankfurt am Main, Germany). Phone: +32-3-260-0861; Web: iscre22.com
Maastricht, The Netherlands **September 2–5**

3rd International Conference on Metal-Organic Frameworks and Open Framework Compounds (MOF2012). Dechema e.V. (Frankfurt am Main, Germany). Phone: +49-69-7564-277; Web: mof-conf.org
Edinburgh, U.K. **September 16–19**

Plastic Pipes XVI. Plastic Pipe Inst. (Budapest, Hungary). Phone: +36-1-212-0056; Web: ppxvi.org
Barcelona, Spain **September 24–26**

PPMA Show 2012. Reed Exhibitions (Surrey, U.K.). Phone: +44-20-8910-7189; Web: ppmashow.co.uk
Birmingham, U.K. **September 25–27**

4th Symposium on Continuous Flow Reactor Technology for Industrial Applications. Teknoscienze S.r.l. (Milan, Italy). Phone: +39-02-26809375; Web: teknoscienze.com
Lisbon, Portugal **September 26–27**

ASIA & ELSEWHERE

15th International Congress on Catalysis (ICC2012). Dechema e.V. (Frankfurt am Main, Germany). Phone: +49-69-7564-129; Web: icc2012.org
Munich, Germany **July 1–6**

8th World Water Congress & Exhibition 2012. International Water Assn. (The Hague, The Netherlands). Phone: +31-70-382-0028; Web: iwa2012busan.org
Busan, South Korea **September 16–21**

21st Annual Flexpo Conference — Polyolefins and Elastomers. Chemical Market Resources (Webster, Tex.). Phone: 281-557-3320; Web: cmrhoutex.com
Bangkok, Thailand **September 26–27** ■

Suzanne Shelley

EXPERIENCE MATTERS. With thousands of installations across the globe in some of the world's toughest conditions and applications, Orion Instruments® proves daily that we are the leading supplier of magnetic level indication. Contact us today to find out how we can apply ORION INSTRUMENTS technology to help solve your level applications.

- **CHEMICAL**
- Oil & Gas Exploration & Production
- Power
- Military
- Refining
- Wastewater
- Pulp & Paper

ORION® INSTRUMENTS
A Magnetrol® Company

GET TOUGH

Jupiter®
Magnetostrictive Level Transmitter

Atlas™
Basic, high-performance MLI suitable for a variety of applications.

Aurora®
Redundant MLI with integrated Guided Wave Radar level transmitter.

Schedule a visit to our manufacturing facility

REVEAL™ • Scan to learn more about REVEAL™ • Scan to learn more about

www.orioninstruments.com • 2105 Oak Villa Boulevard • Baton Rouge, Louisiana • 70815 • 866-55-ORION • 225-906-2343 • f: 225-906-2344

HART® is a registered trademark of the HART Communication Foundation. | FOUNDATION fieldbus™ is a trademark of Fieldbus Foundation. **Circle 39 on p. 76 or go to adlinks.che.com/40268-39** ISO 9001

Convert wastewater and CO_2 into chemicals with this technology

Electrochemical and chemical-precipitation technology from New Sky Energy (Boulder, Colo.; www.newskyenergy.com) allows the conversion of salty wastewater and CO_2 from fluegas into valuable process chemicals, such as soda ash, calcium carbonate, sulfuric acid, bleach and other chemicals.

New Sky's customizable system is designed to be installed onsite at a processing facility to work with the chemistry of that plant's brine waste stream and CO_2 exhaust. "Onsite production of chemicals from readily available waste streams reduces transportation costs and reduces CO_2 emissions," says Deane Little, New Sky CEO.

The New Sky scheme includes a proprietary electrochemical reactor in which Nafion ion-exchange membranes are stacked between alternating anode and cathode plates, and a small voltage (3 V) is applied across the cell. A salt solution entering the cell between the membranes is split into acid, base, hydrogen and oxygen. The base from this reaction can be combined with CO_2 and wastewater to selectively precipitate a variety of magnesium, calcium and other metal salts.

New Sky's combined electrochemical-precipitation process generates a suite of potentially useful chemicals, including carbonates, hydroxides, hydrochloric and sulfuric acids, sodium chloride, sodium sulfate and others.

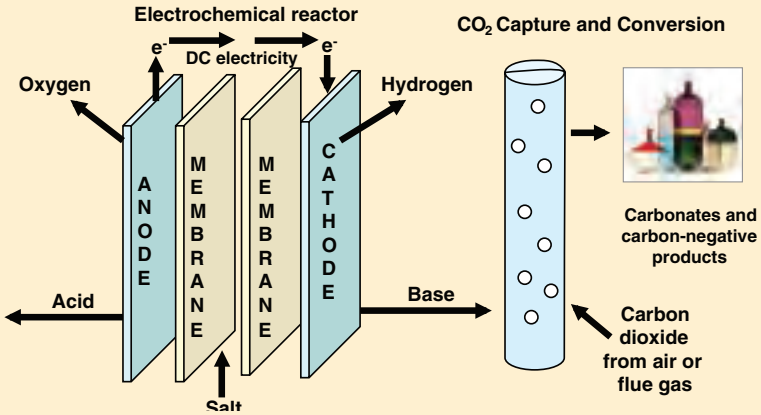

The tunable process is especially appropriate at battery recycling, oil and gas drilling, glass or plastics manufacturing and mining facilities. In economic studies of several cases, New Sky calculates the technology investment for its technology would be repaid in 2.4 yr in the case of using produced water from oil and natural gas drilling to manufacture sodium hypochlorite, and in 3.7 yr in the case of using waste brine to make soda ash for glass manufacturing.

New Sky's initial business model is to license its technology for incorporation at partner sites, as well as to provide consulting services. The company has built two large prototypes, and plans a pilot facility by the end of 2012, and a 3–4 ton/d modular production facility at a client site by the middle of 2013.

A non-crop-based sugar feedstock for bio-based chemicals and biofuels

Proterro Inc. (Princeton, N.J.; www.proterro.com) has demonstrated technology for directly producing sucrose as a feedstock for bio-based chemicals and biofuels that avoids the need for cellulosic biomass and energy crops. Using a genetically engineered strain of photosynthetic cyanobacteria and a unique photobioreactor system, Proterro is able to generate a clean, fermentation-ready sugar at a cost competitive with sugarcane, corn or other energy crops.

The freshwater cyanobacteria naturally secrete sucrose as an osmoprotectant in the presence of salt. They have been engineered and cultivated for maximum secretion of sucrose, while allowing the organisms to maintain all of their regular metabolic functions. These organisms are grown on the surface of a composite fabric material, over which water is trickled. The composite fabric acts as a wick, efficiently distributing a minimal amount of water over the growing surface. Surrounding the gravity-fed fabric surface is a transparent enclosure into which CO_2-enriched air is fed to serve as the carbon source for the sucrose photosynthesis.

Proterro CEO Kef Kasdin reports that the company has successfully tested three photobioreactor systems in two regions of the U.S. "Our system has more geographical flexibility than the production of Brazilian sugarcane and other agricultural approaches," she says, adding that ethanol producers could be among the adopters of Proterro's sucrose.

Metals recovery

Dinnissen Process Technology B.V. (Sevenum, The Netherlands; www.dinnissen.nl) has developed a purpose-built system to recover valuable metals — such as chrome and molybdenum — from highly viscous residual waste from the petrochemical industry. Such waste, which is often contaminated with wood, stone and iron particles, has been almost impossible to process, says the company.

The thick, viscous tar mass (from drums, containers and bags) is first placed in tipper units, which are vibrated and shaken to empty the mass into a scraper unit, which is equipped with scrapers and breakers. The scraper unit processes the waste into a homogeneous material, which is then metered via a worm-wheel conveyor to an incinerator. There, waste products are completely burned, leaving behind pure metal that is cooled in a silo before being packed in bags. More information about the system will be available at the company's Achema exhibition (Hall 5.0, Stand D17).

Desulfurizing biogas

Last month, Lanxess AG (Leverkusen, Germany; www.lanxess.com) introduced Bayoxide E 16, a highly ef-

(*Continues on p. 12*)

Note: For more information, circle the 3-digit number on p. 76, or use the website designation.

Winning copper from low-grade ore

India holds large reserves of low-grade sulfide copper ore containing 0.3 wt.% copper, which cannot be processed through conventional routes since the cut-off grade for treatment in concentrators is about 0.45 wt.%.

India is in short supply of copper and an appropriate technology for processing low-grade ores would contribute to India's economy. Accordingly, a team from the Institute of Minerals & Materials Technology (Bhubaneswar, Orissa, India; www.immt.res.in), led by Professor Lala Behari Sukla, developed a process flowsheet to recover copper metal from the lean sulfide ore of copper available at Malanjkhand, Hindustan Copper Ltd.

Copper-pregnant leach solution obtained from bio-heap leaching of chalcopyrite containing 0.3 wt.% copper was purified through solvent extraction for removal of impurities and then passed through activated carbon to produce an organic-free solution suitable for copper electrowinning.

The team used a mixed culture of acidophilic bacteria, predominantly *Acidithiobacillus ferrooxidans*. It employed a method of repeated subculturing to activate the strain. During each subculturing processes, 2 L of the full-grown media were centrifuged, to collect the total biomass to be used for the next experiments. After six sets of subculturing, a stable iron oxidation rate of 500 kg/m^3/h was achieved.

The team subjected impurity-free solution containing 43 g/L copper and 182 g/L of H_2SO_4 to electrowinning in a continuous mode at a current density of 100 A/m^2 and depletion rate of 4 g/L copper to produce copper sheets of good morphology. About 35 m^3 of electrolytic solution was processed. Cell voltage was about 2.2 V. The amount of copper deposited in the continuous run of 3,515 h was 65.824 kg.

Smooth copper sheets were deposited at the cathode during electrowinning with 99.96% purity.

The team believes its process route is technically feasible and environmentally friendly, and has the potential to replace the conventional process, especially for the treatment of lean copper sulfide ores.

(*Continued from p. 11*)

fective synthetic iron oxide for reducing hydrogen sulfide (H_2S) in biogas that can be added directly to the fermenter. Bayoxide E 16 reacts directly with H_2S to form iron sulfide and sulfur, which together with the fermentation residue, can be used to fertilize fields. Because of the additive's nearly 100% purity, it removes nearly all of the H_2S (typically around 500 mg/m^3, depending on the waste being fermented). As a result, a metering system is not required and the cost of secondary biogas desulfurization by activated carbon absorption is "significantly" reduced, says the company. Removing the H_2S directly inside the fermenter also helps avoid damage from corrosion caused by the formation of sulfuric acid, adds Lanxess.

Focusing on your safety

We offer peace of mind when it comes to your process safety and productivity. Metso is a single source for all your process control needs, from automation systems to intelligent flow control solutions that are proven in the toughest conditions. Our 30,000 professionals based in over 50 countries deliver sustainability and profitability to customers worldwide.

www.metso.com/oilandgas

metso
Expect results

The first synthesis and isolation of a 'heavy ketone'

For the first time, researchers from Riken (Saitama, Japan; www.riken.go.jp) have synthesized stable crystals (photo) of a so-called heavy ketone — a compound in which the carbon of the C=O bond is replaced by Si, Ge, Sn or Pb. These heavy ketones are highly reactive and prone to polymerization, which has made them difficult to synthesize and isolate to study their properties. Computer studies have predicted such compounds may have applications for performing new acid and base reactions, catalysis and for designing new functional materials.

The researchers' first compound is a germanone, with the formula $(Eind)_2Ge=O$, where Eind is a bulky "protection group" — made of 28 carbon atoms and 45 hydrogen atoms (1,1,3,3,5,5,7,7-octaethyl-s-hydrindacen-4-yl) — which prevented the intramolecular polymerization at the Ge=O double bond (diagram). Computational studies and chemical reactions suggest that the Ge=O double bond is highly polarized. The germanone could be reduced into an alcohol, as is observed with ordinary ketones, and it also exhibits a unique reactivity that is not observed with ordinary ketones, including the reaction with acetone without using catalyst, and also the spontaneous trapping of CO_2 gas (at room temperature and 1 atm) to provide a cyclic addition product.

The researchers are now working to synthesize heavy ketones of silicon.

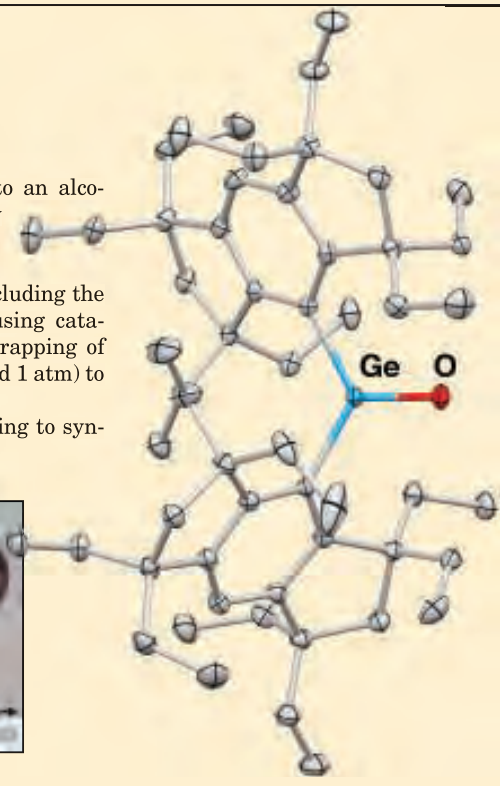

Heat-harvesting

A significant portion of generated energy is wasted as heat. Thermoelectric materials convert waste heat to electricity, and could improve energy efficiency, but most existing thermoelectric materials are expensive to manufacture and difficult to install. Researchers at Purdue University (West Lafayette, Ind.; www.purdue.edu) have collaborated with a team at Jilin University (Changchun, China) in developing a solution-phase deposition method for coating nanoscale crystals of lead-tellurium (a thermoelectric material) onto glass fibers. The techniques used in producing the flexible coated fibers could point the way toward energy harvesting materials that require less raw material and are amenable to large-scale manufacture.

A less-expensive process to recover CO_2 from PSA offgas

At Achema 2012 (June 18–22; Frankfurt am Main, Germany), Union Engineering A/S (Fredericia, Denmark; www.union.dk) will be presenting its patented FlashCO_2 process — both at the exhibition (Hall 9.1, Stand E29) and in a congress lecture (Monday, June 18th at 11:30 in the room Illusion 2). FlashCO_2 enables liquid CO_2 to be produced from H_2 plants at a direct operating cost of around €20–30/ton — significantly lower than the €30–40/ton required using conventional chemical absorption processes, says Michael Mortensen, Union Engineering's chief sales officer.

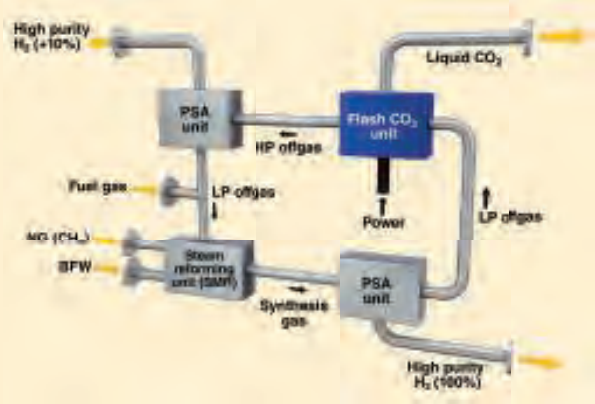

FlashCO_2 was developed to capture CO_2 from the medium-rich CO_2 offgas being purged from pressure-swing adsorption (PSA) units, which are typically used for product purification in H_2 plants. FlashCO_2 (diagram) combines conventional physical adsorption (using chilled methanol) and liquefaction technologies, and eliminates the requirement for steam stripping. Despite the relatively low CO_2 concentration in H_2 PSA offgas (40–55%), the integrated double-loop design makes the plant capable of producing food- and beverage-grade CO_2 at costs competitive with more conventional CO_2 sources, such as ammonia and bioethanol production. Also, the high concentration of H_2 in the purge from the FlashCO_2 unit results in an increase of H_2 production by up to 10% — a benefit not present using traditional absorption processes, says the company.

The first commercial application of FlashCO_2 was a 5 ton/h beverage-grade CO_2 plant for Indura SA (Santiago, Chile; www.indura.net), which takes the PSA offgas from a major petroleum refinery in Conception, Chile and started up in 2007.

Chlorine dioxide single-stage NOx scrubbing technology lowers costs

A new process for removing oxides of nitrogen (NOx) from industrial foul-air and cool combustion exhaust uses ClO_2 in a unique way to remove over 99% of both NO and NO_2 with a single scrubbing stage. The reaction vessel is considerably smaller than those required by conventional wet-chemistry NOx removal processes, and according to the technology's developer, Pacific Rim Design and Development (PRDD; Shingletown, Calif.; www.prdd.net), the equipment is less expensive to install and operate than existing methods, such as wet-scrubbing or selective catalytic reduction.

PRDD's patent-pending process employs proprietary technology that precisely combines the ClO_2 with NOx-containing waste gas stream in a gas-phase reaction chamber. Requiring only 1.5 seconds of residence time within the scrubbing vessel, the process uses chlorine dioxide to react with NO and NO_2, yielding nitric and hydrochloric acids. The mineral acid products of this reaction can be used elsewhere.

The PRDD NOx abatement process is unique because it treats both NO and NO_2 in a single scrubbing stage. Conventional wet-scrubbing processes require three-stage scrubbers to accomplish this, explains PRDD scientist and engineer Robert Richardson. In cases where waste gas streams contain primarily NO_2, single-stage treatment is possible, but gas streams with significant levels of NO require multistage scrubbers because the low-solubility NO must first be converted to water-soluble NO_2, before being removed from a waste gas stream. The PRDD process, which has been demonstrated in two pilot-scale facilities, employs reactions that occur very quickly, allowing high removal efficiencies for both NO and NO_2.

The short residence times and simple, small single-stage reaction vessel design in the PRDD process lowers equipment costs, as well as operational costs, Richardson remarks, allowing companies to cost-effectively meet regulatory requirements for NOx emissions.

PRDD anticipates completing a full-scale facility in the third quarter of 2012 that will be capable of treating 32,000 ft^3/min of waste gas. The company is working on deals to license its technology either as a retrofit, or to be built into new facilities.

Circle 12 on p. 76 or go to adlinks.che.com/40268-12

Aramid nanofibers

Teijin Techno Products Ltd., a Teijin group company (Tokyo, Japan; www.teijin.co.jp) has developed the world's first mass-producible aramid nanofiber. These uniformly sized nanofibers are based on the company's proprietary Teijinconex heat-resistant meta-aramid, and will be marketed in the form of non-woven sheets. Commercial production is targeted for 2014.

These heat-resistant, aramid nanofiber sheets are said to maintain their shape, even at 300°C; are highly resistant to oxidation; and have a high porosity and large surface — properties that make them especially suited for use as separators in lithium ion batteries. Other potential applications are being developed for the new aramid sheets, including separators for capacitors and heat-resistant filters.

A new process for making screens

After eight years of R&D work, Inflotek B.V. (Beringe, The Netherlands; www.) is now commercializing a range of metal screens made with a proprietary, waterjet-cutting technology. Compared to conventional waterjet-cutting methods, Inflotek's process can reliably make hundreds of perforations per hour, which enables the fabrication of industrial process screens with a large number of perforations on a small surface. The screens can have virtually any pattern that can be printed, with slots that are tapered (photo) to reduce sensitivity for plugging, says Frank Stofmeel, sales manager at Inflotek.

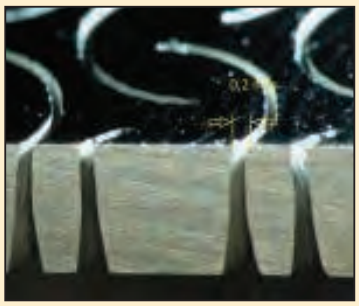

To make the screens, a mixture of water and very fine sand is passed through a proprietary nozzle at high pressure (4,000 bars). The water beam (with sand) emerges from the nozzle at Mach 3, and is narrower (100 µm) than traditional jets (400 µm), enabling smaller slot kerfs with twice the cutting tolerance, says Stofmeel. This much finer beam can cut at speeds 2–3 times faster than a traditional waterjet, thus significantly reducing production costs, he says. Screens made with the micro-waterjet technology have the highest open area of any screen thicker than 2 mm, with open areas typically 50 to 200% greater than wedge wire screens for slot widths below 400 µ, he adds. It can cut steel more than 30 mm thick, without causing distortion, warping, work hardening or thermal stress.

Inflotek is initially focused on screens used in centrifuges for separating solids from liquids, and the screens are currently being trialed in a range of industries, including potash, coal, food and chemicals. The company is also developing a range of screens for pulp processing, fluidized-bed drying, high-wear coarse classification screens and others. The screens will make their commercial debut at Achema 2012 (June 18–22; Frankfurt am Main, Germany; Hall 5.1, Stand D8).

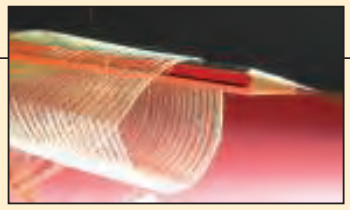

Manufacturing bee silk with bacteria

A partnership between Australian research agency CSIRO (Melbourne, Australia; www.csiro.au) and Lonza Group Ltd. (Basel, Switzerland; www.lonza.com), aims to market new insect silk products globally. Potential applications of insect silk include composite fibers for the aviation and marine industries, and medical applications such as wound repair, drug delivery, repairing and replacing human tissues such as membranes, ligaments, blood vessels and cartilage.

Production of silk at adequate yield and desirable properties including stability, lightness and tensile strength, as in natural silks, has been the aim of a group from several CSIRO divisions in Victoria and the ACT (Australian Capital Territory), and the Dept. of Biomedical Engineering, Tufts University (Medford, Mass.; www.tufts.edu).

Many invertebrates, including silkworms, bees, spiders and ants produce silk. Production of silkworm and spider silks as biomaterials has posed problems due to the large size and repetitive nature of the silk proteins. In contrast, the silk of honeybees (*Apis mellifera*) is made of a family of four small and non-repetitive fibrous proteins. An NMR study reported that honeybee silk proteins have both α-helix and β-sheet structures, and that α-helical conformation predominates.

The group has achieved recombinant production and purification of the four full-length unmodified honeybee silk proteins in *Escherichia coli* bacteria at yields of up to 2.5 g/L — the highest reported expression level of any recombinant silk protein. The previous highest level was the production of a partial-length synthetic spider silk at a yield of 0.36 g/L. Under suitable conditions the recombinant proteins self-assemble to reproduce the native coiled structure. Using a simple spinning system the group has succeeded in producing recombinant silk fibers (photo) with the tensile strength of the native material.

'Visible' photocatalyst

The research groups of Masahiro Miyauchi at Tokyo Institute of Technology (www.eim.ceram.titech.ac.jp) and Kazuhiko Hashimoto at the University of Tokyo (www.light.t.u-tokyo.ac.jp) have developed a photocatalyst that is highly active for the destruction of volatile organic compoiunds (VOCs) using visible radiation. The catalyst, a culmination of a five-year project supported by New Energy and Industrial Technology Development Organization (NEDO), opens the door for applications for photocatalytically destroying harmful VOCs in interiors of buildings and cars with visible light.

The researchers converted photochemically inactive, oxygen-defective TiO_2 — made by the thermal-oxidation of a mixture of Ti_2O_3 and TiO_2 in air — into an efficient visible-light-sensitive photocatalyst by grafting the TiO_2 surface

'Green' polymer

In cooperation with project partners from BASF, the Technical University of Munich and the University of Hamburg, scientists from Siemens' global research unit Corporate Technology have developed a competitive alternative to the standard ABS (acrylonitrite-butadiene-styrene) polymer, which is frequently used in consumer products. The new composite material is a mixture containing polyhydroxybutyrate (PHB), which is made from renewable materials such as palm oil and starch. Because PHB is brittle, polypropylene carbonate (PPC) from BASF is added to make it softer. PPC is 43 wt.% CO_2, which is obtained from power plant emissions using a separation process. More than 70% of the new mixture is made of "green polymers." Bosch-Siemens-Hausgeräte (BSH) has used the new material for vacuum cleaner covers under series production process conditions. ❑

Detecting VOCs with a quantum-tunneling composite

A sensor that detects volatile organic compounds (VOCs) at levels of 10–100 parts per million (ppm) is being developed by Peratech Ltd. (Richmond, U.K.; www.peratech.com), with collaboration from the University of Durham (U.K.; www.dur.ac.uk). The so-called Electronic Nose is based on the company's quantum-tunneling composite (QTC) material — a composite of conductive nanoparticles and a non-conductive polymer. The polymer content of the granular QTC swells when exposed to VOCs, which brings the conductive particles close enough to allow electrons to flow between the particles — an effect known as quantum tunneling. The sensor is said to respond faster than alternative sensing technologies, and rapidly (within seconds) recovers once the VOCs have gone from the surroundings. An additional feature of the QTC technology is that it has very low power requirements, says the company. Peratech is now looking for companies interested in licensing the technology.

with 2–3-nm clusters of amorphous cuperous oxide (CuO), which serves as a co-catalyst. This catalyst shows a tenfold increase in reaction efficiency (with visible light) over conventional nitrogen-doped TiO_2, and almost the same sensitivity as the ultraviolet sensitivity of commercially available anatase-type TiO_2. For example, with the new catalyst, gaseous 2-propanol is decomposed into CO_2 under visible radiation at a rate of 0.20 µmol/h with a quantum efficiency of 10.8%.

The chemists are planning to apply their achievement for real applications, such as self-cleaning, easy to maintain construction materials, as well as air-cleaning materials for use at hospitals and airports. Materials have already been developed as powders and coating solutions, and could be commercially applied within two years. ■

U.S. House approves cybersecurity bill to ease information sharing

Last month, the U.S. House of Representatives voted to pass the Cyber Intelligence Sharing and Protection Act (CISPA), a measure that would ease information sharing among chemical firms and other companies with facilities that are vulnerable to cyberattacks. The bill has been met with much controversy: President Obama has threatened a veto and the Senate has been circulating a different bill aimed at cybersecurity, although no vote has been held in that chamber.

Sponsored by Reps. Mike Rogers (R-Mich.) and Dutch Ruppersberger (D-Md.), CISPA would give businesses and the federal government legal protection to share cyberthreat information with each other. The government does not currently share these data because the information is classified and companies fear violating antitrust laws. The bill would remove legal barriers, making it easier for chemical firms, and other businesses, to do so.

"The intelligence community has the ability to detect these cyberthreats, these malicious codes and viruses, before they are able to attack our networks," says Ruppersberger. "But right now, federal law prohibits our intelligence community from sharing classified cyberthreats with the companies ... that control the networks — the AT&Ts, the Verizons, the Comcasts."

"We have the ability to give them information to protect us, yet we have to pass a law to do that," the Congressman added.

The Obama administration threatened a veto and privacy and civil liberties groups claim that, under CISPA, what is defined as consumer data and permitted to be shared is overly broad. The bill's authors have added amendments to appease concerns, such as limiting the federal government's use of private information and restricting which cyberthreat data can be shared. The Obama Administration is also seeking regulatory mandates for critical infrastructure providers, which are not contained in CISPA, which is one of four cybersecurity bills currently under consideration.

CSB RELEASES NEW SAFETY VIDEO ON DUPONT HOT WORK EXPLOSION

The U.S. Chemical Safety Board (CSB; Washington, D.C.; www.csb.gov) recently released a new safety video detailing a fatal 2010 hot work accident that occurred at the DuPont facility near Buffalo, N.Y.

The video, entitled "Hot Work: Hidden Hazards," features a computer animation showing how hot work being conducted on top of a tank led to a deadly explosion that killed one contractor and injured another.

In the video, CSB chairperson Raphael Moure-Eraso emphasized that hot work is "often seen as a routine activity, but it can prove deadly if fire and explosion hazards are overlooked."

The 11-minute video details the events leading up to the accident, noting that although DuPont personnel monitored the atmosphere above the tank, no monitoring was done to see if any flammable vapor was inside the tank. The CSB investigation found the hot work ignited the vapor as a result of the increased temperature of the metal tank, sparks falling into the tank, or vapor wafting from the tank into the hot work area.

The CSB released its final report and formal safety recommendation at a public meeting in Buffalo on April 19. The video is available to stream or download at CSB's website or YouTube channel (www.youtube.com/uscsb).

GE and Shenhua open cleaner-coal-technology JV in China

GE (Atlanta, Ga.; www.ge.com) recently announced the opening of GE Shenhua Gasification Technology Co., a 50-50 joint venture (JV) with Shenhua Group to advance the development and deployment of "cleaner coal" technology solutions in China.

The new company combines GE's expertise in industrial gasification technologies with Shenhua's expertise in coal gasification and coal-fired power generation. The JV will sell industrial gasification technology licenses in China, conduct research and development to improve cost and performance of commercial-scale gasification and integrated gasification combined cycle (IGCC) solutions and work to advance the distribution of commercial-scale IGCC technology.

Gasification technology has become a critical tool in the expansion of the Chinese economy, allowing a wide variety of industrial products and fuels to be created from low-cost abundant coal resources. With more than 50 licensed facilities in China, GE's gasification technology is one of the most widely deployed in the industry.

Shenhua is one of the world's largest coal and energy companies, with integrated coal production, power generation, railway, port and shipping infrastructure. Shenhua also has a national role in the development of new coal-related technologies.

China and the U.S. are the two biggest energy consumers in the world.

Jacobs receives contract from Evonik for new chemical plant

Jacobs Engineering Group Inc. (Pasadena, Calif; www.jacobs.com) says it was awarded a contract from Evonik Industries AG (Essen, Germany; www.evonik.com) to provide basic engineering services for an investment in a grassroots polyamide-12 production facility in Asia.

Officials did not disclose the contract value. Jacobs has been working closely with Evonik's project team in Marl, Germany to develop the conceptual design for the new plant, which is based on Evonik's existing plants in Germany. Members of the integrated project team are operating from Jacobs' office in Leiden, The Netherlands to undertake the FEED (front-end engineering design) work, supported by Jacobs' office in Mumbai, India.

Under a separate framework contract signed in 2011, Jacobs is providing engineering services as the owner's engineer on Evonik's process industry projects worldwide. ■

Edited by Scott Jenkins

EDUCATION EVOLUTION

To prepare students for globalized industries, chemical engineering academic departments are incorporating new requirements, utilizing IT and connecting with CPI companies

A host of conditions, including globalization of industry, expanding access to information and a shifting workforce profile present challenges for university chemical engineering departments as they prepare aspiring engineers for work. To address the challenges, the educational system for chemical engineering is trying to strike the optimal balance between new and traditional teaching approaches, as well as between core chemical engineering topics and modern engineering applications. Meanwhile, the academic chemical engineering community and the world of industrial chemicals are struggling, with mixed success, to forge connections and relationships.

Macro-level trends

A number of wider trends are having a significant impact in shaping the education enterprise in chemical engineering. Information — and the technology used to locate and organize it — is at the heart of several high-level trends that have both positive and negative consequences for the education of engineers. "There has been a veritable explosion of technical information available," says Sasha Gurke, senior vice president and co-founder of Knovel, an online library of curated technical content. "And the growth of information is still accelerating, while the Internet is maturing," he adds. One result of that is an ever-greater need for efficient and effective informatics tools for mining that information. Gurke suggests that generally, computer software and information management tools are keeping pace. For example, the use of computer-assisted design in engineering is rising, he says.

"In education, access to information has never been greater," says University of Michigan (UM) chemical engineering collegiate lecturer Susan Montgomery. "This has both positives and negatives for students."The wealth of online information allows unprecedented access to the wide range of the latest technical information and ideas, but also sources of temptation for students to take shortcuts.

While most of the core topics taught in chemical engineering courses have remained the same over several decades, the methods for teaching those topics have changed somewhat, primarily through the wider use of information technology (IT). "The use of information technology for teaching chemical engineering has been universal, but I still don't think universities are taking full advantage of the IT tools available," opines Richard Felder, emeritus professor of chemical engineering at North Carolina State University (NCSU; Raleigh; www.ncsu.edu/effective_teaching) and longtime champion of improved teaching.

Bridging the gap

In decades past, university chemical engineering programs have been closely tied to industrial chemical-processing operations in their regions. A large portion of academic chemical engineering research was funded by industry, notes Dan Crowl, the Herbert Dow Professor for Chemical Process Safety at Michigan Technical University (MTU; Houghton, Mich.; www.mtu.edu). Whereas today that is not the case. The modern relationship between the academic and industrial chemical engineering communities is more diverse, dynamic and complex than in the past, but there is a general sense that the academic and industrial chemical engineering worlds are not as integrated as they should be.

"The disconnect between academia and industry in chemical engineering has never been greater," says Sanat Kumar, chair of the chemical engineering department at Columbia University (New York; www.columbia.edu). "It's increasingly polarized."

Crowl suggests that an overall trend within academia over the past several decades has been a generally reduced level of direct industry experience on the part of the faculty members. "There's been a drift away from the industrial experience in U.S. education," he says.

There is a rising awareness, however, that university departments must be connected more to industry, and must continuously foster those relationships, say Mauricio Futran and Henrik Pedersen, the current and past department chairs, respectively, of the chemical engineering department at Rutgers University (Piscataway, N.J.; www.rutgers.edu). "Rutgers is somewhat unique in the number and breadth of the industry partnerships that the department has made," Pedersen added. These include a catalysis consortium, a center for solid-organic particulate matter, individual research collaborations and others. The partnerships are driven by the expertise of the faculty, which tends to be in areas of interest to industry companies, Futran says.

In an example of how connections are made, many departments have established industry advisory boards that meet periodically to provide input to university departments about industrial needs, and other topics, MTU's Crowl points out.

Academics have to go out and seek connections to industry, because there are not many good forums for the two communities to come together, Columbia's Kumar says. He recounts a recent effort to set up an industry-academic discussion group at the New York Academy of Sciences in which academic participation was far higher than industry, by a 90/10% split, Kumar says. So far, it seems like the themes we have picked — bioprocessing, energy, "big data" — have not resonated that strongly with industry, he says.

Knovel's Gurke agrees that broader leadership and coordination for academic-industry initiatives in chemical engineering is lacking. He also agrees that the industry-academic gap is real, despite the efforts on the part of individual universities, individual researchers and companies to establish links between the two sectors. Relationships between universities and engineering-related companies certainly exist, but they are established and cultivated somewhat on an ad hoc basis. "There is no national policy or leadership in this matter," he says.

Universities "can and should do more to integrate practical industry knowledge into their courses, such as by setting up business incubators, participating in industrial R&D and expanding internship programs with local companies," Gurke comments.

The disconnect between academia and industry amplifies existing workforce-related challenges. Gurke explains, "The problem is that, in the past, mentoring of young engineers by older, experienced ones was more prominent, with experienced personnel transferring practical engineering knowledge on a person-to-person basis. Now, streamlined staffing and the retirements of Baby-Boom-aged engineers leave fewer opportunities for in-depth mentoring." Citing an IEEE study that suggests over three-quarters of the knowledge obtained by engineers is acquired after graduation, Gurke says the reality is that young engineers have to obtain that knowledge in other ways. And the relationships between CPI players and engineering schools will play a large role in how effectively this is accomplished.

University chemical engineering programs are exploring a wide range of ways to foster improved connections with industry. An overriding educational goal in the chemical engineering program at MTU is to give students as much fundamental depth as possible, while still relating the education to industrial practice, says MTU's Crowl. For example, in many cases, universi-

universities have moved toward smaller unit operations laboratory equipment that is not as reflective of industrial environments, says Crowl. On the other hand, MTU students work on a pilot-scale, three-story distillation tower with an Emerson control system. "It's an example of how we're trying to make the academic experience connect to the industrial world," Crowl noted.

Other faculty members, such as UM's Montgomery and Ann Marie Flynn, chemical engineering department chair at Manhattan College (Riverdale, New York; www.manhattan.edu Flynn say that it is important to have faculty with industrial experience, especially to teach the product- and process-design courses.

Curriculum changes

A major ongoing challenge faced by university chemical engineering faculty is how to maintain the core chemical-engineering curriculum, while also including key ancillary skills and introducing students to new technologies.

"There's a deep-seeded conservatism in the world of chemical engineering, which means that there is a considerable resistance to change," Kumar says. "It's actually quite remarkable that so little has changed in the chemical engineering curriculum."

"In most ways, the curriculum has remained very much the same; what may be different are the examples used to illustrate the topics," Kumar says. "It's these examples that will bring in some of the newest technologies and latest applications" and be reflective of modern technologies.

Futran and Pedersen, of Rutgers University agree, saying the core chemical engineering topics remain the same after decades of teaching. The problem is that there is very little, if any, room in the curriculum for new topics, Crowl says. "It's very difficult to fit everything in," adds Manhattan's Flynn.

Despite the difficulty, chemical engineering departments are feeling pressure to add more material to their curricula. For example, Montgomery says that a survey of chemical engineering alumni at UM identified a number of topics where recent graduates were somewhat lacking in their preparation for the workplace. These included statistics, six-sigma manufacturing and process equipment troubleshooting. "We've been hearing a lot from industrial engineers that critical thinking skills are important, especially when applied to troubleshooting processes and equipment problems," says UM's Montgomery. In response to the input from alumni in industry positions, UM developed — in conjunction with the alumni board — a required one-credit class covering chemical engineering process economics.

Others pointed to additional areas that should be addressed more in chemical engineering education. For example, sustainability and risk analysis are becoming more important in framing engineering problems. "Risk management and risk analysis are important for engineering design, and should become more prominent in engineering education," says Gurke.

Reflecting the importance of computing and informatics, Columbia chemical engineering students are required to complete a class in programming methods. In addition, they must complete a two-semester chemical engineering design series, where product design is the second-semester subject.

Ancillary skills

Despite the difficulty in fitting material into the traditional chemical engineering curriculum, departments are still making an effort to provide their students with not only technical engineering knowledge, but also skills that are not specific to engineering, and yet important for modern workplace success. These include writing, presentation, language and others.

Communications-related skills have emerged as a focus in many engineering departments. At the University of Michigan, members of the technical communications faculty are also involved in the laboratory and design courses in the chemical engineering department, notes Montgomery.

Students at Manhattan College are required to take a communications class, in which they discuss topics such as technical presentations, email writing, technical communications and others, Flynn explains.

At Columbia, Kumar notes that communications skills are integrated "across the board" in the undergraduate curriculum, so chemical engineering students are required to deliver multiple oral presentations and submit several written reports. Rutgers takes a similar approach.

Aside from communication skills, other non-engineering-specific topics have also emerged as ones that will

EVOLVING TEACHING APPROACHES

With a wide array of new technologies and a fuller understanding of the science behind how students learn, universities have an array of tools with which to engage their young engineers. "Students want an active learning environment," says MTU's Crowl.

Former N.C. State professor Felder cites the increasing use of inductive learning techniques, such as inquiry-based and problem-based learning, in which students are first presented with a challenge and learn the course material in the context of addressing that challenge, as an example of the discipline's movement toward more experiential hands-on instructional strategies.

Also, making expectations clear to students about what problems they are expected to solve is important. Going forward, there will be an increasing use of learning objectives, where instructors articulate what skills should be mastered at different points in the class.

For the past 21 years, Felder has led a popular, three-day workshop for chemical engineering instructors known as the National Effective Teaching Institute (NETI).

The successful workshops have exposed more than 1,000 chemical engineering instructors from over 200 institutions to the latest information from the cognitive science field about how students learn. NETI is also designed to provide instructors with new tools to foster that learning, Felder says.

The chemical engineering department at Manhattan College has utilized a large number of teaching tools and techniques, but has found that its students responded better to a more traditional lecture-based approach.

"One thing I think departments need to be careful of is changing things just for the sake of change," says Annmarie Flynn, chemical engineering department chair at Manhattan College. "It's important to establish a balance between the traditional teaching style and the more experiential, inductive approaches, which are challenging to run effectively in practice," Flynn remarks. "Formal lecture, with repetition of concepts, remains important," Columbia's Kumar adds.

The chemical engineering department at Rutgers strives to teach fundamental topics in a classroom setting, while still using Web-based tools that are available. ❑

help engineering students in their careers. For example, all Columbia engineering students are also required to take a "core program" of general education requirements.

"At Michigan, we try to give students more opportunities to take general electives and pursue minors in their degree program. There's also a university-wide initiative in international education," Montgomery points out.

Knovel's Gurke also recommends a more comprehensive approach to teaching informatics in university engineering courses — even suggesting mandatory informatics classes. "Everyone has visits by a university librarian to explain resources, but more emphasis should be placed on 'how to learn' and how to do it efficiently," Gurke says.

Process hazards requirement

Another area in which additions to the chemical engineering curriculum have been made is process safety and chemical hazards education. The additions are a result of new accreditation requirements introduced in 2012 by the Accreditation Board for Engineering and Technology (ABET; Baltimore, Md.; www.abet.org) to include teaching on chemical process safety and process hazards as part of all university chemical engineering curricula.

One of the factors that led to the new ABET chemical hazards accreditation requirements was the U.S. Chemical Safety Board's (CSB; Washington, D.C.; www.csb.gov) investigation of a 2007 explosion at the T2 Laboratories facility in Jacksonville, Fla. The CSB investigation concluded that one of the causes of the accident was that engineers did not have sufficient instruction on reactive chemical hazards. One of the CSB's recommendations was to change the accreditation requirements to add education on process hazards to the curriculum of chemical engineering departments in the U.S. Universities are addressing this need in a number of ways.

Most university departments are incorporating process safety and chemical hazard information in the context of other classes. "At Rutgers, we have embedded that material into multiple courses," Pedersen says.

At Manhattan, Flynn says the department has incorporated in its laboratories a number of safety features instituted at an industrial cosmetics engineering facility at L'oreal Corp., with which they have a relationship. "It helps to establish a culture of safety among the students," she says. They are also looking at an accident and emergency management class.

At MTU, Crowl says the department has established a student-run safety program in laboratories there that helps students take responsibility for safety. ■

Scott Jenkins

EXPLOSIONS: ARE YOU PREPARED?

Explosion protection equipment can minimize damage, but process understanding is key to optimized solutions

Fike

Fike

Pepperl+Fuchs

Designed for use with square or rectangular explosion vents, FlamQuench SQ technology consists of various layers of high temperature stainless steel that absorb heat produced during combustion. This allows conventional venting to be done indoors with no release of flame

An ECARO-25 (photo, top right) clean agent fire-suppression system is suitable for protecting electronics and high-value assets, thus reducing the threat of needless downtime and business interruption

For industrial signal transmission many users insist on single loop integrity. Others need compact mounting. With a module width of only 12.5 mm and single channel functionality, the new KC-Modules of the K-System combine these two requirements, making them suitable for use in hazardous areas

An explosion is defined as "a rapid increase in volume and release of energy in an extreme manner," and is usually accompanied by high temperature generation and gas release. Flammable gases, vapors, dusts and ambient oxygen — all present in chemical processing facilities — can react to cause an explosion that essentially creates a shock wave.

As a result of modern production technologies and increased production capacity, an explosion is a threat chemical processors confront daily, says Gerd Mayer, president of Rembe (Charlotte, N.C.; www.rembe.com).

While there are Occupational Safety and Health Admin. (OSHA; Washington, D.C.; www.osha.gov) standards and industry guidelines — namely OSHA's Combustible Dust National Emphasis Program and NFPA's 654, 68 and 69 — chemical processors are still often confused when it comes to selecting and installing explosion protection systems.

"Protection is very different than prevention," explains Vahid Ebadat, CEO of Chilworth North America (Princeton, N.J.; www.chilworth.com). "When it comes to explosion protection, what you're saying is that you are anticipating that an explosion will occur, but you have designed your processes and equipment in such a way that when an explosion does occur, people won't be harmed and the facility won't be damaged."

And, he continues, in order to do this, operators need to have a clear understanding of their operations and processes, as well as the chemicals being used and the associated risks they create. "Knowledge of the maximum pressure and the severity of the explosion that could occur as a result of ignition of the flammable gas, vapor or dust cloud atmosphere is imperative," he says.

In addition, the objectives of the facility owners must be evaluated, says Bruce McLelland, national accounts sales manager for explosion protection with Fike Corp. (Blue Springs,

Mo.; www.fike.com), such as how much damage is tolerable and what kind of changes the facility owner is willing to make for protection. "Is it acceptable if, at the end of an event, a vent has worked properly and protected against the worst case scenario, but the processing equipment is destroyed by fire after the explosion?" he asks. "It's good that there wasn't flying debris or injuries or loss of facility, but there is still a loss of equipment and there will be a significant loss in process downtime. Processors need to look at all types of available explosion protection equipment and determine what is acceptable loss to them."

Mayer agrees. He suggests considering three basic requirements when selecting a solution: profitability (the protection solution has to be economical to implement, operate and maintain), reliability (the protected facility has to remain permanently and optimally available for production) and safety (people and machines must be ensured of an explosion-protected environment through constructive and effective directives).

Equipment types

In addition to the use of appropriately rated electrical equipment and intrinsically safe instruments and devices in hazardous areas, there are three main types of explosion protection solutions, each with its own set of pros and cons. Solutions include the following:

Containment. Process equipment can be designed to withstand the maximum explosion pressure. However, containment can be an expensive option because of the special engineering and strength required. Often, once the equipment is built, access to the vessel for routine maintenance is cumbersome. And, it is necessary to maintain the pressure integrity of the vessel for life. Corrosion or other wear and tear can weaken the equipment over time. In practice, this option is usually considered for small vessels or where highly toxic chemicals must not be released.

Explosion suppression. Like a fast-acting fire extinguisher, suppression systems kick in when an explosion starts to develop. When explosion conditions are detected, a suppressant is injected into the dust or vapor cloud to quench and stop an explosion. While this is a viable solution, it can be an expensive option because detectors and sensors, control systems and battery backup equipment are required and must be regularly maintained.

Explosion relief venting. Compared to the first two options, venting is usually the simplest solution. It consists of a panel or door that will rupture or open and release the explosion products (pressure and flame). The problem here, however, is that vents can't normally open inside a building and must be routed to a safe location outside the building, which requires proximity to an outside wall. And, it is not an option when the chemical being released could cause an environmental hazard.

There have been some advances in explosion protection solutions, including suppression systems that offer optical detection to improve the speed of response and stability of detection, and indoor venting systems, referred to as particulate retention and flame-arresting devices, that, under some circumstances, make venting possible when equipment has no easy access to an outside wall. And, these can all be used in conjunction with intrinsically safe instrumentation, the use of which helps reduce — but not always eliminate — the need for explosion protection equipment in some installations, says Robert Schosker, product manager of intrinsic safety with Pepperl+Fuchs Inc. (Twinsburg, Ohio; www.pepperl-fuchs.us).

However, experts agree that what might seem like the best solution may not actually provide the best protection for a given facility. It is highly recommended that chemical processors seek a risk assessment that can classify the hazardous areas, determine the risks and, based upon that information, select the explosion protection solution or solutions that will protect employees, equipment and processes in accordance with the facility owner's objectives.

"Ultimately, the best solution is the one that provides life safety and enables the facility to maintain their business with the least interruption possible," says McLelland. ❑

Equipment News

EXPLOSION-RELATED PRODUCTS

Yokogawa

Newson Gale

Larson Electronics

Oseco

Install these lights in hazardous environments

The portable tower and removable lamp assembly design of the EPL-QP-1X150-100 explosion-proof halogen light tower (photo) provides 1,500 ft^2 of work area coverage with 1,520 lumens of light output. It is designed to provide operators in hazardous locations with a powerful portable lighting solution. Equipped with a 150-W halogen bulb that produces illumination in a wide flood pattern, the explosion-proof lamp housing is suitable for wet areas. — *Larson Electronics LLC, Kemp, Tex.*
www.magnalight.com

Verify grounding with this system

The Earth-Rite static electricity monitoring system (photo) provides a margin of safety when Type C FIBCs or similar static dissipative containers are used to transfer bulk powdered and other solid materials in hazardous-area applications. The system includes an enclosed, intrinsically safe power supply and an electronic monitor. It continuously verifies the existence of a low-resistance path between the container's static dissipative or conductive fibers and a known grounding point, typically through a mechanical grounding clamp affixed to a flexible tab. — *Newson Gale Inc., Jackson, N.J.*
www.newson-gale.com

An explosion vent with extended life

The MV-RD explosion vent (photo) provides extended in-service life and lower burst pressure in smaller sizes. The vent is designed for high cycling applications, such as in dust collectors and baghouses that experience vacuum pressures up to 12 psig (24.4 in. Hg). The vent mounts on enclosures where dust explosions may occur, and will activate to safely relieve pressure in the event of deflagration, preventing a large explosion. It can also be used on bulk storage units and in ductwork applications requiring a square explosion vent. The vent features a high vacuum rating to help extend the life of the vent in applications where high vacuum pressure exists. Its lower burst pressures provide users with the ability to get the required relief area without having to use a larger vent size. It can operate in temperatures up to 450°F and meets OSHA's Combustible Dust National Emphasis Program and NFPA 68. — *Oseco, Broken Arrow, Okla.*
www.oseco.com

This suppression system meets NEP requirements

Type IPD chemical isolation and suppression system (photo, p. 29) provides explosion protection for facilities handling combustible powders. Installed, the system meets the requirements of OSHA Combustible Dust National Emphasis Program (NEP), as well as NFPA 654, 68 and 69. System components include a power supply and bat-

BS&B Safety Systems,

Volkmann

tery backup, a monitoring module indicating system status/drive external relays, a unitized sensor to detect explosion onset and suppression cannons that deliver a safe sodium bicarbonate suppression agent into the protected equipment. The cannon's compact size and low mass simplify installation and allow the unit to be installed at any angle. There is no need for heavy extension piping and nozzles for suppressant dispersion. — *BS&B Safety Systems, Tulsa, Okla*
www.bsbsystems.com

Vacuum conveying system

By using a sophisticated, nitrogen purging function, the INEX vacuum conveying system (photo) reduces oxygen content within the unloaded batch to below 7% (or lower when required), maintaining the material's inert safety, while providing dust-free transport. The INEX features a closed station that can be flushed from within by sucking in the washing liquid, or through clean-in-place. Standard lightweight and pressure-rated systems are available with INEX functionality. — *Volkmann, Inc., Hainesport, N.J.*
www.volkmannusa.com

This loop-powered indicator provides local data

The MLX loop-powered indicator (photo, p. 28) incorporates the LCD from the company's EJX pressure transmitter into a NEMA 4X aluminum housing. Typical applications for the FM-approved, loop-powered indicators are in potentially hazardous environments in the chemical industry. They provide an additional view of the measured value between a field instrument and the control room. This local indication of flow, pressure, liquid level or temperature can provide assistance during maintenance or when troubleshooting a malfunction. The MLX contains a six-digit numerical and alphanumeric displays for engineering units and a 20-segment bar graph indicating 0–100% of full scale. — *Yokogawa Corp. of America, Newnan, Ga.*
www.yokogawa-usa.com ■

Joy LePree

FOCUS ON Software

Siemens Industry Sector

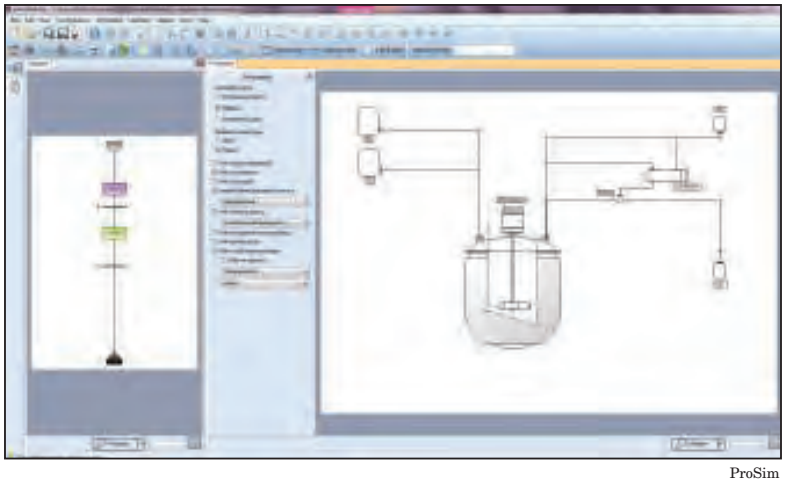

ProSim

Plant-management software for increased integration, and more

This company has expanded its Comos software solution for plant engineering and operation to include considerably enhanced functionality. Comos 10 now provides an enterprise platform for plant engineers and operators that can handle even the largest volumes of data. New functions allow project teams to collaborate with each other across different systems and locations, enabling parallel processing of different work packages. Comos 10 also allows further integration of Comos in the Simatic PCS 7 process-control system (photo). A new interface ensures a consistent, bidirectional exchange of information between both systems, which allows previously serial engineering processes to be organized in parallel. Initial pilot projects have produced time savings of up to 11 weeks (or 12.5%), and up to 315 fewer person-weeks. Cosmos 10 is being released in several stages, the first version became available last month. Achema Hall 11.0, Stand C3 — *Siemens Industry Sector, Industry Automation Div., Nuremberg, Germany*
www.siemens.com

Major updates of gSolids for process design and operation

Last month saw the release of gSolids, a second-generation, integrated drag-and-drop graphical flowsheet environment for model-based engineering and optimization of solids processes. New in gSolids is the ability to handle multiple solid phases, each with its own particle-size distribution. There are also enhancements to a large number of the software's capabilities, such as the use of dynamic modeling to handle batch, continuous and hybrid processes; advanced parameter estimation and optimization capabilities; and integration with the company's gCrystal modeling software and gas-liquid process models. Hall 9.2, Stand C9 — *Process Systems Enterprise Ltd., London, U.K.*
www.psenterprise.com

Track equipment health at large operations

In February, this company introduced Proficy SmartSignal Shield 4.0 software for the oil-and-gas and power industries. The Shield software helps operators detect equipment problems early and avoid surprise equipment failure, thereby increasing productivity while minimizing costs. This software solution provides early warning of impending equipment problems, diagnostic guidance and prioritized actionable intelligence. The Shield software's diagnostic algorithms combine observations on multiple individual sensors to pinpoint failure effects. Beyond vibration and thermal analysis, the solution uniquely models all data on all critical rotating and non-rotating equipment. — *GE Intelligent Platforms, Chicago, Ill.*
www.ge-ip.com/smartsignal

Enhancements for simulation of batch reactors

Released earlier this year, this new version of BatchReactor (photo) combines detailed equipment modeling, reaction engineering and advanced numerical methods to create a state-of-the-art simulation environment for chemists and chemical engineers. By providing a complete understanding of the production recipe, the new simulation software enables users from the pharmaceutical and fine-chemicals industries to test alternative synthesis routes and new production strategies through effective use of simulation in parallel with laboratory and pilot-plant experiments. The software features an efficient thermodynamic package and relies on proven and efficient numerical methods. Hall 9.1, Stand E66a — *ProSim, Toulouse, France*
www.prosim.net

Note: For more information, circle the 3-digit number on p. 76, or use the website designation.

Save man-hours with this electrical-design software

This completely new Electrical software application is said to be a feature-rich design solution for electrical engineers and designers in the plant environment. Pre-released customer testing has demonstrated man-hour savings of up to 30% when compared to traditional design applications, says the company. It is quick and easy to deploy, and has a very open interface, allowing it to be used with design applications from other vendors or as part of this company's Integrated Engineering & Design approach. Electrical can be used on both new projects, as well as on brownfield activities where the integration legacy data is critical. Hall 9.2, Stand C29 — *Aveva, Solutions Ltd., Cambridge, U.K*
www.aveva.com

A new version of a smart plant design and modeling solution

Last month, this company launched CADWorx Plant Professional 2013, the newest version of its AutoCAD-based intelligent 3D plant design and modeling solution. The software features a powerful new pipe routing engine in which the piping components operate as a single system. This allows a plant designer to move, resize and change the specification as a single line without the need to modify each component individually. Another new feature is the Assembly View Pallette. The assembly builder lets the designer build and save a complete assembly of a piping system that can be reused in the future parametrically, thereby boosting the efficiency of the design by allowing for common assemblies used throughout a project to be designed, developed and modeled once, then reused quickly in different areas of the plant system. Hall 9.2, Stand D28— *Intergraph Corp., Huntsville, Ala.*
www.intergraph.com

This release enables more users to perform simulations

The new release of Aspen Plus software, launched in March, is said to significantly improve the user experience in process simulation. The completely redesigned user interface and workflow improve engineering productivity and enable the use of process simulation to a wider range of new users, says the company. Users can now experience a fully integrated simulation environment to easily access other aspenONE Engineering products. This enables easy and intuitive access to the comprehensive physical-properties database, the capital-cost estimating product and the "most-complete" heat exchanger thermal and mechanical design products, says the company. Process engineers can also jump-start projects and optimize operations by efficiently finding and accessing models and data throughout the Aspen Search tool. — *Aspen Technology, Inc., Burlington, Mass.*
www.aspentech.com

Circle 33 on p. 76 or go to adlinks.che.com/40268-33

A tool to test for HART compliance

In April, the new enhanced HART DDL/EDDL (electronic device description language) Host Test Suite v2.0 was released. The test suite is used by suppliers and developers of host products to test compliance of their HART implementation and is used by this foundation to verify and validate compliance of host products submitted for HART registration. The new Suite v.2.0 includes: improved Encoded Test DDs updated to align with the current Test Specifications; test report spreadsheets for documenting test results; new and improved Xmtr-MV v2.5; and other ancillary files needed to facilitate HART DDL/EDDL host testing. Hall 11.V, Stand B29 — *HART Communication Foundation, Austin, Tex.*
www.hartcomm.org

Save energy at data centers and more with this suite

In December, this company introduced its Decathlon suite including software, hardware and services for data centers to provide a single view of IT, facilities and energy management information for improved data access and use, while making data centers themselves more reliable and energy efficient. Decathlon is said to enable better control and proactive maintenance of data center operations, with access to information from multiple systems, and provides potential energy savings of 10 to 50%. Decathlon provides realtime equipment health status to ensure reliability and proactive maintenance. It also transforms energy consumption data into valuable information so that data center operators can optimize power use while maintaining high levels of productivity and reliability. Hall 11.1, Stand A61 — *ABB Warminster, Pa.*
www.abb.com

A tool to help design heat-trace systems

Released at the end of last year, TraceCalc Pro version 2.5 is an industrial heat-trace-system design software that provides users with a step-by-step process to design an effective and efficient heat-trace system for pipes and vessels. Users can input their heat-trace design parameters (such as pipe size and material, insulation type and thickness, service voltage, maximum exposure temperature, pipe length, the number and size of valves and more) into TraceCalc Pro. The software then provides the information needed to complete the heat-trace-system design process, such as the amount of heat loss from the pipe, types of heat-trace products required, number of circuits used, and electrical and thermal performance of the system. — *Tyco Thermal Controls, Houston, Tex.*
www.tycothermal.com ■

Gerald Ondrey

ACHEMA 2012

Show Preview

Funke Wärmeaustauscher Apparatebau

Zeppelin Systems

Kreisel Umwelttechnik

List

The benefits of solvent-free processing

Dry processing — processing in the concentrated phase, with minimal or zero use of solvents — is efficient, economical, and ecological, according to this company. Applications in polymer processing include polymerization and direct devolatilization. Operating at viscosities up to 100,000 Pas, the firm's Kneader Reactor process technology (photo) ensures consistently high product quality and eliminates or at least significantly reduces costs of solvents and recycling. The result is a technology offering a high degree of process flexibility and lower total cost of ownership. Excellent mixing behavior, low shear rates and plug flow contribute to a wide operational window and consistent product quality, even at high capacities. The closed system ensures environmentally friendly operation, with residual monomer contents below 10 ppm. Hall 5.1, Stand D92 — *List AG, Arisdorf, Switzerland*
www.list.ch

Reliable feeding and discharge under extreme conditions

The Rotary Feeder CFH 630 (photo) has been designed to ensure reliable feeding and discharge of product, even at pressures and temperatures of 6 bars and 200°C. The feeder housing is sealed from the process while material is conveyed at rates of up to 100 ton/h. Normally, high temperatures and pressures cause different expansion and deformation of the rotor and the housing. To compensate for these factors, the CFH 630 housing is heated by an integrated temperature control system, which helps to minimize the gap and thus the air leakage. Hall 6.0, Stand A52 — *Zeppelin Systems GmbH, Friedrichshafen, Germany*
www.zeppelin-systems.com

Dry sludges and pastes two ways with one unit

The Combi Fluidization Technology (CFT) combines contact and fluidized-bed (FB) drying, and is especially suitable for the treatment of sludges and pastes. The FB in this horizontal dryer is produced mechanically by a rotating paddle system. For processes under atmospheric pressure, steam can be applied as an additional heat-transfer medium and also serve as inertization. In the CFT dryer, the wet product is immediately encapsulated by the dry product, is evenly distributed throughout the dry product and is dried efficiently. By encapsulating the wet feed, sticky phases or forming crusts on the wall are largely avoided. Hall 4.0, Stand B24 — *Buss-SMS-Canzler GmbH, Butzbach, Germany*
www.sms-vt.com

A wear-resistant rotary valve for abrasive bulk solids

This company has developed a hygienically pure and safe conveyor system for metering and transporting bulk materials. Capable of transporting more than 100 ton/h over distances of over 1 km, every system is energy-optimized and adapted to the user's requirements. Also being exhibited are the wear-resistant rotary valves (photo), which deliver high-performance and high throughput, and are said to increase service life by a factor of 10 to 20 compared to steel valves (depending on the material being conveyed). — Hall 6.0, Stand B82 — *Kreisel Umwelttechnik GmbH & Co. KG, Krauschwitz, Germany*
www.kreisel.eu

Tube-in-tube design augments safety in these heat exchangers

In addition to plate heat exchangers in bolted, brazed, semi- and fully-welded designs, this company will exhibit several products from the shell-and-tube heat-exchanger design. A highlight is the refined safety of the SWP shell-and-tube exchanger (photo), which is based on a tube-in-tube combination that creates a safety space and prevents the operating media from mixing. Also at Achema will be two special types of plate heat exchangers: the FPG, with two plates welded together into a cassette; and the FPDW, with the two plates welded together at the potring to form a leakage space between the plates. Hall 4.0, Stand G24 — *Funke Wärmeaustauscher Apparatebau GmbH, Gronau / Leine, Germany*
www.funke.de

Note: For more information, circle the 3-digit number on p. 76, or use the website designation.

Show Preview

Phoenix Contact

Thermo Fisher Scientific

Rembe

Vega Grieshaber

Distributed signals with a single turn in the field

The new Radioline wireless system (photo) is designed for wireless signal transmission at large facilities. input/output (I/O) mapping is one feature that distributes signals from up to 250 stations within the system without any software. Input signals receive I/O addresses via thumb wheels, with these addresses being mapped to corresponding output modules. Because identical signals can be outputted several times, it is possible to set up smart distribution and signal multiplication in the field. Hall 11.1, Stand A27 — *Phoenix Contact GmbH & Co. KG, Blomberg, Germany*
www.phoenixcontact.com

Perform multiple spectroscopies with a single touch

The Nicolet iS50 FTIR (Fourier transform infrared) spectrometer (photo) is said to be the first research-grade FTIR with one-touch operation. The device features integrated Raman for an accessible and cost-effective compliment to IR characterization, dedicated NIR (near infrared) designed to assist development of quality control methods for bulk samples and touch points for collecting, analyzing and reporting results with one-touch simplicity. Users can initiate attenuated total reflection (ATR), Raman and NIR modules at the touch of a button, enabling access to these techniques without manually changing system components. Hall 4.2, Stand B7 — *Thermo Fisher Scientific, Dreieich, Germany*
www.thermoscientific.com

Moving-object simulations improved with this new version

This company recently released STAR-CCM+ v7.02, a new version of its multidisciplinary engineering simulation solution. The release features a new Overset Mesh capability that allows users to generate an individual mesh around each moving object, which can then be moved at will over a background mesh. The Overset Mesh capability is fully compatible with the full range of unstructured mesh options in STAR-CCM+. With no need to worry about interconnecting meshes or cell distortion, Overset Mesh brings genuine moving object simulation within the grasp of all engineers, says the company. Hall 9.2, Stand C10 — *CD-adapco, London, U.K.*
www.cd-adapco.com

A level detector for hard-to-reach areas

The microwave barrier VegaMIP R62 (photo) is a non-contact sensor that can detect the limit level of solids and liquids in poorly accessible locations. Designed to meet the demands of the bulk solids industry, the device can detect the limit level under adverse environmental conditions, such as dust, fog or high temperatures. It consists of a VegaMIP T61 transmitter and a receiver, which measures the attenuation of the received microwave signal and generates a switching signal. For hard-to-reach or dangerous areas, there is now the receiving unit R62 with remote control, which allows the control unit to be placed in a safe, accessible location. Hall 11.1, Stand C63 — *Vega Grieshaber KG, Schiltach, Germany*
www.vega.com

A rupture disc for pristine processing applications

One of the highlights at this company's stand is the new TC(R)-KUB reverse-acting bursting disc with Gylon gasket (photo), which utilizes the synergies from both the inspected and proven KUB Technology (reverse-acting bursting disc) and the high-tech development found in a Gylon Gasket. This new bursting disc can be installed in

any industrial or chemical area requiring absolute sterility and permeability, for example in the pharmaceutical, biotechnological and food-processing industries. Hall 9.1, Stand C26 — *Rembe GmnH, Brilon, Germany*
www.rembe.de

Many parameters are handled by a single transmitter

The new Signet 9900 SmartPro Transmitter (photo, p. 32D-2) features multi-parameter capabilities, flexible modularity and an auto-sensing, backlit display with "at-a-glance" visibility, even in dark conditions. The transmitter provides a single-channel interface for many different parameters, including flow, pH/ORP, conductivity/resistivity, pressure, temperature, level, salinity and other sensor types that output a 4–20-mA signal. This single-channel, multi-parameter capability and field-upgradable modularity allow users to increase their service level

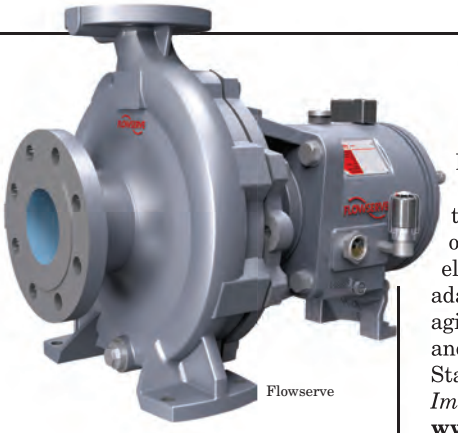

Flowserve

while maintaining reduced inventory levels, says the company. The 9900 is available in both panel or field-mount versions. Hall 8.0, Stand E64 — *Georg Fischer Piping Systems Ltd., Schaffhausen, Switzerland*
www.piping.georgfischer.com

A top-mounted agitator with smart electronics

The new Type MU electric agitator combines efficient agitator technology with the advantages of modern electronics. The controllable agitator has been adapted for the dosing of tanks with volumes of 100 to 1,000 L. Four different modes of operation are provided by the electronics, and the speed can be adapted for different viscosities. The agitators are suitable for both batch and intermittent operation. Hall 8.0, Stand K63 — *sera ProDos GmbH, Immenhausen, Germany*
www.sera-web.com

This ANSI pump now has an ISO companion

An expanded range of this company's Durco Mark 3 ISO chemical-process pumps (photo) will be launched at Achema. The Durco Marc 3 ISO pump range is fully compliant with ISO 2858 (dimensional) and ISO 5199 (design) criteria, and is designed using state-of-the-art hydraulic and modeling software with knowledge gained from more than 30 years of experience with the company's ANSI/ASME B73.1

Müller

Durco Mark 3 ANSI pump. Both ANSI and ISO pump versions feature the IPS Beacon condition monitoring device — a data acquisition, logging and visual alert device that is designed to monitor vibration in addition to temperature. Constructed of stainless steel and mounted on top of the bearing housing, the IPS Beacon delivers early warning notification to users, allowing them to take proactive measures to extend bearing life and mechanical seal of the pump. Hall 8.0, Stand A64 — *Flowserve Corp., Irving, Tex.*
www.flowserve.com

This washing machine cleans drums in a few minutes

The Drum Washing Machine DCM (photo) cleans the inside and outside of 30–200-L drums, with a washing cycle of 5–10 min. Cleaning nozzles within the system can be connected directly to a facility's water loop (2 bars pressue, 35 L/min flowrate), and separate connections for inside and outside washing enables a reduction of water consumption. The units are constructed of stainless steel with EPDM seals. Hall 3.1, Stand A75 — *Müller GmbH, Rheinfelden, Germany*
www.mueller-gmbh.com

This established machine now bags even faster

The Haver Adams will be the centerpiece of this firm's exhibition. Since its launch six years ago, this packaging system, which uses the Form-Fill-Seal principle, has been improved to meet users' demands for speed and product variety. Today, products with poor flow properties and powder-type products with granular components and micro-granulates can be packed into compact, sealed, weather-tight bags at the rate of 2,000 bags per hour. The advantages of this kind of durable packaging include extended storage times in wind and weather, a guaranteed cleanliness along the entire supply chain and an improved price-to-benefit ratio, says the manufacturer. Hall 3.0, Stand F38 — *Haver & Boecker, Oelde, Germany*
www.haverboecker.com ■

Gerald Ondrey

CHEMICAL ENGINEERING
FACTS AT YOUR FINGERTIPS
Department Editor: Scott Jenkins

Spray Drying Parameters

Among the most widely used technologies in the chemical process industries (CPI), spray drying involves dispersing a liquid or slurry in a hot gas to produce a dry powder product. A wide range of pumpable solutions, suspensions and emulsions can be used as spray-drying feeds.

Spray drying allows processors to generate powders with precisely defined properties. By controlling process parameters — including the characteristics of the liquid feed, the method of atomization, the configuration of the dryer and others — chemical makers can control the shape, flow properties and porosity of the solid particles produced. Here, the major considerations of spray drying are outlined.

Atomization

Several methods for atomizing the liquid feed in a spray-drying system are available (Figure 1). For most atomization equipment, the liquid leaves the atomizing head as a thin liquid film. The film fragments upon leaving the atomizing head, and droplets form immediately, driven by the surface tension of the liquid. Because of this, droplet formation depends heavily on the rheological properties of the liquid and its interaction with the heated drying medium just outside the atomizing device.

Rotary. In centrifugal (rotary) atomization, the most common method used in spray dryers, a rotating disc or wheel breaks the liquid stream into droplets. A liquid mist is formed horizontally from the atomizer wheel. Centrifugal atomizers rotate in the range of 5,000 to 25,000 rpm. The size of the droplets produced is roughly inversely proportional to the peripheral speed of the wheel, or disc, which typically have diameters in the range of 5 to 50 cm. The use of variable-speed drives can make the control of the droplet size straightforward. The smallest rotary atomizers handle 1–10 kg/h of liquid feed in the laboratory, while the largest commercial units, driven by 1,000-kW motors, can handle more than 200 metric ton/h.

Nozzle. Atomization with a pressure nozzle involves pressurizing a liquid using a pump, and forcing it through the orifice or a nozzle. Typical orifice sizes are 0.5–3.0 mm, which limits the capacity of the nozzle to 750–1,000 kg/h of liquid feed, depending on pressure, viscosity and solids content of the feed. Larger pressure drops across the orifice produce smaller droplets, so to reduce particle size for a given feedrate, a smaller orifice and higher pump pressure must be provided to maintain the same mass flow. Although simple, the pressure nozzle is often difficult to maintain, especially in multiple-nozzle systems. Most of the difficulty results from plugging, as well as wear of the nozzle insert, which can change the characteristics of the nozzle.

Two-fluid pneumatic. In this type of atomization, the feed interacts with a second fluid (usually compressed air) through a two-fluid nozzle to accomplish the atomization. Particle size is controlled by adjusting the ratio of the compressed air to the feed. Two-fluid pneumatic atomization is used primarily in smaller drying systems.

Sonic atomization. For applications requiring fine droplets at low flowrates, sonic atomization can be used. In this technique, the feed liquid is passed over a surface that is vibrated at ultrasonic frequencies. It is employed in small-capacity dryers when a highly uniform particle-size distribution is required.

GEA Niro

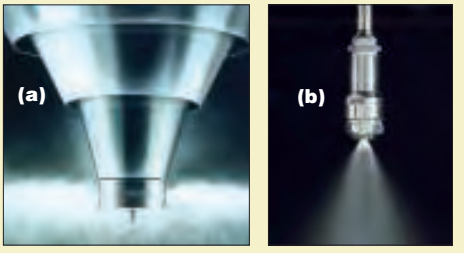

FIGURE 1. Rotary atomizers (a) produce a liquid mist horizontally from the atomizer wheel. Atomization by nozzle (b) often leads to a narrower particle-size distribution

FIGURE 7. This spray drying system is equipped with a heat recovery unit

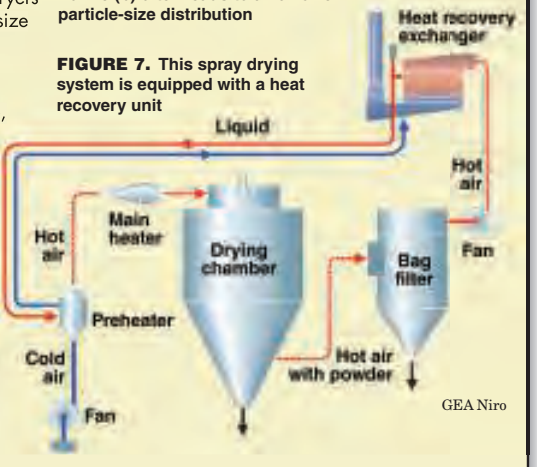

GEA Niro

Dryer configuration

To allow the liquid to evaporate, the flow patterns of the droplets and the gas through the dryer must provide enough contact time. Therefore, the size and geometry of the spray-drying chamber and gas disperser become important parameters. In many spray-drying systems, the atomizer is installed at the roof of a large-diameter drying chamber, and the heated gas is introduced through a roof-mounted air or gas disperser around the atomizer. This creates a co-current flow of gas and droplets and particles. The chamber's height must allow particles sufficient retention time to dry. Larger particle sizes require larger-diameter drying chambers.

The residence time should be selected based on the experience of the product's known drying characteristics and on the desired particle size. This allows direct calculations of the drying chamber volume.

Another configuration involves installing the pressure nozzle at the bottom of the chamber, so that the spray shoots upward from the bottom. This configuration is used in cases where the product is a coarse powder and the production rate is lower.

Collecting dried solids

Coarse powders are most easily collected directly from the bottom of the drying chamber. For fine powders, cyclones or bag filters become the primary collecting points. The particles must be separated from the drying media, which is cooler (due to evaporation) and more humid than before drying.

Gas flow

Heating the drying gas that flows through the spray dryer may be accomplished by direct combustion of natural gas, by indirect heating with shell-and-tube heat exchangers, or by electric heaters (used in small spray dryers). Most gas dispersers are configured with the help of computational fluid dynamics (CFD) analysis to define airflow patterns and temperature distributions within the drying chamber. For most applications, the gas disperser has adjustable guide vanes that allow for fine-tuning. Industrial radial fans are used to move the gas through the system. Sizing of system components can be based on gas flow.

Evaporation rate

Inside a spray dryer, the evaporation rate is directly proportional to the temperature difference from input to outlet multiplied by the mass flow. Values for the outlet temperature are usually determined experimentally, since they depend on the material's equilibrium isotherm, and true equilibrium is never actually reached. The inlet temperature is also determined experimentally, and should be as high as possible without risking product degradation.

Safety

In spray-drying operations, safety procedures related to dust explosions must be considered carefully, including determination of dust explosion pressure rise (K_{st}), the maximum dust explosion pressure (P_{max}), minimum ignition energy (MIE), minimum ignition temperature (MIT), and minimum auto-ignition temperature (MAIT).

Editor's note: The material in this "Facts at Your Fingertips" was adapted from the article cited here: . Moller, J.T. and Fredsted, S., A primer on spray drying. *Chem. Eng.*, November 2009, pp. 34–40.

Draining Vessels

Determine how long it will take for units with flat, cone- or dish-shaped bottoms

Edward H. Steve
Chemical Engineer

Throughout the chemical process industries (CPI), the need to drain a tank or process vessel arises. In batch-type plants, it is a regular occurrence and is one factor that affects the total cycle time per batch and ultimately the entire production capacity of the plant itself.

Some operations rely on draining a freely flowing Newtonian liquid from a process vessel to another vessel or to elsewhere without the assistance of a pump. This article develops the equations that a process engineer can use to easily estimate the time required for draining a vertical, cylindrical process vessel with a flat bottom, a cone bottom or an ASME F&D (dish) bottom. Unlike other articles on the subject [*1*], this one includes the effect of the connected drain line.

Using the equations and the examples in this article, the reader can construct an Excel spreadsheet for repeating the calculations to estimate the approximate drain times for a series of cylindrical, cone-bottom and dish-bottom tanks.

Tanks with other head styles and horizontal and non-cylindrically shaped tanks are not considered here. Meanwhile, this article does not deal with special fluids such as slurries or non-Newtonian liquids.

FLAT BOTTOM

Equation and its basis

Figure 1 shows the height of liquid (h) above the outlet nozzle of a vertical cylindrical flat-bottom tank during draining. The liquid is flowing into the outlet nozzle (point 1) located at x distance above the bottom of the tank and through a pipeline to some terminus (point 2). Equations in this article are based on the assumption that the size of the pipeline is the same size as the outlet nozzle and does not change between points 1 and 2. The pressures above the liquid in the tank and at the terminus are both Pt.

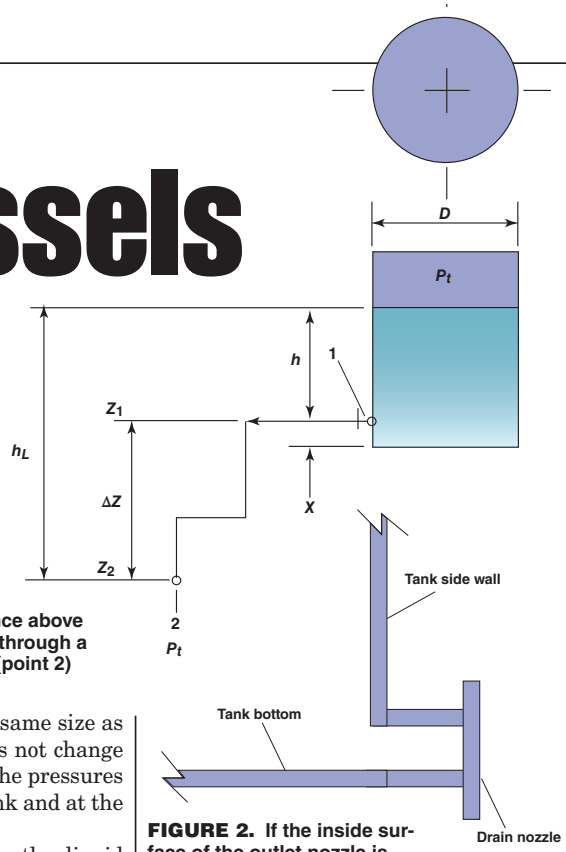

FIGURE 1. In a vertical cylindrical, flat-bottom tank, liquid is flowing into the outlet nozzle (point 1) located at x distance above the bottom of the tank and through a pipeline to some terminus (point 2)

FIGURE 2. If the inside surface of the outlet nozzle is aligned with the inside surface of the tank bottom as shown here, distance x is 0 and h_i incorporates the entire contents of the tank

Before draining begins, the liquid fills the tank to some initial height (h_i) above the outlet nozzle. If the inside surface of the outlet nozzle is aligned with the inside surface of the tank bottom as shown in Figure 2, distance x is zero and h_i incorporates the entire contents of the tank. As draining progresses, h decreases.

The Bernoulli Equation applies to the flow in the pipeline between points 1 and 2:

$$Z_1 + \frac{144P_1}{\rho_1} + \frac{v_1^2}{2g} = Z_2 + \frac{144P_2}{\rho_2} + \frac{v_2^2}{2g} + h_L \quad (1)$$

This article assumes isothermal flow, so the liquid density remains unchanged; because the pipeline size does not change, the velocities at points 1 and 2 are the same. Thus, Equation (1) can be rearranged as follows:

$$h_L = \Delta Z + [(144/\rho)(P_1 - P_2)] \quad (2)$$

The ΔZ term is the change in elevation of the discharge pipeline and is a fixed value.

Because $P_1 = P_t + (h\rho/144)$ and $P_2 = P_t$, Equation (2) becomes:

$$h_L = \Delta Z + h \quad (3)$$

Equation (3) indicates that the friction caused by flow in the pipeline between points 1 and 2 consumes the entire static pressure represented by $\Delta Z + h$. Note that h_L also decreases during draining because differentiating Equation (3) gives the following:

$$dh_L = dh \quad (4)$$

A basic material balance applies to developing the equation needed to predict the drain time for the tank:

In – Out = Accumulation

Because no liquid is being added to the tank, *In* = 0.

Out is the rate of liquid discharge from the outlet pipeline and is given by [*3*]:

$$Q = 19.65\, d^2\, (h_L/K)^{0.5} \quad (5)$$

Because h_L decreases during draining, Q decreases as well. Therefore, the Reynolds Number (NRe) in the pipeline also changes during draining.

The K in Equation (5) is the total resistance to flow and is the sum of four individual resistances:

$$K = K_{Entrance} + K_{Valves\&Fittings} + K_{Pipe} + K_{Exit} \quad (6)$$

The values for two of the resistances in Equation (6) are found in the litera-

AVERAGE PIPELINE FRICTION FACTOR

The upper plot in Figure 3 results when calculated values of friction factor [*8*] for 3-in., schedule-40 pipe with roughness 0.00015 are plotted as a function of NRe on arithmetic coordinates. The lowest value for NRe is 2,000. Note the sharp decrease in *f* at values much less than 500,000 NRe.

Inspection of the data shows that the value of *f* drops by approximately 0.002 between 100,000 and 300,000 NRe; it drops only 0.0005 between 300,000 and 500,000 NRe. Because the value of *f* at fully turbulent flow (f_T) is given as 0.018 [*9*], and the value is 0.0181 at 500,000 NRe, no significant reduction in *f* occurs at values greater than 500,000 NRe.

The lower plot in Figure 3 shows *f* as a function of NRe up to 500,000 NRe. The superimposed Excel Trendline indicates that the equation of the curve for that plot is $y = 0.1804x^{-0.1822}$. The fit of the Trendline is not perfect, but is sufficient for calculating an average *f*.

The average friction factor (f_{AVE}) can be calculated by determining the area under the plot and dividing by the included range of NRe. For the lower plot in Figure 3, the basic mathematics are:

$$f_{AVE} = \frac{\int_{NRe_1}^{NRe_2} 0.1804\,x^{-0.1822}}{NRe_2 - NRe_1} \qquad \text{(B1-1)}$$

Integrated and expanded with values for NRe gives:

$$f_{AVE} = \left[\frac{0.1804}{1-0.1822}\right]\frac{\left[500{,}000^{(1-0.1822)} - 2{,}000^{(1-0.1822)}\right]}{(500{,}000 - 2{,}000)} = 0.0201 \qquad \text{(B1-2)}$$

Plots like Figure 3 were constructed for schedule-40 pipe in sizes of 1, 1.5, 2, 3, 4, 6 and 8 in. After judging what should be the value for NRe_2 for each pipe size, f_{AVE} was calculated. Table 1 presents the f_{AVE} value as well as the range of NRe used and the plot equation for each pipe size; the friction factor at complete turbulence from the literature [*9*] is also indicated for reference. ❑

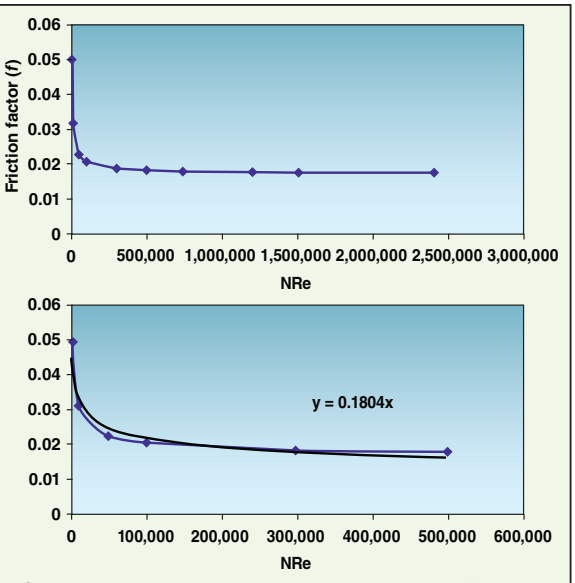

FIGURE 3. These plots show calculated values of friction factor (*f*) for 3-in. schedule-40 pipe with roughness 0.00015 plotted as a function of NRe. The top graph shows no significant reduction in *f* at >500,000 but a sharp decrease at values <<500,000. The bottom graph narrows in on NRe up to 500,000 and provides a suitable, fitted trendline equation for calculating an average *f*

ture [*4*] and are accepted as independent of NRe:

$K_{Exit} = 1$

For a sharp edged opening:

$K_{Entrance} = 0.5$

Values for other entrance conditions can be found in Ref. *4*.

However, values for the other two resistances (K_{Pipe} and $K_{Valves\&Fittings}$) must be found through some analysis.

In general, the resistance to flow through straight pipe is given by [*5*]:

$$K_{Pipe} = f\,(L_{pipe}/D_{pipe}) \qquad \textbf{(7)}$$

For a given length of pipe with a given inside diameter, the (L_{pipe}/D_{pipe}) ratio is constant no matter what the flow might be. The friction factor (*f*), however, is a function of NRe so K_{Pipe} is not constant as the flow decreases during drainage. A way to avoid iterative calculations is to use an average friction factor (f_{AVE}) in Equation (7) to calculate K_{Pipe}. The box, Average pipeline friction factor (above) discusses that approach to calculating f_{AVE} and Table 1 lists the results for various sizes of schedule 40 pipe.

The literature reports [*6*, *7*] that a three-constant (3-K) method should be used to calculate the resistances to flow through valves and fittings because they vary with NRe. Because the flow changes during draining, average values can also be used when determining $K_{Valves\&Fittings}$. The box, Average resistance to flow in valves and fittings (p. 37), discusses an approach to calculating these averages, and Table 2 lists the results for various sizes of several types of valves and fittings that could be part of a drain line.

TABLE 1. AVERAGE FRICTION FACTOR FOR SCHEDULE 40 PIPE (ROUGHNESS ε = 0.00015)

Pipe size, in.	NRe_1	NRe_2	*f* vs. NRe plot equation	f_{AVE}	f_T
1	2,000	500,000	$y = 0.1323x^{-0.1411}$	0.0241	0.023
1.5	2,000	300,000	$y = 0.1722x^{-0.1764}$	0.023	0.021
2	2,000	300,000	$y = 0.1903x^{-0.1858}$	0.0222	0.019
3	2,000	500,000	$y = 0.1804x^{-0.1822}$	0.0201	0.018
4	2,000	500,000	$y = 0.1933x^{-0.1908}$	0.0194	0.017
6	2,000	740,000	$y = 0.1904x^{-0.1908}$	0.0178	0.015
8	2,000	1,200,000	$y = 0.1815x^{-0.1869}$	0.0163	0.014

Obviously, *K* can then be calculated for the variable flow in the drain line by summing the values of the four individual resistances according to Equation (6).

Returning to the basic material balance, *Accumulation* is the rate of volume reduction in the tank. The volume (gallons) in the tank above the outlet nozzle at any time is given by:

$$V_{CY} = 7.48(\pi D^2 h)/4 \qquad \textbf{(8)}$$

The volume decreases with time according to the first derivative of Equation (8):

$$\frac{dV_{CY}}{d\theta_f} = 7.48\frac{\pi D^2}{4}\frac{dh}{d\theta_f} \qquad \textbf{(9)}$$

Substituting Equation (4) into Equation (9) gives the following:

$$\frac{dV_{CY}}{d\theta_f} = 7.48\frac{\pi D^2}{4}\frac{dh_L}{d\theta_f} \qquad \textbf{(10)}$$

Putting the pieces of the basic material balance together yields the mathematical version with flow units of gal/min:

$$0 - 19.65d^2\sqrt{\frac{h_L}{K}} = 7.48\frac{\pi D^2}{4}\frac{dh_L}{d\theta_f} \qquad \textbf{(11)}$$

Equation (11) can be re-arranged into a form that can easily be integrated:

$$d\theta_f = \frac{7.48\pi D^2\sqrt{K}}{-19.65(4)d^2}\frac{dh_L}{\sqrt{h_L}} \qquad \textbf{(12)}$$

Using the following model:

TABLE 2. AVERAGE RESISTANCE TO FLOW IN VALVES AND FITTINGS

Item	D_n, in.	K_i	K_d	$K_i(1+K_d/D_n^{0.3})$	K_1	NRe_1	NRe_2	K_1/NRe ave	K_f ave	K_f [10]
Tee, flow-through (flanged)	1	0.05	4	0.2500	150	2,000	300,000	0.0025	0.2525	0.460
	1.5	0.05	4	0.2476	150	2,000	300,000	0.0025	0.2501	0.420
	2	0.05	4	0.2459	150	2,000	300,000	0.0025	0.2484	0.380
	3	0.05	4	0.2435	150	2,000	300,000	0.0025	0.2460	0.360
	4	0.05	4	0.2419	150	2,000	300,000	0.0025	0.2444	0.340
	6	0.05	4	0.2395	150	2,000	300,000	0.0025	0.2421	0.300
	8	0.05	4	0.2379	150	2,000	300,000	0.0025	0.2404	0.280
90-deg. elbow (flanged)	1	0.091	4	0.4550	800	2,000	1,200,000	0.0043	0.4593	0.690
	1.5	0.091	4	0.4506	800	2,000	1,200,000	0.0043	0.4549	0.630
	2	0.091	4	0.4475	800	2,000	1,200,000	0.0043	0.4518	0.570
	3	0.091	4	0.4432	800	2,000	1,200,000	0.0043	0.4475	0.540
	4	0.091	4	0.4402	800	2,000	1,200,000	0.0043	0.4444	0.510
	6	0.091	4	0.4360	800	2,000	1,200,000	0.0043	0.4402	0.450
	8	0.091	4	0.4330	800	2,000	1,200,000	0.0043	0.4373	0.420
45-deg. elbow (threaded, standard)	1	0.071	4.2	0.3692	500	2,000	1,200,000	0.0027	0.3719	0.368
	1.5	0.071	4.2	0.3656	500	2,000	1,200,000	0.0027	0.3683	0.336
	2	0.071	4.2	0.3631	500	2,000	1,200,000	0.0027	0.3657	0.304
	3	0.071	4.2	0.3595	500	2,000	1,200,000	0.0027	0.3622	0.288
	4	0.071	4.2	0.3571	500	2,000	1,200,000	0.0027	0.3597	0.272
	6	0.071	4.2	0.3536	500	2,000	1,200,000	0.0027	0.3563	0.240
	8	0.071	4.2	0.3512	500	2,000	1,200,000	0.0027	0.3538	0.224
Gate valve (standard)	1	0.037	3.9	0.1813	300	2,000	740,000	0.0024	0.1837	0.184
	1.5	0.037	3.9	0.1796	300	2,000	740,000	0.0024	0.1820	0.168
	2	0.037	3.9	0.1783	300	2,000	740,000	0.0024	0.1807	0.152
	3	0.037	3.9	0.1766	300	2,000	740,000	0.0024	0.1790	0.144
	4	0.037	3.9	0.1754	300	2,000	740,000	0.0024	0.1778	0.136
	6	0.037	3.9	0.1737	300	2,000	740,000	0.0024	0.1762	0.120
	8	0.037	3.9	0.1726	300	2,000	740,000	0.0024	0.1750	0.112
Ball valve (standard)	1	0.017	4	0.0850	300	2,000	740,000	0.0024	0.0874	0.069
	1.5	0.017	4	0.0842	300	2,000	740,000	0.0024	0.0866	0.063
	2	0.017	4	0.0836	300	2,000	740,000	0.0024	0.0860	0.057
	3	0.017	4	0.0828	300	2,000	740,000	0.0024	0.0852	0.054
	4	0.017	4	0.0822	300	2,000	740,000	0.0024	0.0846	0.051
	6	0.017	4	0.0814	300	2,000	740,000	0.0024	0.0838	0.045
	8	0.017	4	0.0809	300	2,000	740,000	0.0024	0.0833	0.042

$$\int \frac{dx}{\sqrt{x}} = 2\sqrt{x} \qquad \textbf{(12A)}$$

And integrating between the initial and the final values yields:

$$\theta_f = \frac{7.48\pi D^2\sqrt{K}}{-19.65(4)d^2}\left[2\left(\sqrt{h_{L2}}-\sqrt{h_{L1}}\right)\right] \qquad \textbf{(13)}$$

Drain-time equation for a vertical, cylindrical tank with a flat bottom. Clearing the minus sign and combining the constants gives the equation for the drain time from a vertical cylindrical tank with a flat bottom (in minutes):

$$\theta_f = \frac{0.5979D^2\sqrt{K}}{d^2}\left[\left(\sqrt{h_1}-\sqrt{h_2}\right)\right] \qquad \textbf{(14)}$$

For a flat bottom tank, note that:

$$h_{L1} = \Delta Z + h_i \qquad \textbf{(14A)}$$

$$h_{L2} = \Delta Z \qquad \textbf{(14B)}$$

Example calculation

As an example, consider a 2,000-gal, vertical flat-bottom cylindrical vessel with a 7-ft inside diameter (D) that initially contains 1,000 gal of liquid. The outlet nozzle is 2-in., schedule 40 (d = 2.067 in.), located as illustrated in Figure 2. A 2-in. gate valve is mounted on the nozzle; the drain line contains 20 ft of 2-in., schedule-40 pipe and three 90-deg. elbows, and the change in elevation (ΔZ) is 3 ft (pipe length is included in the 20 ft). The draining time is found with the following steps:

Step A. Because h_i incorporates the entire contents of the tank, Equation (8) is re-arranged to solve for the value of h_i:

$h_i = (4V_{CY}) / (7.48\pi D^2) = 3.47$ ft

Step B. For the 20 ft of 2-in. pipe, L_{Pipe}/D_{Pipe} is 20/0.17225 or 116.1. When multiplied by the appropriate f_{AVE} from Table 1 (0.0222), K_{Pipe} is 2.577.

Step C. Using Table 2, $K_{GATE\ VALVE}$ is 0.1807 and $K_{90DEG\text{-}ELBOW}$ is 0.4518; the value for $K_{VALVES\ \&\ FITTINGS}$ is, therefore, (0.1807 + 3 × 0.4518) or 1.5361.

Step D. Summing up yields the following K portion:

K = 0.5 + 1.5361 + 2.577 + 1
= 5.6131

$K^{1/2}$ = 2.369

Step E. From Equation (14A):

$h_{L1} = \Delta Z + h_i$
= 3 + 3.47
= 6.47 ft

$h_{L1}^{1/2}$ = 2.5436

Step F. From Equation (14B):

$h_{L2} = \Delta Z$
= 3 ft

$h_{L2}^{1/2}$ = 1.732

Step G. Using Equation (14), the estimated drain time is 13.2 min.

Note that when the bottom of the cylindrical tank is not flat, the derivation of the drain time equation becomes more complicated.

AVERAGE RESISTANCE TO FLOW IN VALVES AND FITTINGS

The literature reports [6, 7] that the resistance to flow in a valve or a fitting should not be considered constant as had been previously reported [5] but should be considered to vary with Reynolds Number (NRe) according to [7]:

$$K_f = (K_1/\text{NRe}) + K_i\,[1 + (K_d/D_n^{0.3})] \quad \text{(B2-1)}$$

There is a set of three constants K_1, K_i and K_d for each specific valve or fitting. The table in Ref. 7 should be the source of the values because the constants have been updated from those given in Ref. 6.

Note that (K_1/NRe) is variable; the $K_i\,[1 + (K_d/D_n^{0.3})]$ term is constant for any given pipe size. As the influence of the variable part becomes small (approaches zero), K_f becomes equal to the constant. An average value for K_f can be calculated by adding an average value of the variable part of the equation to the constant part.

The first plot in Figure 4 shows calculated values of K_f for various sizes of a flow-through-tee, plotted as a function of NRe on arithmetic coordinates. The lowest value for NRe is 2,000 while the largest value is the estimated beginning of fully turbulent flow from a Moody chart [5]. Note the sharp decrease in K_f for all sizes at low NRe due to the variable part of the equation becoming less significant.

Inspection of the (K_1/NRe) data for the flow-through-tee shows that the value decreases by 0.0015 between 50,000 and 100,000 NRe; it drops 0.001 between 100,000 and 300,000 NRe and 0.0003 between 300,000 and 740,000 NRe. Based on those differential data, no significant reduction occurs above 300,000 NRe.

The lower plot in Figure 4 shows K_1/NRe for the flow-through-tee as a function of NRe up to 300,000 NRe; K_1 is 150. The superimposed Excel trendline confirms that the equation of the curve is $y = 150x^{-1}$.

The average value of K_1/NRe can be calculated by determining the area under the plot and dividing by the included range of NRe. For the lower plot in Figure 4, the basic mathematics are:

$$\left(\frac{K_1}{\text{NRe}}\right)_{AVE} = \frac{\int_{\text{NRe}_1}^{\text{NRe}_2} 150x^{-1}}{\text{NRe}_2 - \text{NRe}_1} \quad \text{(B2-2)}$$

Integrating and expanding with values for NRe gives:

$$(K_1/\text{NRe})_{ave} = \frac{[150\,(\ln 300{,}000 - \ln 2{,}000)\,]}{(300{,}000 - 2{,}000)} = 0.0025 \quad \text{(B2-3)}$$

Note that this average value applies to all pipe sizes because K_1 is related to the type of fitting or valve, not to the size.

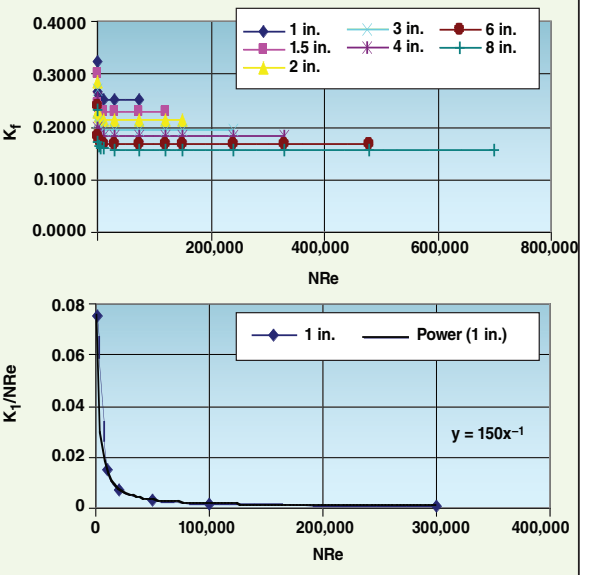

FIGURE 4. Resistance to flow in a flow-through tee (K_f, first graph) decreases sharply for all sizes at low NRe because the variable part of the equation (K_f/NRe, second graph) becomes less significant

The average value of K_f for any size flow-through tee is then $(K_1/\text{NRe})_{ave}$ plus the constant related to that size.

After judging what should be the value for NRe_2 for each fitting and valve, $(K_1/\text{NRe})_{ave}$ was calculated for a flow-through tee, 90- and 45-deg. elbows, and a gate and a ball valve. After calculating the constant part of Equation (B2-1), the average value for K_f was easy to determine.

Table 2 presents the applicable constants, the range of NRe used and the average K_f value for each pipe size of the various fittings and valves listed; the constant K_f value from the literature [10] is also indicated for reference. ❑

CONE BOTTOM

Figures 5 and 6 depict a vertical process vessel comprised of an upper right circular cylinder and a lower circular right cone. This article assumes that there is a liquid level in the upper portion, as shown, before draining begins.

While liquid is still in the upper part during draining, the liquid fills the cylinder to some height (h) and the entire cone to height h_C; the height of liquid above the outlet nozzle located at the bottom of the cone is $(h + h_C)$.

Liquid drains from the outlet nozzle (point 1) to some terminus (point 2) as discussed above. The reader can reason that $h_L = \Delta Z + h + h_C$ and that Equation (4) is still valid for the cylinder.

During draining, the height of liquid in the cylinder decreases, and the liquid surface descends into the cone; then both the cross-sectional area and the height of the liquid in the cone decrease.

Because the geometries of a cylinder and a cone are different, so are the individual drain times. The total drain time for the tank, therefore, is the sum of the times required to drain both portions. Each time must be calculated separately.

Cylindrical portion. For draining the cylindrical portion, Equation (14) applies because the geometry is identical to a flat bottom tank. But, the initial and final values for h_{L1} and h_{L2} must be defined carefully:

$$h_{L1} = h_i + h_C + \Delta Z \quad \textbf{(14C)}$$

$$h_{L2} = h_C + \Delta Z \quad \textbf{(14D)}$$

Because the value for h_i is related only to the volume of the liquid in the cylindrical portion, the volume in the cone must be subtracted from the total volume in the tank before calculating h_i with Equation (15).

Cone portion. Figure 5 depicts the cone bottom only. Note that the following discussion can be adapted to a cone tank by itself, if appropriate.

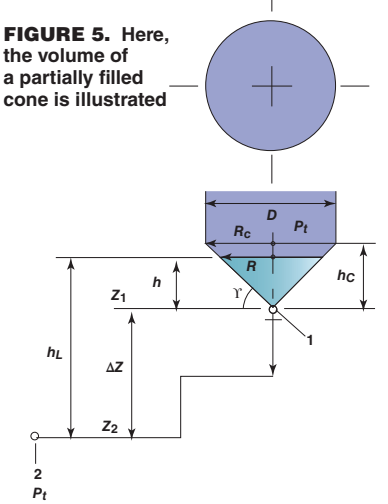

FIGURE 5. Here, the volume of a partially filled cone is illustrated

The volume of liquid (gallons) contained in the circular right cone shown in Figure 5 is given by the following:

NOMENCLATURE

a	radius of a spherical sector, ft	h_L	loss of static pressure due to fluid friction, ft	P_2	pressure at outlet of drain pipeline, psi	V_{CY}	liquid volume in a cylindrical tank, gal
d	inside diameter of outlet nozzle and drain pipeline, in.	h_{L1}	initial loss of static pressure due to fluid flow, ft	P_t	pressure above liquid in tank and at outlet of drain pipeline, psi	x	height of outlet nozzle above flat bottom, ft
D	inside diameter of tank, ft	h_{L2}	final loss of static pressure due to fluid flow, ft	Q	rate of liquid discharge, gal/min	Z_1	elevation of outlet nozzle, ft
D_n	nominal pipe size, in.	K	total resistance coefficient*	R_C	radius of a right circular cone, ft	Z_2	elevation of outlet of drain pipeline, ft
D_o	outside diameter of tank, ft	K_d	resistance coefficient in 3-K method related to diameter of valve or fitting, in.$^{0.3}$	R_D	radius of spherical portion of an ASME F&D head, ft	ΔZ	change in elevation of drain pipeline, ft
D_{Pipe}	inside diameter of outlet pipeline, ft	K_f	resistance coefficient for valve or fitting*	R_S	radius of sphere used to describe spherical sector, ft	γ	cone angle, deg.
f	friction factor*	K_i	resistance coefficient in 3-K method related to type of valve or fitting*	v_1	fluid velocity at inlet of outlet nozzle, ft/s	θ	total time to drain a tank with a cone or a dish bottom, min
f_{AVE}	average friction factor*	K_1	resistance coefficient in 3-K method related to NRe*	v_2	fluid velocity at outlet of drain pipeline, ft/s	θ_c	time to drain a cone bottom, min
f_T	friction factor at fully developed turbulent flow*	L_{Pipe}	length of drain pipeline, ft	v_S	depth of a spherical sector, ft	θ_B	time to drain an ASME F&D (dish) bottom, min
g	acceleration due to gravity, ft/s^2	NRe	Reynolds number*	V_B	liquid volume in a dished head, gal	θ_f	time to drain a flat bottom tank or a cylinder, min
h	height of liquid, ft	P_1	pressure at inlet of outlet nozzle, psi	V_C	liquid volume in a cone, gal	ρ_1	density of liquid at inlet of outlet nozzle, lb/ft^3
h_B	depth of an ASME F&D head, ft					ρ_2	density of liquid at outlet of drain pipeline, lb/ft^3
h_C	height of liquid in a right circular cone, ft						
h_i	initial height of liquid in cylindrical portion of a tank, ft						

* Dimensionless

$$V_C = 7.48[(\pi R^2 h)/3] \quad \textbf{(16)}$$

Note that determining the radius of the liquid in the cone is a matter of trigonometry:

$$R = h/(\tan \gamma) \quad \textbf{(17)}$$

The value of angle γ is a function of the construction of the cone so it remains constant; Equation (17), therefore, correlates the height and radius of liquid in the cone during draining.

Liquid drains from the outlet nozzle (point 1) to some terminus (point 2) as discussed above. Again, the reader can reason that $h_L = \Delta Z + h$ and that Equation (4) is still valid for the cone.

Substituting Equation (17) into Equation (16) gives the following:

$$V_C = 7.48\pi h^3/[3(\tan \gamma)^2] \quad \textbf{(18)}$$

The rate of volume reduction in the cone during the draining process is given by the first derivative of Equation (18) with respect to time:

$$\frac{dV_C}{d\theta_c} = \frac{7.48\pi h^2}{(\tan\gamma)^2}\frac{dh}{d\theta_c} \quad \textbf{(19)}$$

But $h_L = \Delta Z + h$, so $h = h_L - \Delta Z$ and:

$$h^2 = h_L^2 - 2h_L\Delta Z + \Delta Z^2 \quad \textbf{(20)}$$

Substituting Equation (4) and Equation (20) into Equation (19) then gives:

$$\frac{dV_C}{d\theta_c} = \frac{7.48\pi\left(h_L^2 - 2h_L\Delta Z + \Delta Z^2\right)}{(\tan\gamma)^2}\frac{dh_L}{d\theta_c} \quad \textbf{(21)}$$

Putting together the pieces of the basic material balance for the cone gives the mathematical version with flow units of gal/min:

$$0 - 19.65d^2\sqrt{\frac{h_L}{K}} = \frac{7.48\pi\left(h_L^2 - 2h_L\Delta Z + \Delta Z^2\right)}{(\tan\gamma)^2}\frac{dh_L}{d\theta_c} \quad \textbf{(22)}$$

Equation (22) can be rearranged into a form that can easily be integrated:

$$d\theta_c = \frac{7.48\pi\sqrt{K}}{19.65d^2(\tan\gamma)^2} \bullet \left(h_L^{1.5} - 2h_L^{0.5}\Delta Z + \Delta Z^2 h_L^{-0.5}\right)dh_L \quad \textbf{(23)}$$

Equation for a cone-bottom. Integrating Equation (23) between h_{L1} and h_{L2}, clearing the minus sign, combining the constants and grouping items of like exponents gives the expression for the drain time from a cone bottom:

$$\theta_c = \frac{1.1959\sqrt{K}}{d^2(\tan\gamma)^2} \bullet \left[0.4\left(h_{L1}^{2.5} - h_{L2}^{2.5}\right) - 1.333\Delta Z \bullet \left(h_{L1}^{1.5} - h_{L2}^{1.5}\right) + 2\Delta Z^2\left(h_{L1}^{0.5} - h_{L2}^{0.5}\right)\right] \quad \textbf{(24)}$$

An example will show how the total drain time is calculated for a cone bottom tank.

Example calculation

The 2,000 gal, cone-bottom tank shown in Figure 6 contains 1,000 gal of liquid. The tank inside diameter is 7 ft (D), the height of the bottom cone is 3.5 ft (h_C) and the bottom nozzle is 2 in., schedule 40 (d = 2.067 in.). A 2-in. gate valve is mounted on the nozzle. The drain line contains 20 ft of 2-in. schedule-40 pipe and three 90-deg. elbows, and the change in elevation (ΔZ) is 3 ft (pipe length is included in the 20 ft). To determine the total drain time, the calculations are:

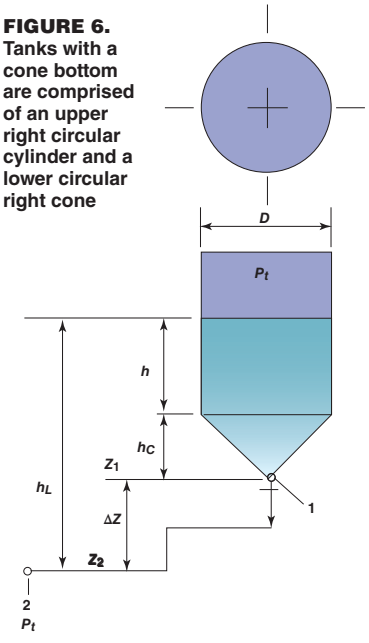

FIGURE 6. Tanks with a cone bottom are comprised of an upper right circular cylinder and a lower circular right cone

Step A. Using $R = R_C$ (which = $D/2$) and $h = h_C$ in Equation (16), the total volume in the cone bottom is 336 gal.

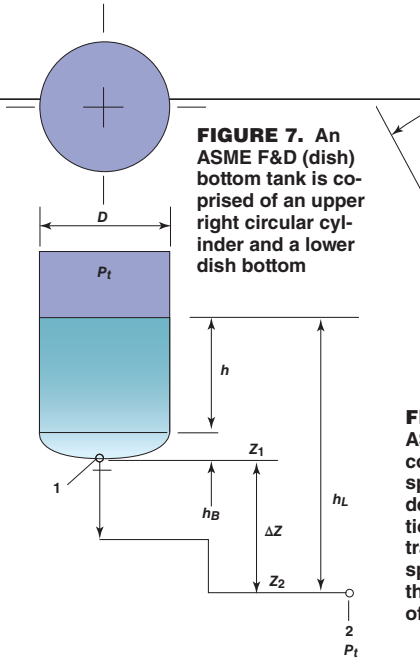

FIGURE 7. An ASME F&D (dish) bottom tank is comprised of an upper right circular cylinder and a lower dish bottom

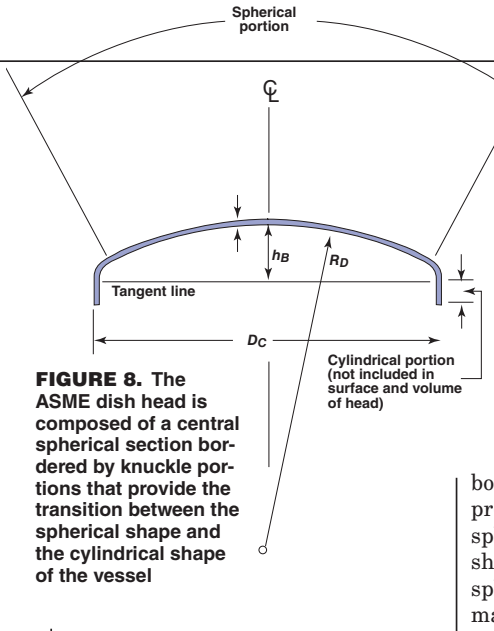

FIGURE 8. The ASME dish head is composed of a central spherical section bordered by knuckle portions that provide the transition between the spherical shape and the cylindrical shape of the vessel

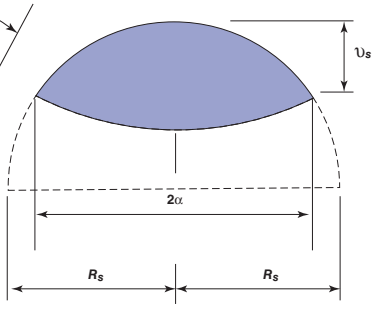

FIGURE 9. Here, the geometry of a spherical sector is illustrated

Step B. The initial volume in the cylindrical portion is 1,000 – 336 or 664 gal.

Step C. Using Equation (15):

h_i = 2.307 ft

Step D. The same K applies (as in the previous, flat-bottom tank example calculation)

$K^{1/2}$ = 2.3692.

Step E. For the cylinder:

1. $h_{L1} = h_i + h_C + \Delta Z$
   $= 2.307 + 3.5 + 3 = 8.807$ ft
   ${h_{L1}}^{1/2} = 2.5436$
2. $h_{L2} = h_C + \Delta Z$
   $= 3.5 + 3 = 6.5$ ft
   ${h_{L2}}^{1/2} = 2.5495$
3. Using Equation (14), $\theta_f = 6.8$ min

Step F. For the cone:

1. $\tan \gamma = h_C/R_C = 3.5/(7/2) = 1$
   $[(\tan \gamma)^2] = 1$
2. $h_{L1} = h_C + \Delta Z = 3.5 + 3 = 6.5$ ft
   ${h_{L1}}^{2.5} = 107.717$
   ${h_{L1}}^{1.5} = 16.572$
   ${h_{L1}}^{0.5} = 2.5495$
3. $h_{L2} = \Delta Z = 3$ ft
   ${h_{L2}}^{2.5} = 15.588$
   ${h_{L2}}^{1.5} = 5.196$
   ${h_{L2}}^{0.5} = 1.732$
4. Using Equation (24), $\theta_c = 4.03$ min

Step G. Total drain time for the entire tank is:

$\theta = \theta_f + \theta_c = 6.8 + 4.0 = 10.8$ min

Calculating the drain time for a process vessel with an ASME F&D (dish) bottom head requires a similar procedure, but the time for draining the bottom head requires a different mathematical expression.

ASME F&D (DISH) BOTTOM

Figure 7 depicts a vertical process vessel comprised of an upper right circular cylinder and a lower ASME F&D (dish) bottom. While liquid is still in the upper part during draining, the liquid fills the cylinder to some height (h) and the entire dish to height h_B; the height of liquid above the outlet nozzle is ($h + h_B$).

Liquid drains from the outlet nozzle (point 1) to some terminus (point 2) as discussed above. Once again, the reader can reason that $h_L = \Delta Z + h + h_B$ and that Equation (4) is still valid for the cylinder.

During draining, the height of liquid in the cylinder decreases, and the liquid surface descends into the dish; then both the cross-sectional area and the height of the liquid in the dish decrease.

Because the geometries of a cylinder and the dish are different, so are the individual drain times. The total drain time for the tank, therefore, is the sum of the times required to drain both portions. Each time must be calculated separately.

Cylindrical portion. For draining the cylindrical portion, Equation (14) applies because the geometry is identical to a flat bottom tank. But, the initial and final values for h_{L1} and h_{L2} must again be defined carefully:

$$h_{L1} = h_i + h_B + \Delta Z \quad \textbf{(14E)}$$

$$h_{L2} = h_B + \Delta Z \quad \textbf{(14F)}$$

Because the value for h_i is related only to the volume of the liquid in the cylindrical portion, the volume in the dish must be subtracted from the total volume in the tank before calculating h_i with Equation (15).

Dish portion. As Figure 8 (see Assuming dish is spherical, p. 40) shows, an ASME F&D head is composed of a central spherical section bordered by knuckle portions that provide the transition between the spherical shape and the cylindrical shape of the vessel; the radius of the spherical portion (R_D) is approximately equal to the inside diameter of the tank (D) and the depth of the dish to the tangent line (h_B) is approximately 0.169 D. Per the calculation in the box, Assuming dish is spherical (p. 40), modeling the entire head shape with a spherical sector introduces only a small error into the draining theory.

Using the basic Equation (B3-1) (see Assuming dish is spherical, p. 40) with $\upsilon_S = h$ and $R_S = D$, the volume of liquid (gal) contained in the partially filled dish shown in Figure 10 is given by:

$$V_B = 7.48[(\pi D h^2) - (\pi h^3/3)] \quad \textbf{(25)}$$

As with the other shapes, the rate of volume reduction in the dish during the draining process is given by the first derivative of Equation (25) with respect to time:

$$\frac{dV_B}{d\theta_B} = 7.48\left(2\pi Dh - \pi h^2\right)\frac{dh}{d\theta_B} \quad \textbf{(26)}$$

Liquid drains from the outlet nozzle (point 1) to some terminus (point 2) as discussed above. The reader can reason that $h_L = \Delta Z + h$ and that Equation (4) is still valid for the dish. Because $h_L = \Delta Z + h$, the following are true:

$$h = h_L - \Delta Z \quad \textbf{(27)}$$

$$h^2 = {h_L}^2 - 2h_L\Delta Z + \Delta Z^2 \quad \textbf{(28)}$$

Substituting Equation (4), Equation (27) and Equation (28) into Equation (26) then gives:

$$\frac{dV_B}{d\theta_B} = 7.48\left[\begin{matrix}2\pi D\left(h_L - \Delta Z\right) \\ -\pi\left({h_L}^2 - 2h_L\Delta Z + \Delta Z^2\right)\end{matrix}\right]\frac{dh_L}{d\theta_B} \quad \textbf{(29)}$$

Putting together the pieces of the basic material balance for the dish gives the

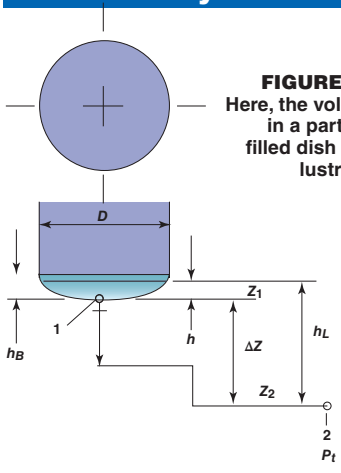

FIGURE 10. Here, the volume in a partially filled dish is illustrated

ASSUMING DISH IS SPHERICAL

As Figure 8 [*11*] shows, the shape of an ASME F&D (dish) head is spherical up to the extremities where knuckle portions make the transition from sphere to the cylindrical shape of the vessel shell. The radius of the spherical portion is the outside diameter of the tank [*12*]. To simplify the mathematics of draining with an error of less than 5%, the ASME F&D head can be considered a spherical segment as explained below.

The volume of the spherical segment with one base shown in Figure 9 is given by Equation (B3-1) [*13*]:

$$V_B = (\pi/3)\, v_S^2\, (3R_S - v_S) \quad \textbf{(B3-1)}$$

For an ASME F&D head, v_S is approximately $0.169D$ [*12*]; R_S can be approximated by the inside diameter of the tank because the thickness of the head is small by comparison. Substituting these values into Equation (B3-1) and solving for V_B gives:

$$V_B = 0.08467D^3, \text{ ft}^3 \quad \textbf{(B3-2)}$$

$$V_B = 0.6333D^3, \text{ gal} \quad \textbf{(B3-3)}$$

Because the actual volume (in gallons) in a dish head is approximately $0.606D^3$ [*12*], the error due to assuming that the head is a spherical sector is as follows:

$$\%\text{ERROR} = [(0.6333/0.606) - 1]100 = 4.51\% \quad \textbf{(B3-4)}$$ ❑

mathematical version with flow units of gal/min:

$$0 - 19.65d^2\sqrt{\frac{h_L}{K}} = 7.48\begin{bmatrix} 2\pi D(h_L - \Delta Z) \\ -\pi\left(h_L^{\,2} - 2h_L\Delta Z + \Delta Z^2\right) \end{bmatrix}\frac{dh_L}{d\theta_B} \quad \textbf{(30)}$$

Equation (30) can be re-arranged into a form that can easily be integrated:

$$d\theta_B = \frac{7.48\pi\sqrt{K}}{-19.65d^2} \bullet \begin{bmatrix} (2D + 2\Delta Z)h_L^{\,0.5} - h_L^{\,1.5} \\ -\left(2D\Delta Z + \Delta Z^2\right)h_L^{\,-0.5} \end{bmatrix} dh_L \quad \textbf{(31)}$$

Equation for a dish-bottom. Integrating Equation (31) between h_{L1} and h_{L2}, clearing the minus sign, combining the constants and grouping items of like exponents gives the expression for the drain time from a dish:

$$\theta_B = \left[\frac{1.1959\sqrt{K}}{d^2}\right] \bullet \begin{bmatrix} 1.333(D + \Delta Z)\left(h_{L1}^{\,1.5} - h_{L2}^{\,1.5}\right) \\ -0.4\left(h_{L1}^{\,2.5} - h_{L2}^{\,2.5}\right) \\ +2\left(2D\Delta Z + \Delta Z^2\right)\left(h_{L1}^{\,0.5} - h_{L2}^{\,0.5}\right) \end{bmatrix} \quad \textbf{(32)}$$

Example calculation

An example will show how the total drain time is calculated for a tank with a dish bottom.

The 2,000 gal dished bottom tank shown in Figure 7 contains 1,000 gal of liquid; the diameter is 7 ft (D) and the bottom nozzle is 2-in., schedule 40 (d = 2.067 in.). A 2-in. gate valve is mounted on the nozzle. The drain line contains 20 ft of 2-in., schedule-40 pipe and three 90-deg. elbows. The change in elevation (ΔZ) is 3 ft (pipe length is included in the 20 ft). The drain time is calculated by the following steps:

Step A. The total volume in the dish is $0.606D^3$ (see Assuming dish is spherical, above) or 208 gal.

Step B. The initial volume in the cylindrical portion is 1,000 – 208 or 792 gal.

Step C. Per Equation (15), h_i is 2.75 ft

Step D. $h_B = 0.169D$ = 1.183 ft

Step E. The same K applies (from the flat bottom tank); so $K^{1/2}$ = 2.3692

Step F. For the cylinder:

1. $h_{L1} = h_i + h_B + \Delta Z$
   = 2.75 + 1.183 + 3 = 6.933 ft
   $h_{L1}^{1/2}$ = 2.633 ft
2. $h_{L2} = h_B + \Delta Z$
   = 1.183 + 3 = 4.183 ft
   $h_{L2}^{1/2}$ = 2.045 ft
3. Using Equation (14), θ_f = 9.55 min

Step G. For the dish:

1. $h_{L1} = h_B + \Delta Z$
   = 1.183 + 3 = 4.183 ft
   $h_{L1}^{2.5}$ = 35.787 ft
   $h_{L1}^{1.5}$ = 8.555 ft
   $h_{L1}^{0.5}$ = 2.045
2. $h_{L2} = \Delta Z$ = 3 ft
   $h_{L2}^{2.5}$ = 15.588
   $h_{L2}^{1.5}$ = 5.196
   $h_{L2}^{0.5}$ = 1.732
3. Using Equation (32), θ_B = 3.16 min

Step H. Total drain time for the entire tank is:

$\theta = \theta_f + \theta_B$ = 9.55 + 3.16 = 12.7 min ■

Edited by Rebekkah Marshall

Acknowledgements

Thanks to Professor Ron Darby, of Texas A&M, for providing the table of 3-K constants from his book. Thanks also to Van Zhao, process engineer at IPS, for critically reviewing the manuscript.

Author

Edward H. Steve (esteve41@comcast.net) is a chemical engineer who works with companies on an as-needed basis. He has 46 years of design and operating experience in the chemical, chemical specialty, renewable energy, pharmaceutical chemical, pharmaceutical, electronics, consumer goods and biotechnology industries. He is the author of 17 other articles on unsteady state heat transfer in process vessels, fluid flow and solids storage. In addition to wide process engineering experience, Steve has management experience as COO, department head, team leader and production supervisor in large and small companies. He has a B.Ch.E. degree from Cornell University, is a registered professional engineer in Pennsylvania and New Jersey, is an emeritus member of AIChE and a member of Chemical Consultants Network (www.chemconsultants.org).

References

1. Foster, Thomas C., Time required to empty a vessel, *Chem. Eng.*, May 4, 1981, p. 105.
2. Crane Company, Flow of Fluids, Technical Paper 410, Stamford, CT, 1991, pp. 1–5.
3. op. cit., pp. 3–4.
4. op. cit., pp. A-29.
5. op. cit., pp. 2–8.
6. Darby, Ron, Correlate Pressure Drop through Fittings, *Chem. Eng.*, July 1999, pp. 101–104.
7. Darby, Ron, "Chemical Engineering Fluid Dynamics", 2nd Ed., Marcel Dekker, New York, 2001, Table 7-3, pp. 210–211.
8. Serghides, T.K., Estimate friction factor accurately, *Chem. Eng.*, Mar. 5, 1984, pp. 63–64.
9. Crane, op. cit., p. A-26.
10. Crane, op. cit., p. A-27ff.
11. Dimoplon, William, Jr., How to determine the geometry of pressure vessel heads, *Hydrocarbon Process.*, August 1974, adaptation of Figure 2, p. 71.
12. op. cit., p. 73.
13. Tuma, Jan J., "Engineering Mathematics Handbook", McGraw-Hill, New York, 1970, p. 30.

PowerDyne™

Pure Performance

For Steam Mains and Tracers

Long Service Life

- Air jacket eliminates inefficient cycling
- Tight sealing reduces wear

Energy Conservation

- Mirror-polished disc minimizes steam loss
- Hardened trim for reliable operation

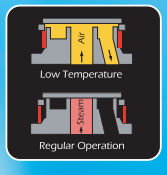

Increased Productivity

- Built-in air vent discharges initial air
- Automatic venting reduces start-up time

Easy Maintenance

- Replacement module for quick response
- Inline body reduces cost of ownership

Reduce Life Cycle Cost

Up to Supercritical — 3700 psig

TLV CORPORATION
13901 South Lakes Drive, Charlotte, NC 28273-6790
Phone: 704-597-9070 Fax: 704-583-1610
E-mail: tlv@tlvengineering.com
For Technical Service 1-800 "TLV TRAP"
http://www.tlv.com

Member of FCI Fluid Controls Institute, Inc. Technical Resources for Instrumentation and Fluid Control

Manufacturer
TLV CO., LTD.
Kakogawa, Japan
is approved by LRQA Ltd. to ISO 9001/14001

ISO 9001/ISO 14001

Circle 53 on p. 76 or go to adlinks.che.com/40268-53

Dynamic Modeling for Steam System Control

Dynamic modeling fills in the gaps of steady-state modeling and provides a more complete, reliable and efficient analysis

Ali Bourji, David Ballow and **Martha Choroszy**
WorleyParsons

One of the most energy-intensive utilities for many facilities in the chemical process industries (CPI) is the steam system. Traditionally, steam-use optimization has centered on efficient heat transfer and eliminating waste [*1*]. Further optimization can involve a broader look at how steam supply and consumption interact dynamically throughout a large complex. This type of optimization often results in increased interconnectivity and interdependency.

Many CPI facilities have a central steam-production area containing boilers and boiler feedwater treatment, as well as additional steam generators scattered throughout the facility (for example in the petroleum refining sector there are ethylene and catalytic cracking units). If a facility is built in several stages, as is often the case, steam generating systems may be separated by considerable distances. Over these distances, the stability of the integrated steam system could be jeopardized by inappropriate control strategies. How should one go about setting up a control strategy and verifying that it is stable and appropriate for a particular complex?

Steady-state modeling and steam balances only show the endpoints of system behavior. Dynamic modeling fills in the space between these endpoints providing a more complete analysis. With potentially billions of dollars in capital investment depending on a reliable supply of steam, employing dynamic modeling during the design development of integrated systems is worth the extra effort. This article breaks down the task of setting up a control strategy into four basic steps (Figure 1).

FUNDAMENTAL INVESTIGATIVE QUESTIONS

To understand a system's behavior, start by gathering as much information as possible. Ask fundamental questions, such as these:

1. What units are the big users?
2. What units are the big producers?
3. How does steam demand change for different operating scenarios?
4. Are there any equipment limitations?
5. What is the nameplate capacity of each major system component?
6. Are there limitations to achieving nameplate capacity?
7. Has the root cause of any limitation been determined?
8. In the case of commonly occurring upsets, do they have a pattern or connected event?

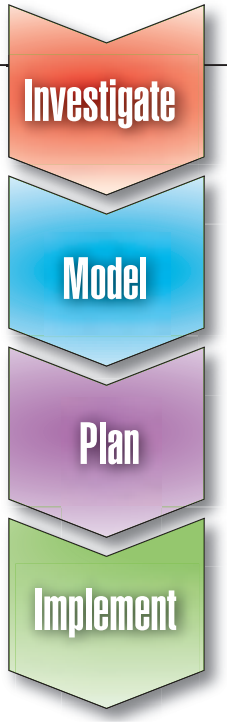

FIGURE 1. An effective control strategy can be broken down into four stages

Investigate

In order to properly control any system, a thorough understanding of the interactions within the system (the system behavior) is essential. Understanding system behavior begins with gathering as much information as possible about a given process or facility. Ask some fundamental questions, such as those outlined in the box above.

For an existing operational facility, there is no better resource to answer these questions than the senior operations staff. They have direct knowledge of how the system behaves in realtime during real upsets under real conditions. Defining these upsets will become an essential input to dynamic model development.

For new facilities, this investigative exercise may still prove valuable for the complex. It is still necessary to draw on the knowledge of experienced operators who have run similar systems in the past. Supplementing their knowledge and experience with the appropriate process engineering and modeling techniques will allow for sufficiently accurate system emulation.

Model

In the typical workflow of modern process design, a steady-state model is usually developed to facilitate the creation of utility balances and to study various operating cases. A wide array of modeling software has been developed [*2*] and is in use within the CPI. When choosing the platform for the steady-state model, keep in mind the potential for running the model dynamically.

Steady-state modeling is essential, but a plant will never truly achieve steady state. To achieve a reliable and stable steam supply throughout the complex, the fully integrated steam system must be analyzed in a dynamic state to understand the probable interactions between the system components. Operating facilities are

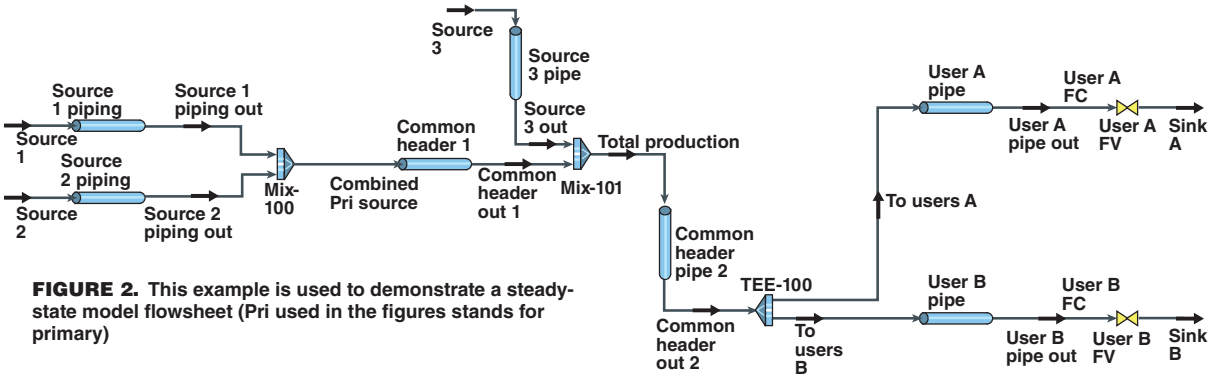

FIGURE 2. This example is used to demonstrate a steady-state model flowsheet (Pri used in the figures stands for primary)

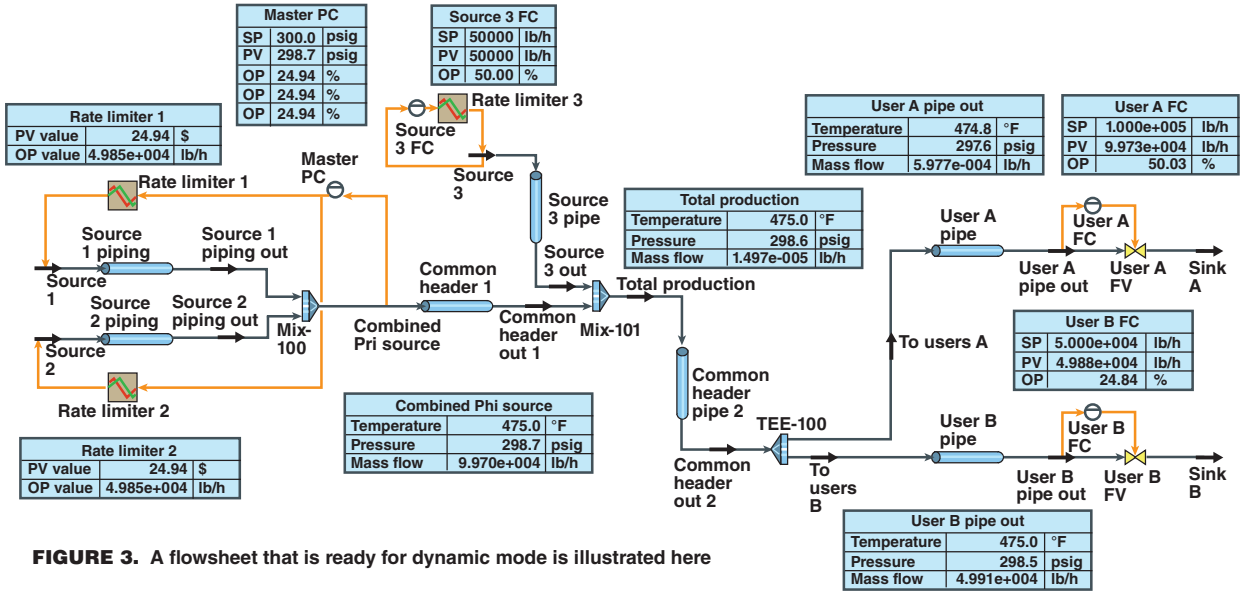

FIGURE 3. A flowsheet that is ready for dynamic mode is illustrated here

generally not able to risk a major shutdown in order to test system responses to the upsets of interest. The next best option is to model the system dynamically. The dynamic model becomes a testing platform on which control concepts can be proven and adjusted if necessary [3].

Dynamic process simulations fill the gap between different steady-state operating cases, showing a more complete picture of system behavior. Using the knowledge gained during the investigative process, a model can be constructed that will be useful for testing the system under changing conditions.

Example. Suppose the system to be modeled consisted of three sources and two users of steam. The steady-state model flowsheet may look like Figure 2. In this example system, two sources of steam exist on one end of a main steam header, while a third source sits close to the process user areas.

This same simulation flowsheet can be adapted for dynamic evaluation by adding some basic controls as shown in Figure 3.

Using this source-sink model of a steam distribution header, some of the aspects of the system behavior can be explored. The system may have two design cases that result in different steam balances. The steady-state model gives a snapshot of what is happening when everything is stable. Table 1 shows what these data may look like.

Switching to a dynamic analysis gives a more complete picture of the system behavior in the time between the two operating cases. At this point, the previous consultation with operators who understand the system comes into play. Using the knowledge gained from the operators, the design engineer must account for the time factors involved in transitioning from normal to alternate operation. For this example, users in Area B are reducing demand to reach the alternate operating mode. Through consultation with the operators, it becomes clear that this demand reduction normally takes place over a 2-min period. Figure 4 is a graph of what this may look like in a dynamic simulation.

Starting from a steady state corresponding to normal operation, the demand reduction begins at 120 seconds. The User B demand is ramped steadily downward for the prescribed two minutes. The source-steam flow controllers initiate a corresponding reduction in steam production to maintain the system balance. This production decrease is typically achieved through some type of master

pressure controller. The master pressure controller senses the steam distribution-header pressure and drives the steam producer to increase or decrease production to maintain the desired header pressure.

A major limiting factor in controlling steam header pressure is the response time of the steam generating source. These sources respond very slowly due to the mass of water and steel that must absorb and release energy to affect a change in the system flow. This thermal inertia can cause differing response times on flow increases and decreases at different capacities.

In this example, the Source 1 and 2 characteristics are such that their response is limited to a rate of 10% of total capacity per minute. Figure 5 shows a plot of the pressure at the main sensing point for Sources 1 and 2.

Again starting from steady state and introducing the disturbance at 120 seconds, the header pressure initially rises due to the slow response time of Sources 1 and 2. The sluggish nature of these steam sources also contributes to the overcompensation and severe drop in header pressure. The sources are eventually able to compensate for the change in steam demand, but a large oscillation has been experienced in the interim. These types of oscillations can cause process upsets throughout a large facility. Note that this example is for illustrative purposes only and some of this lag can be attenuated with careful tuning.

A validation step is essential to verify the model's ability to emulate the system behavior. Typically, a model review is performed involving key personnel from engineering and operations departments. The information gained during the investigative step regarding common upset events is particularly useful at this stage. Ideally, the model is put through a series of known scenarios, and the resulting predicted response is compared to the known response. Any required fine tuning can be implemented, and the model can be used for subsequent analysis with a reasonable degree of confidence. The model can also be used to predict system behavior under new conditions.

TABLE 1. STEADY-STATE RESULTS FOR TWO OPERATING SCENARIOS

Name	Normal operation		Alternate operation	
	Pressure (psig)	Mass Flow (lb/h)	Pressure (psig)	Mass Flow (lb/h)
Source 1	300.0	125,000	300.0	50,000
Source 2	300.0	75,000	300.0	50,000
Source 3	299.6	50,000	300.3	50,000
Total production	299.1	250,000	299.8	150,000
To users in A	298.0	100,000	298.7	100,000
To users in B	298.7	150,000	299.7	50,000

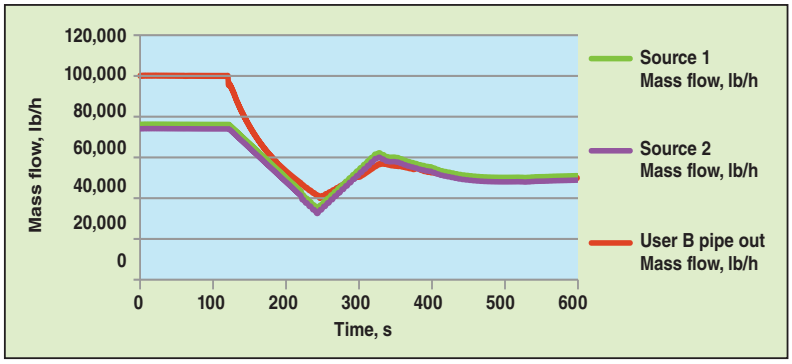

FIGURE 4. The dynamic behavior of steam sources during transition, as discussed in the example, is shown here

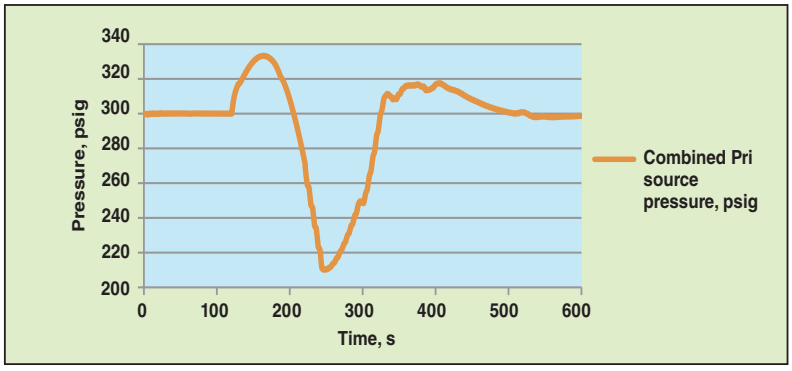

FIGURE 5. This plot shows the dynamic response of main header pressure as given in the example

Once validated, the model will provide valuable insight into system behavior and interactions. It is the high degree of interconnectivity in facilities that results in greater efficiencies, but can lead to unexpected interactions. A well-constructed dynamic model can lead to the discovery of these interactions and will allow a facility time to develop a plan for controlling the integrated system.

If the model is emulating an existing system, step testing can be used to develop actual system behavior data. Incremental changes of a tolerable magnitude can be made during the operation of a facility. The magnitude of the change need only be greater than the noise band of the target dependent variable. Proper planning and preparation is essential for this type of testing, since there is a risk of upsetting an operating unit. All test parameters must be documented and agreed upon prior to testing.

Plan

Using the developed and validated system model, a master control strategy can be developed. Using engineer-

MASTER CONTROL STRATEGY KEY CONSIDERATIONS

In assembling a preliminary control strategy for steam systems, the following key considerations should be included:

1. How will the header pressure be measured and maintained?
2. Is it better to maintain a set point target at one position in the complex header system, or to maintain an average pressure based on multiple readings across the header?
3. Should all boilers be fired symmetrically at the same load?
4. Should boilers be fired in groups with the same load selected for each boiler in a group?
5. Are some boilers better left "base loaded" at a fixed firing rate?
6. Are there any waste streams being fired?
7. What constraints need to be incorporated into the control strategy?

ing judgment and insights gained throughout the model development and testing, a preliminary control strategy is assembled. Some key considerations in such a strategy include those shown in the box above.

The control strategy will likely be a combination of traditional proportional-integral-derivative (PID) controllers and logic triggered actions. Steam load shedding is an example of logic triggered actions. Load shedding can be implemented if major steam users need to be shed in order to recover from an upset scenario. The input of experienced operations personnel is essential in developing a ranking of the major steam users that can be shed. This ranking will allow the development of steam shed actions resulting from steam-header pressure loss [*3*].

Once the preliminary control strategy is established, it can be incorporated into the dynamic model. Confidence in the selected controls will be gained by rerunning the previous model cases using the tuned model and planned control strategy. Perturbing this model using upsets from model development will show the effectiveness or ineffectiveness of the proposed control scheme. Initial tuning parameters can be developed along with any adjustments to sensing locations and final control-element characteristics (such as control valve sizes). The dynamic model can then be used to predict reactions to more severe upsets that are not reasonable to attempt in an operating unit.

Implement

Implementation of the control scheme is the final step. All of the modeling, checking and rechecking should result in confidence in the new master-control scheme and provide useful predictive data for implementation in a new facility or for navigating an existing facility's management-of-

change (MOC) procedures.

The planned scheme must first be documented in all relevant engineering documents. Piping and instrument diagrams, process flow diagrams, control narratives and instrument loop diagrams are examples of these documents. Once all documentation is in place, a thorough review will take place to ensure nothing has been overlooked in either hazards or operability. This is typically done within the framework of an established plant or project hazard-analysis procedure, such as an MOC procedure or a hazard and operability study (HAZOP).

Prior to activating the new control scheme, all components, including the software components, must be tested to ensure proper functionality. ■

Edited by Dorothy Lozowski

References

1. Jaber, David, McCoy, Gilbert A., and Hart, Fred L., Follow these Best Practices in Steam System Management, *Chem. Eng. Prog.*, December 2001.
2. Currie, Jonathan, and others, "Steam Utility Systems are not 'Business as Usual' for Chemical Process Simulators", AIChE Archived Presentations, March 15, 2011.
3. Bourji, Ali, Ballow, David, and Choroszy, Martha, Find Benefits in Automating Boiler Systems, *Hydrocarbon Proc.*, October 2011.

Authors

Ali Bourji is a senior technical director at WorleyParsons (6330 West Loop South, Bellaire, TX 77401; Email: ali.bourji@worleyparsons.com; Phone: 713-407-5000). Bourji received his B.S.Ch.E. and M.S.Ch.E. from the University of Houston and his Ph.D. from Lamar University. He is a professional engineer and a member of AIChE and AFPM (formerly NPRA). Bourji is the author of numerous publications and serves on the Chemical Engineering Ph.D. Advisory Council at Lamar University.

David Ballow is a principal process engineer at WorleyParsons (6330 West Loop South, Bellaire, TX 77401; Phone: 713-407-5000) and is a professional engineer. He received a B.S.Ch.E. from Louisiana Tech University and is a member of AIChE.

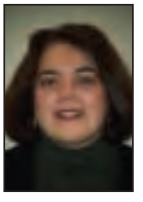

Martha Choroszy is a chief process engineer at WorleyParsons (6330 West Loop South, Bellaire, TX 77401; Phone: 713-407-5000). She received a B.S.Ch.E. from the Massachusetts Institute of Technology and an M.B.A. from Tulane University. She is a licensed professional engineer in Texas and a member of AIChE and NFPA. She is the author of numerous publications, a recipient of Tulane's Allen Vorholt Award and has served as a Blue Ribbon Panel Member to define the national agenda for the U.S. Core Combustion Research Program.

STEAM

MAGNETROL

ECLIPSE MODEL 705

First in guided wave radar.
Foremost in steam applications.

Do your high-pressure vessel environments get you steamed? Rely on the Eclipse Model 705 for liquid level detection that delivers precise readings in saturated steam applications up to 2250 psi at 650ºF.

Our steam probe technology utilizes both a patented mechanical steam target and patented firmware algorithms for continuous compensation control of the signal propagation delay through the vapor space.

The Eclipse Model 705 introduced guided wave radar technology to industrial control applications and was the first to pioneer steam compensation measurement. Make it your foremost choice for high-pressure performance.

When things get hot, depend on SIL 3 Certified Eclipse Model 705 and Magnetrol, the level control experts. ***www.magnetrol.com***

SIL 3 Certified — Safety • Integrity • Level

Magnetrol®
your **preferred partner** at the RIGHT LEVEL for 80 years

1-800-624-8765 • info@magnetrol.com

Circle 35 on p. 76 or go to adlinks.che.com/40268-35

Distillation: Avoid Problems During Tower Startup

Practical procedures for both effective startup and problem analysis are discussed here for a depropanizer that experienced downcomer seal loss

André Bernard
NOVA Chemicals (Canada) Ltd.

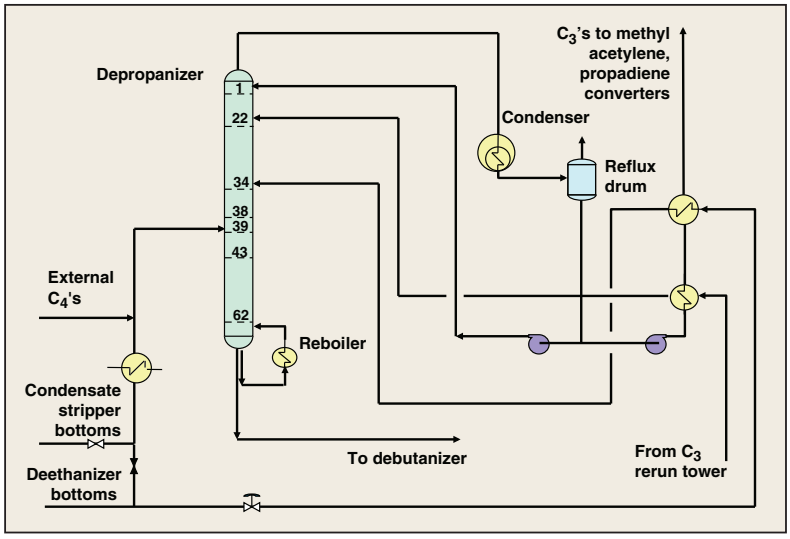

FIGURE 1. Shown here is a schematic process flow diagram of the depropanizer and its ancillaries

A variety of performance problems can arise in distillation towers during startup. Many are caused by equipment, hardware or process conditions. Hardware issues may be related to instrumentation, tower internals or ancillaries. Instrumentation malfunctions are also common during startup and are predominantly related to liquid level indicators, online analysis of key components and in some cases, flowmeters. If not properly compensated, flowmeters can mislead the operator on streams operating outside the normal design envelope. Vessel-isolation blinds, valve alignments or unexpected obstructions in valves can also restrict or misdirect flows. Any of these issues could lead to hazardous conditions and ultimately process incidents.

Anomalies in tower internals, such as obstructions, mechanical damage or poor installation can also cause towers to perform poorly. Meanwhile, issues related to process conditions could arise in all operations conducted from the point of shutdown to getting the tower ready for startup, during the startup itself, and ultimately during steady-state operation. The presence of unexpected impurities, such as water, are also known to cause problems during distillation, or in some cases may result in pressure surges.

Meanwhile, oxygen-freeing practices, and methodologies to introduce the feed stream can lead to cold temperatures that are below the minimum allowable temperature of the piping or tower material. Unstable thermosyphon or reboiler stalling, caused by low loads or premature start of the reboiler, can also cause tower instability. Similarly, tray or packing hydraulic loads that are outside the equipment capability can significantly impact fractionation efficiency by allowing either flooding or operation below turndown.

Although some of these problems ultimately require the process to be shut down so that the tower can be inspected internally, that should be the last resort. Good startup planning and procedures can go a long way toward preventing operating problems in the first place. If problems do arise, appropriate knowledge of the system is essential for identifying the corrective actions that are effective and the least invasive to process operations. Specifically, the use of diagrams that define the tray-stability limits and expected operating lines, and support effective startup planning, can help to demystify the analysis of poor tower performance.

This article illustrates the use of these practical tools through a troubleshooting exercise with a depropanizer tower at NOVA Chemicals' Corunna site. The Corunna site is an olefins plant with a front-end crude unit and a back-end aromatics unit. The plant has the flexibility to crack naphtha and heavy atmospheric gas oil (HAGO), produced by the crude unit. It also has the capability of cracking natural gas liquids (NGLs).

Depropanizer description

The depropanizer is a 147-ft tower with a diameter of 7.5 ft and a total of 62 trays. The first 33 trays (from the top) are conventional two-pass sieve trays. Trays 34 to 62 are high-capacity trays. Heat is supplied to the bottom reboiler by low-pressure steam. Propylene refrigeration (3°C) provides

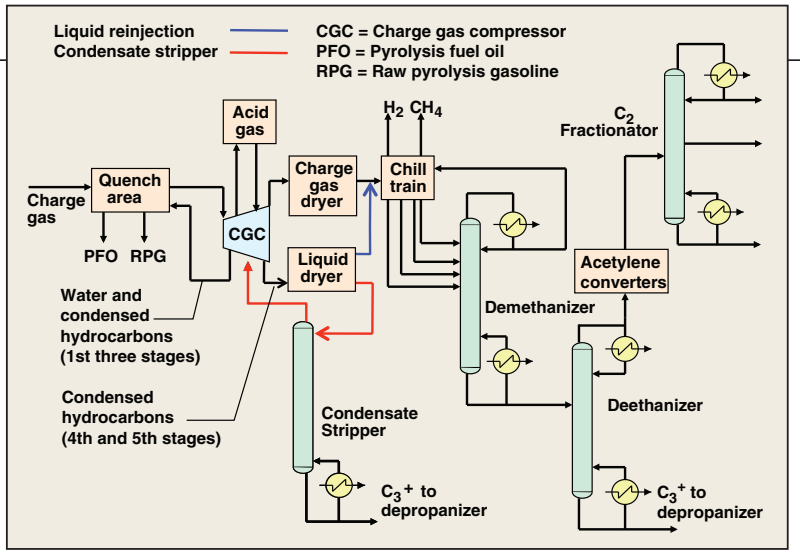

FIGURE 2. This flow diagram shows the liquid re-injection mode and condensate stripper operating mode

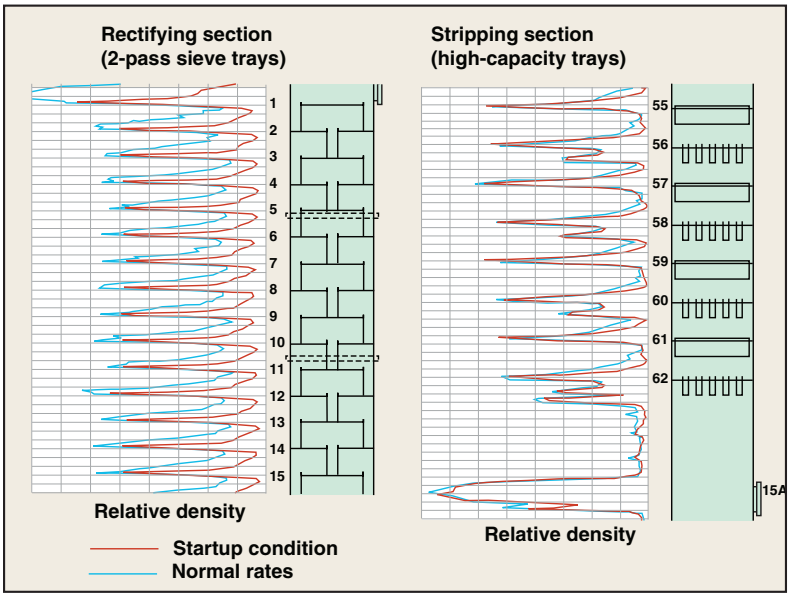

FIGURE 3. This gamma scan of the depropanizer compares normal operating load to the startup conditions

cooling to the overhead condenser.

As shown in Figure 1, the tower has two main feed points at Tray 34 and Tray 39. The feed is distributed by trough distributors at those locations. A third minor feed point, which accommodates a small recycle stream from the C_3 rerun tower is located on Tray 22. The tower normally receives feed from the deethanizer bottoms at Tray 34 and the condensate stripper bottoms at Tray 39. External C_4s can be processed from time to time and are mixed with the condensate-stripper feed. The olefins unit has the ability to run with or without the condensate stripper.

As shown in Figure 2, condensed hydrocarbons from the charge-gas compressor's 4th and 5th stage are dried in liquid dryers and can either be processed by the condensate stripper or mixed with dry charge gas, upstream of the chill train (liquid re-injection path [*1*]). Re-injection of this liquid stream to the charge gas enhances condensation in the first propylene chiller. Process loads are then reduced in the chill train but increased in the deethanizer and depropanizer.

In the liquid re-injection configuration, the depropanizer is entirely fed from the deethanizer bottom. Because of nozzle size and distributor limitations the feed is split between Tray 34 and Tray 39. Tray 34 feed is cooled through cross exchange with the depropanizer overhead product. Feed to Tray 39 is cooled against cooling water. Without cooling, the feed would enter the tower with a significant vapor fraction, which would shift the tray loads from the stripping to the rectifying section.

From a startup standpoint, the liquid re-injection configuration (Figure 2), offers two advantages. First, given the low feedrate during startup, this arrangement provides more load on the deethanizer and depropanizer, which helps in meeting turndown. Second, the movement of material from the front to the back end of the plant is sequential. As such, the depropanizer does not see any feed until the deethanizer has been inventoried. The plant is therefore normally started with the liquid re-injection configuration.

NOMENCLATURE

A_E	=	Pipe-equivalent slot area, ft^2
A_D	=	Pipe-equivalent of downcomer area, ft^2
A_h	=	Hole area, ft^2
a_D	=	Downcomer area, ft^2
C	=	Constant given by Equation (9)
C_v	=	Discharge coefficient, unitless
D_{eq}	=	Equivalent diameter, ft
F_1	=	Factor, equivalent to unity (F_1 = 1) for most tower larger than 4 ft in diameter [*6*]
F_2	=	Factor given by Equation (11)
g	=	Gravitational acceleration, 32.2 ft/s^2
K_1	=	Constant (0 for sieve deck)
K_2	=	Dry pressure drop coefficient, in./(ft/s)^2
K_C	=	Number of velocity head lost
L_D	=	Downcomer liquid rate, lb/h
l_D	=	Downcomer length, ft
N_{slot}	=	Number of downcomer slots
P_1	=	Lower tray pressure, in. of liquid
P_2	=	Upper tray pressure, in. of liquid
ΔP_D	=	Downcomer pressure drop, in. of liquid
ΔP_T	=	Tray deck pressure drop, in. of liquid
V	=	Total vapor rate, lb/h
V_D	=	Downcomer vapor rate, lb/h
$(V_D)_{cr}$	=	Downcomer critical vapor rate, lb/h
V_T	=	Tray vapor rate, lb/h
f	=	Pipe friction factor, unitless
f_n	=	Fraction of V_D flowing to the downcomer n
ρ_V	=	Vapor density, lb/ft^3
ρ_L	=	Liquid density, lb/ft^3

Depropanizer startup problems

Sequence of events. Feed from the deethanizer to the depropanizer started ramping up roughly 15 h after the charge gas compressor was

brought to minimum governor speed.

Steam to the reboiler was started 10 h later. The depropanizer was operated in the liquid re-injection mode for the following 12 h. Throughout this period, several moves were made on the reflux and reboil rate. Since these operations were unsuccessful in bringing the tower bottom within specification, the operation mode was transitioned to the condensate stripper scheme. Furthermore, roughly 5,000 lb/h of off-spec C_4's from storage was fed to the depropanizer through the external C_4's feed point to help load the tower. The tower was still performing poorly and process engineering support was then requested by operations.

Depropanizer troubleshooting. Prior process engineering work [2] done on startup conditions highlighted the risks associated with operating high-capacity trays below their minimum liquid limit. There was concern that the tray load might not be sufficient to seal the downcomers. However, an initial high-level review of the operating conditions did not reveal anything abnormal.

As described in Table 1, the tower operating conditions were not significantly different from the pre-shutdown ones. Plant data also suggested that the upper section was working fine, since reflux changes and overhead composition were varying as expected. The stripping section, however, was performing poorly.

Simulation work and a gamma scan on the tower were then conducted. The Operations Dept. was asked to maintain stable conditions, regardless of performance, for the duration required to conduct the gamma scan on the tower. The intent of the scan was to determine if any mechanical anomalies were present inside the tower and to assess the tray-loading profile.

The gamma scan results (Figure 3) indicated no mechanical anomalies and no sign of flooding. Vapor-liquid disengagement looked better compared to a previous scan done at a normal plant rate. Many of the high-capacity trays showed a clear vapor space equivalent to the vapor space above the reboiler return and the bottom tray. Scanning across the tray could not provide any information with regard to the downcomer operation. Based on the work done by Urbanski and others [3], it is assumed that tray weeping cannot be determined by the gamma scan.

The tower was simulated with inputs reflecting operating conditions sustained at the time of the scan. The intent of the simulation was first to ensure that the trays were operating within their hydraulic capabilities. The operating point relative to flooding was calculated using the Kister and Haas correlation [4] for the sieve tray section.

The operating point for the high-capacity trays was plotted on the tray operating window obtained from the tray vendor. The simulation results estimated the sieve tray operation at 72–73% of flood, which compare to 68–70% of flood for the pre-shutdown operation. The high-capacity tray operating points are shown on Figure 4 and compared against loads calculated for pre-shutdown operation. As for the sieve tray, the startup conditions showed loads slightly higher than pre-shutdown.

Tray loading calculations were consistent with the gamma scan results, which supported the conclusion that the trays were not flooded but rather were operating at low rates. Some of the key information gathered was structured into a problem analysis matrix, as shown in Table 2. The concept of problem analysis is to look at what, where and when the problem is — and is not — and to look at differences and changes, as well. It was clear from Table 2 that the main change was the low feedrates in the C_3 area. A review of previous startups concluded that the plant had never been brought up to steady-state conditions at such low rates. A light feed slate similar to pre-shutdown conditions explained the lower rates to the C_3 and C_4 area. This

TABLE 1. PRE- AND POST-SHUTDOWN OPERATING CONDITIONS

	Pre-shutdown	Post-shutdown
		(at time of Gamma Scan)
Feed from the deethanizer, thousand lb/h	112.8	105.6
Feed from the condensate stripper, thousand lb/h	63.0	72.8
External C_4's, thousand lb/h	0	5 (off-spec C_4s)
Reflux rate, thousand lb/h	98.9	94.3
LP steam to reboiler, thousand lb/h	24.2	26.3
Tower pressure, psig	123	122
Tower pressure drop (in. H_2O)	111	112

TABLE 2. PROBLEM ANALYSIS

Deviation: Depropanizer bottom stream C_3s outside specification

	Is	Is not	Differences	Changes	Probable cause
What	**Object:** Depropanizer bottom stream **Defects:** C_3s outside product specification	**Object:** Deethanizer **Defects:** Bottom specification	• Feedrates • Properties • Process conditions • Composition • Trays	• Low rates in C_3 area	
Where	Depropanizer stripping section	Depropanizer rectifying section	• Tray type • Composition • Hydraulic load • Temperature • Properties	• Low rates in C_3 area	• High capacity tray turndown not met
When	Startup	Pre-shutdown	• Path to low-rate operation	• Low rates in C_3 area	• Stripping section tray downcomer unseal • Stripping section tray weeping

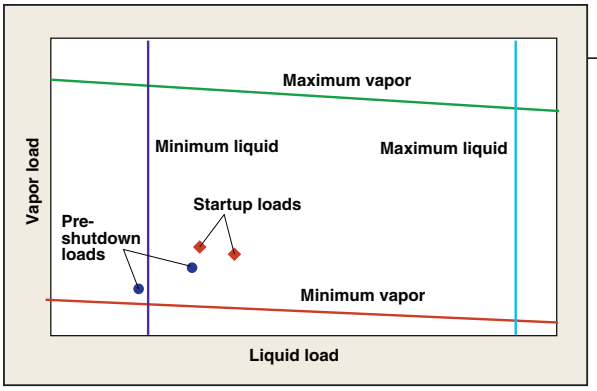

FIGURE 4. This diagram shows the high-capacity trays' operating limits, with the pre-shutdown and startup operating points

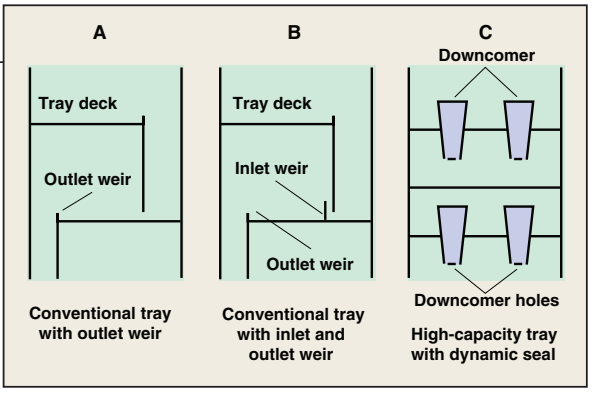

FIGURE 5. Typical downcomer arrangements for conventional and high capacity trays are shown here. The downcomer positive seal is shown on (A) and (B), while the downcomer dynamic seal is shown on (C)

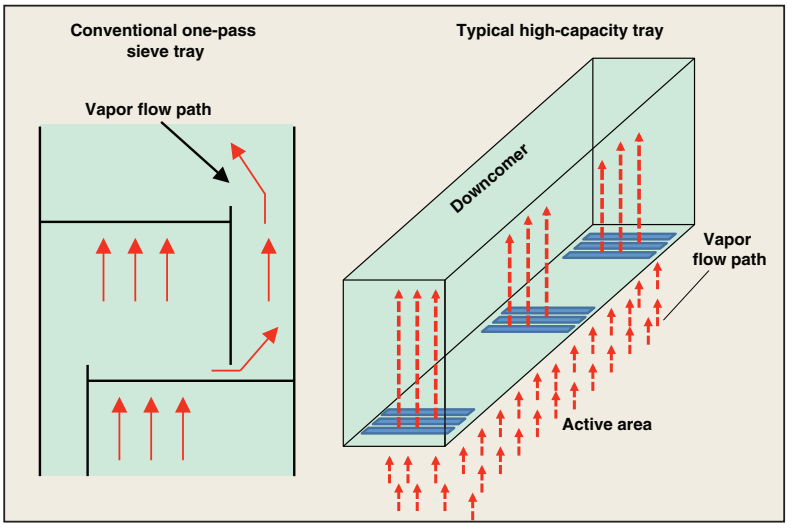

Pipe equivalent diameter	Equivalent fittings	*Kc*
D_E	Entrance	0.5
D_E	45° elbow	0.2
D_D	45° elbow	0.2
D_D	Straight length	$f\ l_D/D_D$
D_D	Exit	1

Pipe equivalent diameter	Equivalent fittings	*Kc*
D_E	Entrance	0.5
D_D	Straight length	$f\ l_D/D_D$
D_D	Exit	1

FIGURE 6. These illustrations compare the vapor flow path across a conventional, one-pass tray (left) and a typical high-capacity tray (right) with a pipe-fitting analogy for estimating the downcomer pressure drop

explained, to a certain degree, why this problem had never been experienced before.

The tray type and the path to low-rate operation were two other key components to this analysis, which led to the conclusion that the probable cause was an unsealed downcomer or a tray weeping problem in the stripping section.

When a tray is turned down from high to low rates, the downcomers and the tray deck are already sealed. However, at the early stage of starting up a distillation tower, vapor tends to flow through the downcomers and liquid weeps down the holes on the tray deck. To break this path, a good balance between vapor and liquid flowrates needs to be established, so that sufficient vapor seals the tray deck and sufficient liquid seals the downcomers. As such, turndown conditions will differ between a tray being brought from high to low rates, and a tray brought from a cold startup.

The tray type is another significant difference that explains why the problem occurred in the stripping section and not in the rectifying section. As shown on Figure 5, high-capacity tray downcomers differ from those of conventional trays in the way the downcomer seals itself. In a high-capacity tray, liquid falls on the active area of the tray below through a number of slots in the bottom of the downcomer. Sufficient liquid flow is required to maintain a positive liquid head over the slots (this is a dynamic seal).

Insufficient liquid causes the downcomer to run empty, which opens up the slots. Vapor is then free to flow upward through the slots of the downcomer.

In conventional trays, mechanical barriers ensure a constant inventory of liquid in the downcomer. If the outlet weir height exceeds the clearance of the downcomer, the liquid head in the downcomer cannot drop below the outlet weir height when the tray deck is sealed.

An inlet weir can also be present, weir), or if the outlet weir height is less than the downcomer clearance, the downcomer seal becomes dynamic. In this case, the two-pass sieve trays have a downcomer design similar to the one described Figure 5A.

As indicated on the problem analysis summarized in Table 2, this problem did not occur in the deethanizer. The deethanizer tower is also equipped with high-capacity trays; however, the potential for under loading the deethanizer was recognized when evaluating startup conditions. Startup material balances were developed to ensure sufficient load on the deethanizer, especially the stripping section. Feed pre-heat to the deethanizer was bypassed until reaching full plant rates. Operators were also reminded to maximize reflux.

Performance of the deethanizer tower was also carefully monitored throughout the startup as it is a key

element for bringing the ethylene product within specification.

Corrective actions

The troubleshooting exercise described above revealed that the high-capacity trays downcomers were not sealed. It was also believed that, since a fair chunk of vapor was flowing through the downcomers, not enough was left to seal the tray deck. As a result, poor vapor-liquid contact was causing the lack of fractionation that was observed.

Increasing the liquid load and forcing it down the tower to seal the downcomers was believed to be one reasonable solution to this problem. The action plan called for an increase of offspec C_4's rate from 5,000 to 25,000 lb/h, increasing reflux and reducing the reboil rate for a few hours. The reduction in reboil rate was done to ensure that liquid would flow down the tower. The reboil rate would be re-established once the tower showed signs of recovery. The tower bottom C_3 composition met the specification within the hour that followed the changes described above.

Quantifying tray seal limits

Use a tray stability diagram. The analysis described above was able to determine the cause of the problem. However, the tray seal limits had not been determined quantitatively. Rather, the action plan was based on intuition, and its success relied on good problem analysis, and a little bit of luck. Tower stability during startup has been discussed by Kister [*4, 5*] who promotes the use of a startup stability diagram. Such a stability diagram is based on a liquid-vapor rate plot that shows the tray-deck seal limit and downcomer critical velocity.

The downcomer critical velocity is defined as the vapor velocity at which liquids can no longer descend freely through the downcomer but become entrained by vapor instead. The vapor flow distribution between the tray deck and the downcomer must be understood to establish those limits. The vapor balance across the tray can be described by Equation (1).*

$$V = V_D + V_T \quad (1)$$

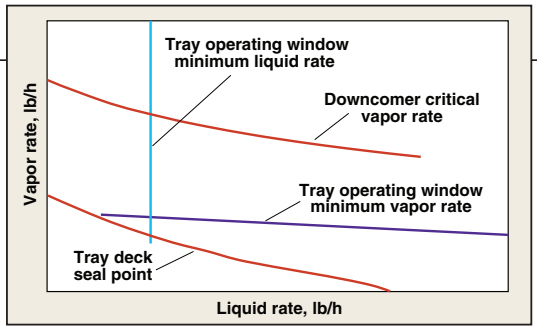

FIGURE 7. This figure shows the post-event analysis of a tray-stability diagram

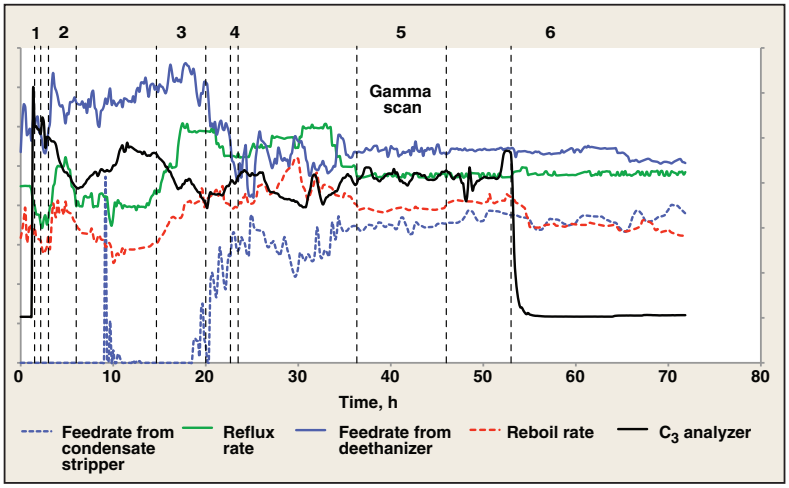

FIGURE 8. The trends of the key process variables are shown here for the depropanizer startup. Period 1, 2, 3, 4 and 6 show the C_3 composition trending down. As shown, steady conditions were maintained during Period 5 to enable a gamma scan to be performed on the tower

The pressure balance is provided by Equation (2):

$$P_1 - P_2 = \Delta P_D = \Delta P_T \quad (2)$$

For startup conditions, the pressure drop across the tray can be assumed to be equivalent to the tray dry pressure drop, which is determined by a variation of the orifice Equation (3):

$$\Delta P_T = K_1 + K_2 \frac{1}{\rho_V \rho_L} \left(\frac{V_T}{3600 A_h} \right)^2 \quad (3)$$

For the sieve tray deck, the value of $K_1 = 0$ and $K_2 = 0.186/C_v^2$.

The pressure drop for vapor flowing up the downcomer is estimated by modeling the downcomer as a pipe. The geometry of the different components of the downcomer is converted into a pipe-equivalent diameter through the following expression:

$$D_{eq} = \frac{4(\text{Cross-section area})}{\text{Wetter perimeter}} \quad (4)$$

Figure 6 shows the differences between a one-pass sieve tray and a typical high-capacity tray downcomer with regard to the pipe-analogy concept. In the high-capacity tray, vapor flows upward from the active area, directly through the slots of the downcomer (pipe entrance), then flows through the downcomer (straight pipe length), and exits the downcomer (pipe exit).

The conventional tray forces the vapor flow to change direction twice (2 x 45-deg pipe elbow) and therefore causes more resistance to vapor flow than the high-capacity tray. In both cases, the pressure drop through the straight length of the downcomer is insignificant and therefore not included in the equation.

The multiple slots and number of downcomers on the high-capacity tray add to the complexity of developing the downcomer pressure-drop relationship. Knowing that the pressure drop across each downcomer is equal, the calculation can then be limited to a single downcomer. The pressure drop calculation was broken down by elements. For the downcomer entrance, the pressure drop was established based on the dimension of a single slot.

* All terms are defined in the Nomenclature box on p. 49.

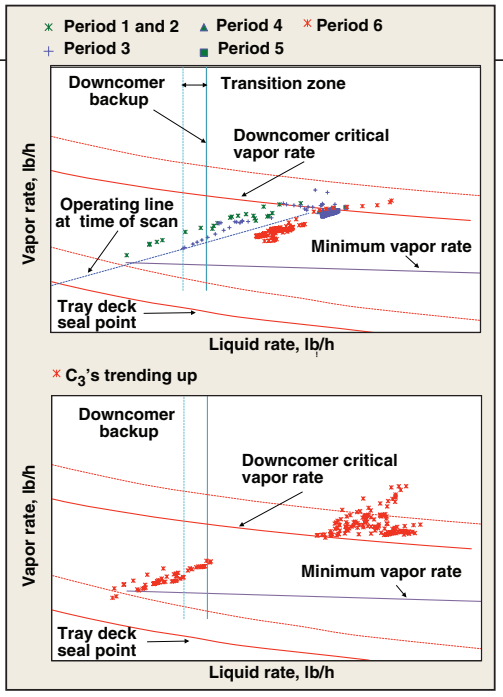

FIGURE 9. This figure shows the operating data (of the critical vapor-rate and tray seal-point) on the stability diagram for the different periods described on Figure 8. Uncorrected data (red dashed curves), and data corrected for 20% reduction in the perforation area (red solid curves) are shown

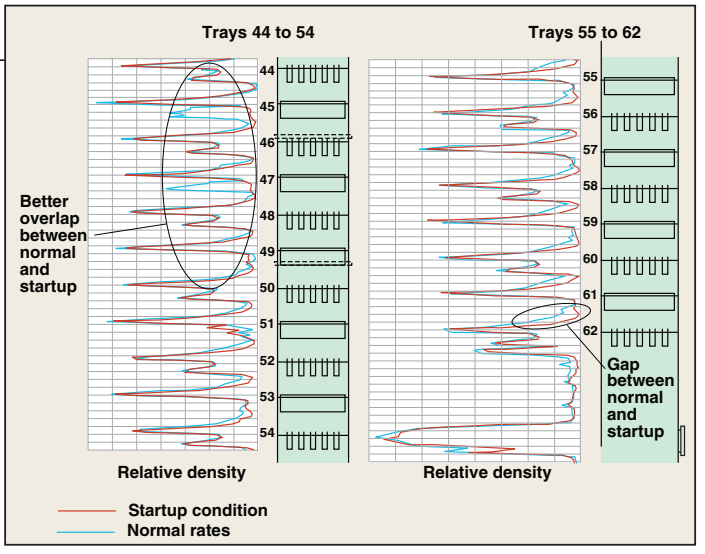

FIGURE 10. This gamma scan shows a suspected entrainment of liquids on startup from the bottom trays to trays 45, 47, 48 and 49

Assuming even distribution within one downcomer, the total downcomer vapor flow, V_D, was divided by the total number of slots and multiplied by factor f_1, as described by Equation (5A). Factor f_1 represents the fraction of V_D flowing to a single downcomer. A_E represents the pipe-equivalent slot area, based on the slot-equivalent diameter. The pressure drop from vapor exiting the downcomer can be calculated from Equation (5B). The total downcomer pressure drop can be obtained by the summation of Equations (5A) and (5B).

$$\Delta P_D = \Delta P_{D1} + \Delta P_{D2} \quad (5)$$

$$\Delta P_{D1} = \frac{6}{g\rho_V \rho_L}\left[\frac{V_D}{3{,}600}\right]^2 0.5\left[\frac{f_1}{N_{slot} * A_E}\right]^2 \quad (5a)$$

$$\Delta P_{D2} = \frac{6}{g\rho_V \rho_L}\left[\frac{V_D}{3{,}600}\right]^2\left[\frac{f_1}{A_{D1}}\right]^2 \quad (5b)$$

Writing the above equations for each downcomer will provide correspondence between the fraction of V_D (expressed by f_n, where n = downcomer number) and the pipe-equivalent area A_{Dn}. f_n can then be determined using Equation (6):

$$\sum f_n = 1 \quad (6)$$

The ratio of Equation (3) and Equation (5) provides the relationship between V_T and V_D.

$$V_D = \frac{V}{1 + C^{-0.5}} \quad (7)$$

$$V_T = \frac{V}{1 + C^{0.5}} \quad (8)$$

Where:

$$C = \frac{gK_2}{6A_h^2} * \frac{1}{\left[0.5\left(\frac{f_1}{n_{slot}A_E}\right)^2 + \left(\frac{f_1}{A_{D1}}\right)^2\right]} \quad (9)$$

Using the value of V_T, the tray-deck seal limit was determined from the correlation in Ref. [4, 5]. The downcomer critical vapor rate was determined by Equation (10).

$$(V_D)_{cr} = a_D F_1 F_2 \left(\frac{\sigma}{\rho_V}\right)^{0.5} \quad (10)$$

F_1 = 1 and F_2 is given by:

$$F_2 = \left(\frac{L_D}{V_D}\right)^{-0.25} \quad (11)$$

Where L_D is assumed equal to L.

The stability diagram, as shown in Figure 7, is built by plotting the total vapor and liquid rate corresponding to the seal deck limits established from Prince and Chan's correlation. The total vapor and liquid rate corresponding to Equation (10) and (11) provides the critical downcomer vapor velocity limit. Figure 7 also includes the minimum stable liquid and vapor rate obtained from the tray vendor.

Key process variables applied on the depropanizer are plotted against time (Figure 8). The tower pressure is not plotted, as it remained relatively constant throughout this period. For simplicity of presentation, the time scale starts at 0 hour just before the C_3 analyzer started reading.

The plot is subdivided in time interval periods, where Periods 1, 2, 3, 4 and 6 show the C_3 composition in the bottom of the depropanizer trending down. Period 5 represents the conditions sustained during the gamma scan.

Using plant data, the bottom tray load was calculated from the tower bottom product and low-pressure (LP) steam flowmeters. The actual bottom-tray vapor rate was estimated by multiplying the ratio of the simulated bottom-tray vapor to LP steam rate by the actual measured rate of LP steam to the reboiler. The liquid load of the bottom tray was estimated by adding the above calculated vapor rate to the actual tower bottoms flowrate.

The data were segregated by periods, as shown in Figure 8, and plotted on two stability diagrams. The first diagram in Figure 9 shows the data selected for the time when the depropanizer bottom C_3 composition was trending down and also includes the gamma scan time interval. The bottom diagram plots the data for which the depropanizer's bottom C_3 composition was trending up.

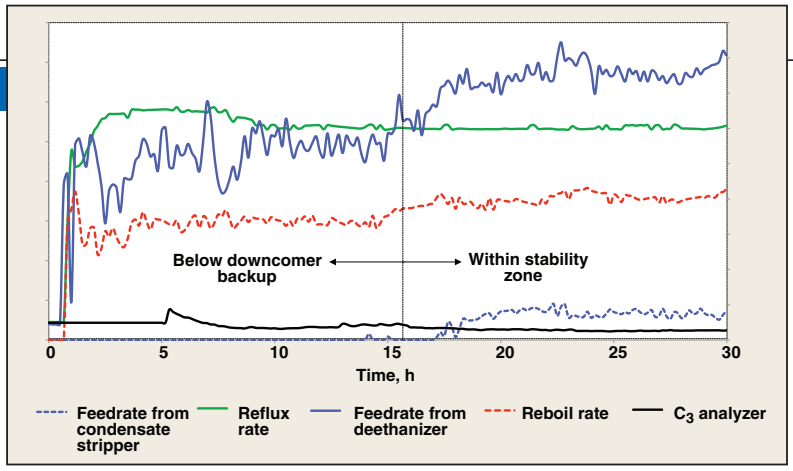

FIGURE 11. The historic trends of key process variables for the depropanizer startup are shown here for the subsequent startup

The downcomer critical vapor-rate limit and tray-deck seal point previously calculated are illustrated by the red dashed line on Figures 8 and 9. Note that those limits were calculated with the assumption of clean trays. However, this tower is known to foul, especially in the bottom section. The tower had been in service for more than three years and this startup was the result of an unplanned outage.

To account for fouling, the total perforation area on the tray deck (A_h in Equation (3) was reduced until the stability limits aligned with the depropanizer's bottom C_3 composition behavior. This exercise suggested that roughly 20% of the perforated area was plugged. This moves the stability limits down (see the solid red lines).

Note that as those limits are moving, so will jet flood. As a result, the trays are expected to flood prematurely. (In other words, if the lower operating limit is lower, then the jet flood limit would also be lower; under these conditions, if the tray were pushed, it would flood at a lower load than expected). Assuming clean downcomers, the minimum liquid load defined by the vendor operating window should remain unchanged. This limit is identified on Figure 9 as downcomer backup and is defined by the liquid rate in the downcomer that ensures a sufficient liquid level over each downcomer slot.

A transition zone for C_3 composition has been identified on the plot, in which the trend was found to go either way. The minimum vapor rate defined by the tray operating window should, in theory, move down if the perforation area is reduced. However, this limit was found to not play a major role in this event and data were insufficient for evaluating the change. A drop similar to the seal point of the tray deck would be the best estimate.

Except for the critical vapor limit of the downcomer, all other limits shown on Figure 9 always apply, regardless of the operating mode. However, the critical vapor limit of the downcomer only applies during startup. Vapor is forced to flow across the tray deck once a sufficient amount of liquid seals the downcomer. The max vapor rate then becomes limited by the onset of jet flood.

Note that the tower was operated in liquid-reinjection mode up to the end of Period 3, as shown on Figure 8. Near the end of Period 3, the tower operation mode was transitioned to the condensate stripper configuration.

While the tower was operated in liquid-reinjection mode, the operating points, as shown on Figure 9, were spread on each side of the downcomer backup limit. Most of the operating data falls within the stable region for Period 1, 2 and 3 and the tower C_3 composition trends downward.

The reduction in reflux and reboil rates near the end of period 2 causes the C_3 composition to trend up again. This transition aligns with the operating points suddenly falling below the downcomer backup limit. Similarly, the increase of reflux and reboil rates at the beginning of Period 3 brings the operating points above the backup limit, which is also associated with a drop of C_3's.

The operating point ramped from the backup limit to slightly above the minimum vapor rate limit, and stayed within the stable region for more than two hours. It is believed that the tray sealed itself during that period. Because the tray was sealed, the critical vapor rate limit of the downcomer no longer applied and the tower should have recovered efficiency. Proper adjustment of reflux and reboil rates at that stage should have been all that was required to bring the bottom stream within its C_3 specification.

However, as the C_3 composition was trending down, the operation mode was transitioned to the condensate-stripper scheme. Initially in the transition, the deethanizer bottoms fed the depropanizer at Tray 34 and Tray 39. The bottom of the condensate stripper is intended to feed the depropanizer at Tray 39. To avoid dilution and benefit from the pre-fractionation work done by the condensate stripper, the deethanizer bottoms must feed the depropanizer at Tray 34 only. If not done properly, the transition of the feed could upset the tower and cause the downcomer to go dry.

Experience demonstrated that feeding the depropanizer to a single feed point when operating in liquid-reinjection mode can cause the vapor rate to exceed the system limit at the feed location. It is suspected that the deethanizer stream feeding at Tray 39 was re-directed to Tray 34 before the condensate stripper started to offload the deethanizer. As such, the full flow would have gone to Tray 34, causing significant vapor entrainment and depriving liquid on the trays below the feed point.

The above suspicion is supported by the liquid level in the tower sump, which dropped from 76 to 40% over a one-hour period. A spike in the overhead product flow, which is controlled from the reflux drum level in a level to the flow-cascade loop, also supports this suspicion. The transition matches the time at which the C_3 composition spiked up and then started dropping again in Period 3, just before the first pounds of material from the condensate stripper were fed to the depropanizer. At this point, the downcomers of the high-capacity trays are assumed to be relatively dry with the operating point above the critical vapor-rate limit of the downcomer. The only way to re-seal the downcomer was to drop the operating point back into the stable area until the downcomer sealed itself. At this point, process conditions

could be re-established for a stable and on specification operation.

As shown on Figure 8, operation was kept relatively stable while a gamma scan was being performed on the tower (Period 5). The cluster of data representing this period is right on the critical vapor-rate limit. This suggests that the downcomer was not sealed but operated close to the conditions that were required to seal it.

The extent of liquid entrainment is limited and cannot be easily identified on the scan. Figure 10 compares the gamma scan between Trays 44 to 54 and to that for the region from Trays 55 to 62. A larger gap exists when comparing the startup and normal rate scan on Tray 55 to 62, which suggests lower froth height with the startup condition.

The normal and startup gamma scans overlap better on Trays 45, 47, 48 and 49, suggesting a potential liquid backup from the lower trays at the startup condition. Given the lower rates, the entrained liquid might not show signs of flooding but might cause an internal recirculating loop to form inside the tower.

Figure 8 shows that a small reduction in reboiler duty and a small increase in reflux kicked off a huge drop in the tower bottom's C_3 composition. The reboil rate was further reduced one hour later, but the tower downcomers had already sealed themselves. This confirms that the conditions sustained during the gamma scan were relatively close to being within the stability zone. As shown on Figure 9, the cluster of operating points is well within the stable zone for Period 6.

Subsequent startup

An unplanned outage occurred within a few weeks from the above startup. Again, during this period, no work or vessel entry was done on the depropanizer. The same startup procedure and feed slates were followed again on the plant restart. However, additional steps were added on the procedure to ensure feed cooling and reflux maximization on the depropanizer.

Proper feed locations and transition between operating modes was re-emphasized. The tower was started on liquid-reinjection mode and transitioned to condensate stripper mode once stable. Figure 11 shows the key process variable progression over time, and Figure 12 provides the operating points and expected operating line. The key process variables on Figure 11 progress in a more controlled fashion than those observed in the previous startup (Figure 8).

The cluster of operating points plotted on the stability diagram shows a normal load progression. Initially, vapor and liquid flows through both — the holes of the tray deck and the downcomers — resulting in poor fractionation. Then, as feedrates are increased, vapor and liquid traffic increases in the tower. A liquid level is

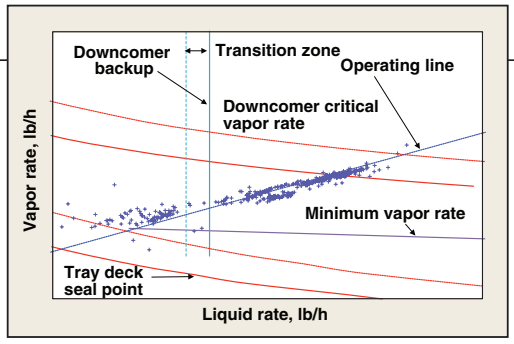

FIGURE 12. This figure shows the operating data on the stability diagram for the subsequent startup

eventually established in the dowcomers and seals them forcing vapor to flow across the tray deck. Vapor flowing across the holes of the tray deck provides sufficient pressure to prevent liquid from falling through the holes. At that point the tray is considered sealed and within the stability zone. By following this path, the critical vapor-rate limit for the downcomer becomes irrelevant.

Note how well the operating points follow the simulated operating line for loads above the downcomer backup. The cluster of data is more sparse and does not line up as well with the operating line at loads below the downcomer backup limit. This makes sense because the tower loses efficiency when operated below its downcomer backup limit.

Analysis

The poor performance of the depropanizer during the first startup was initially attributed to the low feedrates in the C_3 area. However, by the time the depropanizer was started up, feed rates were ramped up to planned production rates, which were low but similar to pre-shutdown levels. The tower could not fractionate properly as those rates were met. Intuition suggested that — even with the operating point is within the vendor's tray-operating window — the downcomer was still unsealed.

The theory at the time relied on the path to low rates on the tray. Establishing the tray-stability diagram clarified what had actually happened. The low liquid limit identified as downcomer backup will apply, whether the tray is brought to that limit from high to low, or from low to high loads. If the tray load progresses smoothly from below the downcomer limit through the stable zone, the downcomer's critical vapor-rate limit should become irrelevant, as the downcomer is already sealed when crossing this limit. If the tower load is quickly brought up above the downcomer's critical vapor velocity, the downcomer might not seal itself and liquid would be entrained out of the downcomer.

The most effective way to correct this problem is to move the operating point down within the stability zone. The problems encountered during the first startup are not attributed to feed rates but rather to the feed-lineup sequence during the transition to the

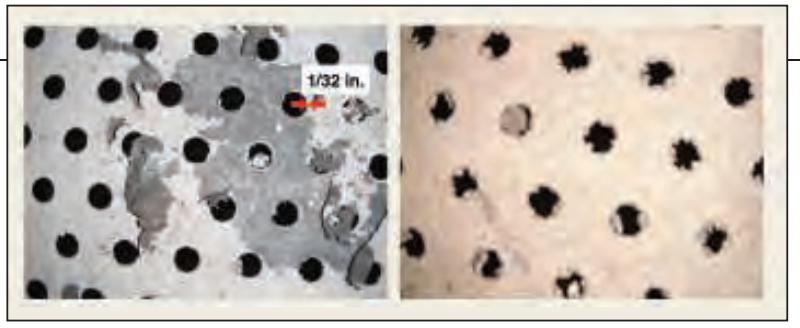

FIGURE 13. Shown here is photographic proof of the reduced effective hole diameter on the depropanizer's high-capacity trays located in the stripping section

condensate-stripper operating mode. Plant data suggest that the downcomers were sealed prior to the transition. An inappropriate feed-lineup sequence is believed to have caused significant liquid entrainment at the feed point, which caused the downcomers of the trays below that feed point to empty out. At that time, the operating point was above the critical vapor rate, and tray stability could only be re-established by reducing the tray load. The deethanizer bottom stream, which feeds the depropanizer at the same location as the condensate stripper bottom stream, should not be switched to the other deethanizer bottom stream until the condensate stripper bottom stream is fully operational. This will temporarily affect the tower efficiency, but will ensure a smooth transition and prevent unsealing the downcomers.

The deethanizer is also equipped with high-capacity trays. Process work done around startup conditions highlighted conditions required to satisfy the minimum liquid limit on the vendor-specified tray operating window. The tower load ramped up smoothly from below the minimum liquid limit to a point within the tray window. As such, the downcomer's critical vapor rate limit has never been a concern.

Tower inspection

More than two years after this incident, the depropanizer was opened and inspected during a scheduled plant turnaround. The inspection revealed no mechanical anomalies. The sieve trays in the rectifying section were found to be clean.

However, in the stripping section, a thin layer of polymer was found on the surface of the tray. The polymer was hard and strongly bonded to the metal surface (Figure 13), coating the circumference of the holes and reducing each hole's effective area.

The post-event analyses described earlier suggested a 20% reduction of the perforation area. This represents a reduction in diameter of around 1/16 in. for 1/2-in. holes, or equivalent to a layer of approximately 1/32 in. covering the circumference of each hole. The polymer was scraped off a small area of the tray deck to highlight the polymer layer covering the circumference

of the holes, which is illustrated on the left side of Figure 13. The un-scraped area in the same picture would suggest little fouling at first sight. However, the polymer coating over the tray also covered the circumference of all the holes with a layer thickness more or less similar to the one displayed on the scraped area. The fouling was more severe on some trays, as shown on the right-end side of Figure 13. On average most of the trays had a reduction in hole area of approximately 20%.

Downcomer seal-loss symptoms

When downcomers become unsealed, a significant portion of the vapor flows through the downcomer and bypasses the active area of the tray. Depending on the extent, there might not be sufficient vapor flowing across the tray deck to prevent weeping or dumping of liquids. As such, little contact occurs between vapor and liquid, which is evidenced by a significant reduction in fractionation.

However, a reduction or loss of fractionation itself, even though symptomatic, is not sufficient to conclude that a loss of downcomer seal has occurred. Flooding will also cause a significant reduction in fractionation. These two operational anomalies can be distinguished by differences in tower pressure drop. In general, a loss of downcomer seal will be associated with low tower pressure drop, while high pressure drop is indicative of flooding.

The combination of poor fractionation and low pressure drop suggests unsealed downcomers but could also be the result of mechanical anomalies, such as tray manways left open or damaged tray panels. Gamma scan of the tower will help in ruling out mechanical anomalies and will provide additional information with regard to flooding. For instance, a scan showing very little froth and no mechanical anomalies, along with low pressure drop and poor fractionation, is a strong indicator of unsealed downcomers.

The use of a tray-stability diagram could replace the need for a gamma scan. However, as demonstrated with the depropanizer example, certain conditions like fouling could mislead the investigators, where a gamma scan would provide the missing link for proper diagnosis.

In summary, the loss of a downcomer seal is very likely if:

- Poor or no fractionation is observed
- The tower has low pressure drop
- Operating points are outside the tray-stability diagram, and
- The gamma scan is showing little to no froth and doesn't show signs of any mechanical anomalies

Re-establish a downcomer seal

It is one thing to recognize unsealed downcomers, but quite another to implement a suitable remedy. Any situation where one tower is incapable of

meeting product specifications puts a high level of stress on the engineering decision makers. Even if the diagnosis is accurate, plant management can easily lose faith if the remedy does not provide positive results in a timely fashion. This leads to further troubleshooting and eventually shutdown and tower entry, once all options have been exhausted.

The tray-stability diagram is a powerful tool that not only helps to diagnose a problem, but also reveals which one of the limitations has been violated. Operation below the downcomer backup limit requires an increase in tray load to ensure a proper downcomer seal. This can be accomplished either by increasing throughput or by false loading the tower with reflux and reboil. On the opposite end, operation above the downcomer's critical vapor rate requires a reduction in load to reseal the downcomer. This is accomplished by reducing throughput or by a temporary slump of the tower. The stability diagram also helps to quantify the deviation from the stability limits, allowing for proper direction in the magnitude of the change required for sealing the downcomers. The absence of a stability diagram leaves the troubleshooter to a trial-and-error approach, which could become time-consuming. In such case, one approach is to proceed with a tower slump followed by a smooth transition to loads historically demonstrated. This should reestablish tray efficiency. ■

Edited by Suzanne Shelley

References

1. Bernard, A., and R. Hayden, Planning and Designing the Modernization of the Recovery Area of a Flexible Cracker, AIChE Spring Meeting, Ethylene Producers Conference, April 2004, New Orleans, La.
2. Bernard, A., Post-revamp startup planning and support, *Petroleum Tech Quarterly*, Q4 2007.
3. Urbanski, N., and others Gamma Scanning a Column Containing Closely Spaced Trays, Annual Meeting AIChE 1999, Dallas, Tex.
4. Kister, H.Z., "Distillation Design," McGraw-Hill, 1992.
5. Kister, H.Z., When tower startup has problems, *Hydrocarbon Proc.*, February 1979.
6. Kister, H.Z., "Distillation Operation," McGraw-Hill, 1990.
7. Kister, H.Z., "Distillation Troubleshooting," Wiley-Interscience, 2006.
8. Summers, D,R., Performance diagrams — All Your Tray Hydraulics in One Place, Annual Meeting AIChE 2004.

Author

André Bernard is a process engineer with NOVA Chemicals (Canada) Ltd. (Email: bernara@novachem.com; Phone: 519-862-2911 ext. 2350). He has more than 20 years of experience in plant operations and process design. He holds B.S.Ch.E. and M.S.Ch.E. degrees from l'École Polytechnique de Montréal in Canada. He is a member of the American Institute of Chemical Engineers, and registered professional engineer in the provinces of Ontario and Québec in Canada.

CFD Analysis of Heat Transfer From Flares

A way to obtain conservative estimates for the temperatures at the support structures of a flare system

Tushar Bhad, Sumanta Sarkar and Arvind Kaushik
Hydrocarbon IC, Larsen & Toubro Ltd.

A gas flare is an elevated vertical conveyance found accompanying oil wells, gas wells, drilling rigs, petroleum refineries, chemical plants, natural gas plants and so on. Although modern flare systems are specifically designed to reduce the thermal radiation, pollution and acoustic impact of a flare, a considerable amount of radiation is nevertheless emitted by an operational flare as a result of burning large quantities of combustible gases. The emitted radiation increases the temperature of the flare support structure and nearby structures. Therefore, it is essential to correctly estimate heat transfer from the flares to the structures when designing structures, selecting their materials of construction (MoC), selecting protective paints and so on.

Flare vendors sometimes provide temperature data on structures vis-à-vis distances from the flare tip based on predictions from their proprietary software, experimental data or correlations. In most of the cases, these predictions are based on two-dimensional (2D) planes, and detailed temperature data on three-dimensional (3D) geometries of the structures are not available.

In reality, the temperature of a flare support structure and the surrounding structures depends on several factors, such as the ambient air velocity and direction, the geometry of the flare tip and the composition of the combustible gases. Therefore, correct estimation of the predicted temperature is very difficult unless a detailed mathematical modeling of the entire system is carried out.

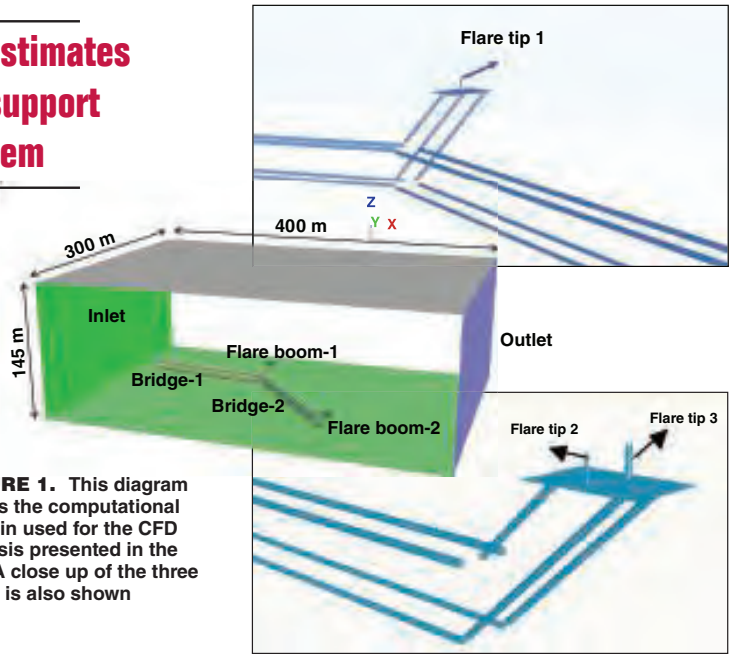

FIGURE 1. This diagram shows the computational domain used for the CFD analysis presented in the text. A close up of the three flares is also shown

Computational fluid dynamics (CFD) is the best tool to model such a system, incorporating all of the complexities to predict how flares will perform under realistic operating conditions with respect to different wind speed and direction. This is generally not possible with less-sophisticated software packages.

This article presents a CFD analysis for predicting the temperatures of neighboring structures of flares. Designing structures associated with flares is traditionally done based on industry practices. However, this may lead to over- or under-designing of the structures depending on the anticipated temperature of the structures when flares are under full load operation. Although several software packages are available for predicting the radiation intensity around a flare, only CFD takes account of the geometrical aspects, process variables, ambient air direction and temperature, combustion reactions and all modes of heat transfer in a 3D domain to accurately predict temperature of structures associated with flare systems, and thus eliminates the uncertainties associated with designing those structures.

In the current study, a comprehensive CFD analysis combining the effects of fluid flow, combustion and heat transfer — including radiation — has been carried out for an offshore oil-and-gas process complex having multiple flares, handling different gas compositions and mass flowrates. The adopted methodology is generic in nature and applicable to any flare system that may be present in any plant in the chemical process industries (CPI).

Four cases were studied for four

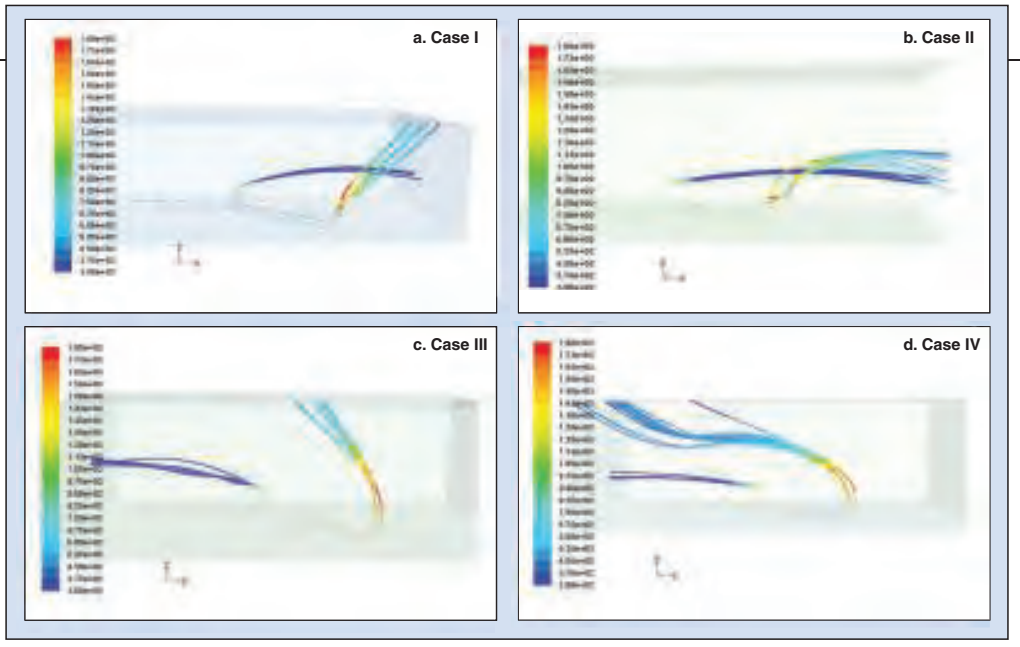

FIGURE 2. The influence of the wind direction and velocity can be seen in the temperature path lines for the four cases discussed in the text

different ambient conditions involving two wind directions and two wind speeds to find out the maximum temperature of the structures under full-load operation of flares. Steady-state heat-transfer analyses were carried out using a general-purpose, commercial CFD code. To take care of the effects of convective and radiative heat transfer from flares to the structures, combustion and radiation were also modeled. All of the combustible components of the different gases were converted to equivalent methane, and a single-step methane-oxidation reaction was modeled to limit the number of species present in the domain. The maximum temperature of the flames was predicted to be around 1,900°C. Also, it will be shown that even at full load operation and for the most adverse ambient conditions, temperature for the support structures and the connecting bridges would be well within the maximum allowable limit of structural steel.

Analysis approach

In the current study, CFD analyses are carried out for an offshore oil-and-gas process complex having three flares. These flares are disposed to atmosphere through tripods. The 3D domain are comprised of the two flare tripods and the interconnecting bridges. Steady-state heat-transfer analyses were carried out using a general-purpose, commercial CFD code considering a rectangular computational domain. Although the three flares are supposed to burn different gases, all the combustible components of the different gases were converted to equivalent methane and a single-step methane-combustion reaction ($CH_4 + 2O_2 = CO_2 + 2H_2O$) was modeled using eddy dissipation model. Radiation was modeled using the P1 model. The ideal gas law is used to determine density as a function of temperature. Heat transfer from the structural members to the ambient is modeled by providing a wall heat-transfer coefficient and ambient temperature. Four different cases were studied involving two wind directions and two wind speeds.

Mathematical model

Gas phase equations. The steady-state continuity and momentum equation of the gas phase are given as Equations (1) and (2). The source term, S_p, results from combustion. The component of velocity in coordinate direction x is given in Equation (2), which includes pressure, gravitational force (buoyancy effects), and the generalized source term. Equations for the y and z components are similar.

$$\frac{\partial}{\partial x_i}(\rho u_i) = S_p \tag{1}$$

$$\frac{\partial}{\partial x_j}(\rho u_i u_j) = -\frac{\partial p}{\partial x_i} + \frac{\partial \tau_{ij}}{\partial c_j} + \rho g_i + F_i + S_p \tag{2}$$

Model for turbulence. The model employed in the present simulation is the standard k-ϵ model proposed by Launder and Spalding. This employs two partial differential equations to estimate the velocity length scales of turbulence:

$$\frac{\partial}{\partial t}(\rho k) + \frac{\partial}{\partial x_j}(\rho u_j k) = \rho P - \rho\varepsilon + \frac{\partial}{\partial x_j}\left[\frac{(\mu_l + \mu_t)}{\sigma_k} \cdot \frac{\partial k}{\partial x_j}\right] \tag{3}$$

$$\frac{\partial}{\partial t}(\rho\varepsilon) + \frac{\partial}{\partial x_j}(\rho u_j \varepsilon) = C\varepsilon_1 \frac{\rho P \varepsilon}{k} - C\varepsilon_2 \frac{\rho\varepsilon^2}{k} + \frac{\partial}{\partial x_j}\left[\frac{(\mu_l + \mu_t)}{\sigma_k} \cdot \frac{\partial \varepsilon}{\partial x_j}\right] \tag{4}$$

In the above two equations, P represents the production term given by Equation (5).

$$P = \nu_t\left[\frac{\partial u_i}{\partial x_j} + \frac{\partial u_j}{\partial x_i} - \frac{2}{3} \cdot \frac{\partial U_m \delta_{ij}}{\partial x_m}\right]\frac{\partial u_j}{\partial x_j} - \frac{2}{3} k\delta_{ij} \tag{5}$$

The energy equation used to solve for enthalpy is given by Equation (6). The source term, S_h, in the energy equation includes combustion and radiation heat-transfer rates:

$$\frac{\partial}{\partial x_i}(\rho v_i h) = -\frac{\partial}{\partial x_i}\left(\Gamma_h \frac{\partial h}{\partial x_i}\right) + S_h \tag{6}$$

Owing to a higher temperature of the flame, radiation is the predominant mode of heat transfer from the flame to the structures. In the current modeling, radiation has been modeled using a commercial code. In the commercial radiation model, radiation flux (q_r) is

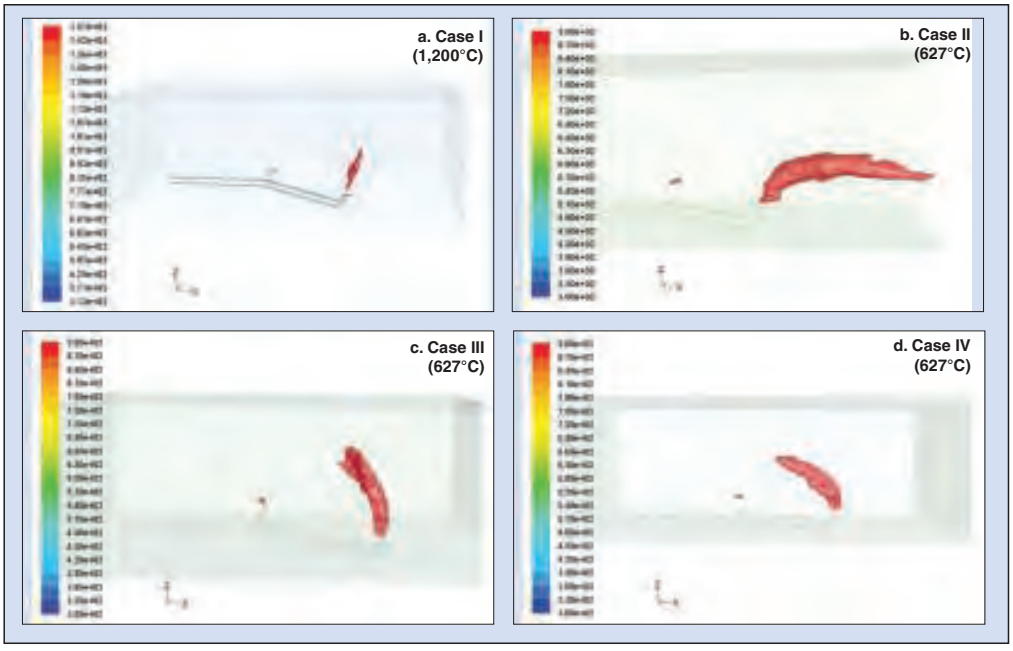

FIGURE 3. Shown here are iso-surface plots for the four cases. For Case I (iso-temperature 1,200°C) represents the flame shape. Those for Cases II–IV (iso-surface for 627°C) represent the direction and spread of the fluegas plume

defined by Equation (7), as follows:

$$-\nabla \cdot q_r = aG - 4an^2\sigma T^4 \quad (7)$$

Where G is the incident radiation, a is the absorption coefficient, n is the refractive index of the medium and σ is the Stefan-Boltzmann constant. The expression for radiation flux can be directly substituted into the energy equation to account for heat sources (or sinks) due to radiation.

Fuel combustion has been modeled using the eddy dissipation model. Combustion of methane is rapid and the combustion is said to be mixing-controlled, hence chemical kinetic rates can be safely neglected. The commercial code provides a turbulence-chemistry interaction model (eddy dissipation model), based on the work of Magnussen and Hjertager [*1*]. The net rate of production of species due to reaction r, $R_{i,r}$, is given by the smaller (that is, the limiting value) of the two expressions below, Equations (8) and (9).

$$R_{i,r} = v'_{i,r} M_{w,i} A\rho \frac{\varepsilon}{k} \min_R \left(\frac{Y_R}{v'_{R,r} M_{w,R}} \right) \quad (8)$$

$$R_{i,r} = v'_{i,r} M_{w,i} AB\rho \frac{\varepsilon}{k} \frac{\sum pY_p}{\sum_j^N v''_{j,r} M_{w,j}} \quad (9)$$

Where Y_p is the mass fraction of any product species, Y_R is the mass fraction of a particular reactant, A is an empirical constant equal to 4.0 and B is an empirical constant equal to 0.5.

In Equations (8) and (9), the chemical reaction rate is governed by the large-eddy mixing time scale, k/ϵ. Combustion proceeds whenever turbulence is present (k/ϵ > 0), and an ignition source is not required to initiate combustion.

Modeling and meshing

Geometry modeling and meshing are carried out using a commercial CAD (computer aided design) tool. The model consists of a rectangular domain (420 m × 300 m × 145 m) as shown in Figure 1. Bridges and flare support structures have been modeled at their respective locations considering only the main load-bearing members. This domain has been aligned with the wind direction. At the lower side, the domain boundary has been considered at a distance of 7 m from the bottom of the bridges. Close-up views of the flares along with the inclined support structures are shown as insets to Figure 1. The geometry has been meshed using a combination of structured (hexahedral) and unstructured (tetrahedral) elements with total number of volume elements as 2.7 million.

Boundary conditions

The following boundary conditions were used for performing the CFD analyses:

1. The mass-flow inlet boundary condition was used at the air inlet corresponding to air velocity of 15 knots (7.6 m/s).
2. The ambient air temperature was taken as 300K.
3. The pressure outlet boundary condition was specified as zero gauge pressure at the outlet boundaries.
4. The side walls and lower wall of computational domain are modeled as free slip walls.
5. The mass flow inlet boundary conditions used at the tips of the three flares are as follows:

Flare tip 1:	7 kg/s
Flare tip 2:	17 kg/s
Flare tip 3:	146 kg/s

6. The wall heat-transfer coefficient was calculated by Morgan co-relation, which was used to model the convective heat transfer.
7. The structural elements were modeled as thin surfaces with a thickness of zero.

Case studies

A total of four different cases have been studied for four different ambient conditions. The objective is to ascertain the maximum possible tem-

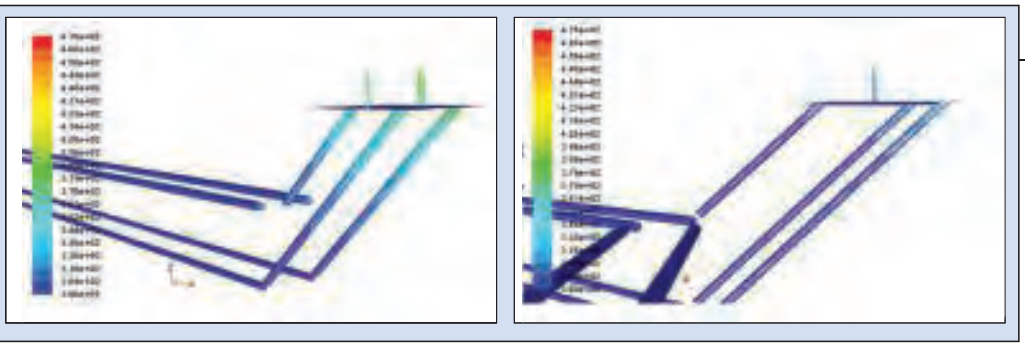

FIGURE 4. The temperatures of the supporting structure is shown here for Case I. Temperatures at discreet points for Cases I–IV are summarized in Table 1

TABLE 1. SUMMARY OF RESULTS FOR CASE I–IV

Case Number	I	II	III	IV
Wind direction	Normal	Normal	Opposite	Opposite
Wind speed, knots	15	30	15	30
Bridge 1 temperature, °C	29	28	30	30
F-2 Boom temperature, °C	60	61	60	54
F-2 Platform temperature, °C	121	122	126	135
Bridge 2 temperature, °C	62	39	54	52
F-1 Boom temperature,°C	182	195	187	164
F-1 Platform temperature, °C	282	352	332	321

perature (or worst case scenario) on the structures in the presence of combined convective and radiative heat transfer with different wind speeds and wind directions.

Case I: Normal wind direction, wind velocity at 15 knots. Figure 2a shows the path-line plots for plumes coming from the flares. These lines are the steady-state temperatures on the path-lines of plumes. Owing to the low mass flowrate of Flare 1 (low momentum, subsonic flow), one sees that the plume is diverted almost immediately along the direction of air flow. The maximum temperature is found to be limited to within a very small region near the tip of Flare 1 due to dissipation of heat from the hot plume to the large ambient surroundings.

For Flare 2 and Flare 3, the mass flowrate of the combustible gas is much higher, and flow velocity comes in the sonic to supersonic region. This leads to the generation of steeper plumes that are not as easily deflected by the ambient air flow. Also, due to the higher mass flowrate of combustible gas, a larger region is covered under the high temperature zone. The maximum temperature of the flames is calculated to be around 1,900°C.

Figure 3a presents an iso-surface (a surface having the same property everywhere) of the flares for 1,200°C. This plot gives an idea about the flame region having a temperature greater than 1,200°C. Anywhere outside the iso-surface, the temperature will be less than 1,200°C.

The steady-state temperature profile of the structures nearest to the flares are shown in Figure 4. The maximum temperature on the F-1 platform is calculated to be 282°C, whereas the same for F-2 is calculated to be 121°C. From the contour plot it can be seen that the maximum temperature of 282°C is limited to a very small region near the corner adjacent to the Flare 3.

The first column of Table 1 summarizes the maximum predicted temperatures of the structural elements.

Case II: Normal wind direction, wind velocity at 30 Knots. The parameters for Case II are the same as Case I except the wind speed has been doubled. Path line plots for temperature and the contour plot for temperature on iso-surface are shown in Figures 2b and 3b. There one sees that the higher ambient-air velocity causes the fluegas plumes to become horizontal more quickly as compared to the base case (Case I). The temperatures predicted for the support structures are presented in column 2 of Table 1.

Case III: Opposite wind direction, wind velocity 15 knots. For this case, the parameters are the same as Case I except the direction of the wind is reversed. The stream line plot for temperature and the contour plot for iso-temperature of 900K (627°C) are presented in Figures 2c and 3c. Streamline plot for Case II shows similar temperature and dispersion of the plume as the base case with the only difference being in the direction of plume.

Column 3 of Table 1 summarizes the predicted temperatures on the various support structures of the platforms for Case III.

Case IV: Opposite wind direction, wind velocity at 30 knots. For this final case, the parameters are the same as Case II except the wind direction is reversed. The stream line plot for temperature and contour plot for iso temperature of 627°C are presented in Figures 2d and 3d. The streamline plot for Case IV shows that the combined plume of Flare 2 and Flare 3 is diverted toward the living quarter platform owing to the higher wind speed. However, the plume gets dissipated as it moves away from the F-1 platform because of turbulence. The last column of Table 1 summarizes the predicted temperatures on the support structures and platforms for Case IV.

NOMENCLATURE

- P Pressure
- u, v, w Velocity components in the x, y, z directions
- x, y, z Three spatial directions
- S Volumetric rate of heat generation
- T Static temperature
- t Time
- k Turbulent kinetic energy
- ϵ Dissipation rate of kinetic energy
- ϕ Specific property, dependent variable
- ∂ Symbol for partial differential
- ρ Density
- Γ Diffusion coefficient
- μ Dynamic viscosity
- C Specific heat
- D Mass Diffusion coefficient
- $\nabla(x)$ Divergence of the variable x
- e Internal Energy per unit mass
- G Rate of generation of turbulent energy
- h Specific enthalpy
- 2D Two dimensional
- 3D Three dimensional

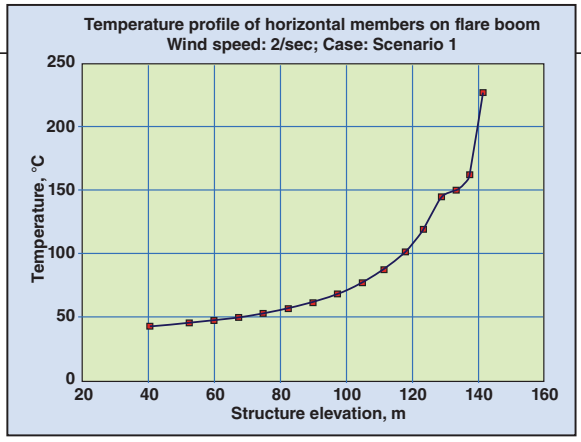

FIGURE 5. This graph plots the temperature variation along the boom length predicted by a flare-modeling software for a past project

Validation of results

Owing to limited or non-existing availability of actual field data, it is very difficult to validate results for this analysis. However, it has been attempted to compare the CFD analysis results with data from some past projects for comparable mass flowrates of the combustible gas as given below:

- CFD predicted maximum temperature compared (gas load: 146 + 17 = 163 kg/s) with the results of a flare modeling software predicted temperature (for 133 kg/s gas load) for a similar flare boom
- Maximum temperature predicted by CFD analysis was 352°C for the F1 platform while the predicted temperature for the reference case was 228°C, as shown in Figure 5. The reference case temperature was lower owing to the relatively lower mass flowrate of combustible gas (133 kg/s versus 163 kg/s for the case under consideration)
- The predictions from this CFD analysis for temperatures on the flare boom are believed to be conservative values for the designing of structures influenced by radiation from flares

Challenges

The following are some of the general challenges encountered while modeling a flare system:

- The handling of a considerably large size domain and therefore a relatively large mesh count
- The combination of both high- and and low-speed flows may be encountered depending on a flare's design. This results in a convergence problem
- Getting a converged solution for a system involving both combustion and radiation modeling in the large domain is challenging
- Multi component systems involving multiple species require high computation time
- Multiple case runs to arrive at the maximum possible temperature on the structures for safe design be-

comes time consuming
- There is a limited availability of experimental and field data for flares, which makes validation of results rather difficult

Broader applications

The methodology adopted to carry out the current study is generic in nature and the same steps can be followed to perform CFD analysis of any flare system and associated structures for any chemical process plant, refinery, oil-and-gas production facility and so on.

The same modeling technique is applicable to predict temperature around any hot gas stack, for example fluegases from incinerators, furnace stack, DG set stack and so on. However, this would not require modeling of the complex combustion reactions since the fluegas composition and the temperature data are often made available by the vendor or designer of the combustion system.■

Edited by Gerald Ondrey

References

1. Improving the Safety Standard of an Offshore Platform, Fluent News Letter, Spring 2001.
2. Stephen Ferguson, Computer Flow Simulation Provides New Insight into Hurricane-resistant Platform Design, Exploration & Production: The Oil & Gas Review 2006.
3. ANSYS Fluent user manual.

Authors

Arvind Kaushik is senior deputy general manager (R&D) at Larsen & Toubro Ltd. (Email: arvind_kaushik@lntenc.com). He has over 23 years of experience in the design of thermal equipment, process optimization, energy conservation in process plants, dynamic simulation of process and power plants, commissioning and trouble-shooting in India and overseas. He leads a team of mechanical and chemical engineers in the Thermal Engineering Group of R&D for innovations in design of waste heat recovery equipment. His areas of interest include solar thermal energy, low temperature thermal desalination, thermal energy storage systems, dynamic simulation of power plants, energy optimization of industrial processes and commissioning and trouble-shooting of process equipment. Kaushik is a post graduate (M.Tech) chemical engineer from Indian Institute of Technology (IIT; Kanpur, India), since 1990.

Tushar P. Bhad is an assistant manager, Hydrocarbon IC, R&D, Larsen & Toubro Ltd. (Mumbai 400072, India at Larsen & Tourbo Ltd. Mumbai, India; Email: tushar_bhad@lntenc.com). He has over three years of experience in the area of CFD modeling of thermal and fluid systems having various applications involving modeling of multi-phase flow, turbulence, combustion and heat transfer. At present his areas of interest include fluid flow, heat transfer, and modeling of multi-phase flow, combustion and radiation modeling using CFD. He has published papers in the CFD conferences and jointly filed for an Indian Patent in the year 2010. Bhad is a post graduate thermal engineer from WCE Sangli, India.

Sumanta Sarkar is deputy general manager (R&D) at Larsen & Toubro's Hydrocarbon IC (Email: sumanta_sarkar@lntenc.com). He is a post graduate (M. Tech.) chemical engineer from ITT, Kharagpur, and has 17 years of experience in the areas of CFD analysis, design & rating of thermal equipment and systems, operation, technical services, project execution, feasibility studies and technology evaluation. His current areas of interest are troubleshooting and design analysis of fluid & thermal systems through CFD modeling, involving multuphase flow, turbulence, reaction and heat transfer with combustion and radiation. He is a recipient of the Outstanding Young Chemical Engineer Award (IIChE) in 2007 and has published several papers in various CFD forums in India and abroad. He has jointly filed for an Indian Patent for Horizontal Heat Recovery Unit in the year 2010.

A Novel Equation for Isothermal Pipe Flow

A newly derived equation for isothermal gas flow in pipes yields improved mass flux predictions

Jung Seob Kim, SK E&C USA, Inc.
and **Navneet Singh,** Bayer CropScience LP

Compressible flow in pipes is common in the chemical process industries (CPI) and is typically associated with density changes in gases that are subjected to pressure variations. Gas flow conditions can be described using an adiabatic or isothermal flow equation. For conservative piping design, the isothermal model is favored, but it overpredicts mass flux through pipes.

The conventional isothermal model is relatively simple and more applicable to long, uninsulated pipelines. Flow conditions in long pipes and the flow of fluids with a low specific heat ratio (~1.0) are approximately isothermal. The temperature of the fluid is essentially constant and equal to the originating station temperature.

The homogeneous equilibrium model improved (HEMI) for pipe flows, developed by Kim and Dunsheath to better account for the change in density along the entire pipe length has been presented for all fluids [*1*]. Kim and Dunsheath noted that the term ρd*P* within the flow equation would result in somewhat higher mass flux than would be expected. This finding can be applied to the isothermal flow equation of ideal gases by manipulating the Bernoulli equation.

This article describes a novel isothermal pipe flow equation that better represents the properties of gas flow in a pipe and yields more accurate predictions of mass flux. The article also compares the calculation results of the two isothermal equations (novel versus conventional) using an example piping system. The newly derived, isothermal flow equation presented here is called the "novel isothermal pipe flow equation" for ideal gases (to differentiate it from the "conventional isothermal pipe flow equation").

One of the reasons for the preferential use of the isothermal flow equation, as compared to the adiabatic equation, is that the mass flux predictions are conservative. However, inappropriate calculations of average density using the conventional isothermal equation leads to non-conservative results, in terms of piping design. These results can lead to piping systems that lack the capacity to handle the mass flow. The novel isothermal equation yields more conservative results and correctly sized piping systems.

NOMENCLATURE

a,1,b	stations	*P*	absolute pressure, Pa
D	pipe inside diameter, m	R	universal gas constant, 8314.47 Pa-m^3/kg-mole-K
f	Fanning friction factor		
G	mass flux, kg/s-m^2		
G_c	critical mass flux, kg/s-m^2	*T*	absolute fluid temperature, K
L	pipe length, m	*υ*	velocity, m/s
M	gas molecular weight	*v*	specific volume, m^3/kg
Ma	Mach number	Δ	arithmetic difference
N	overall loss coefficient, 4fL/D + ∑K (total flow resistances of fittings)	ρ	fluid density, kg/m^3

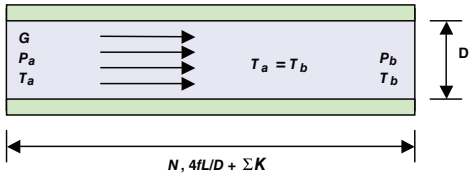

FIGURE 1. Parameters for typical isothermal flow of ideal gases in pipes include friction and fitting losses

Isothermal pipe flows

The novel isothermal pipe flow equation described in this article better represents the nature of isothermal pipe flow. Typical isothermal flow of ideal gases in a pipe with friction is shown in Figure 1. An ideal gas is one that obeys the equation of state for ideal gases. The compressibility factor (*Z*) of ideal gases is 1. The overall loss coefficient (*N*) includes pipe friction losses, in terms of $4fL/D$, as well as all fitting losses of ΣK. The loss coefficient of a frictional element can be included either as the equivalent length or the number of velocity heads. The temperature for isothermal flow is constant across the entire pipe length, and flow at constant temperature is very convenient to model. Elevation changes in pipelines can be neglected if gas densities are relatively small. In the problems presented here, there are no elevation changes for horizontal pipes (Figure 1).

Conventional equation

The designer of pipe flow systems favors an isothermal pipe flow equation because it is simple and conservative. There are numerous isothermal equations, but all are analogous to Equation (1) [*2–11*]. The mass flux (*G*) is determined from the calculated value of G^2. The choking conditions set a limit on the maximum pipe mass flux for a given set of pipe flow conditions. This means that lowering the pipe outlet

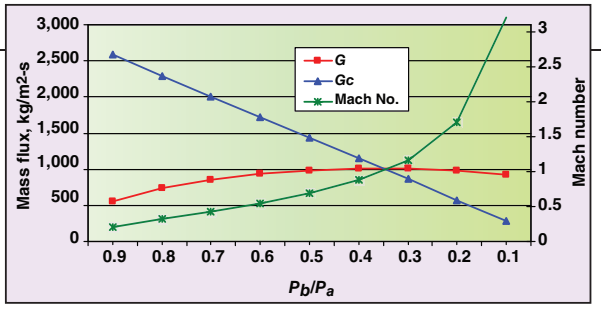

FIGURE 2. Mass flux predictions with the conventional isothermal flow equation tend to be higher because the equation does not correctly account for gas density changes

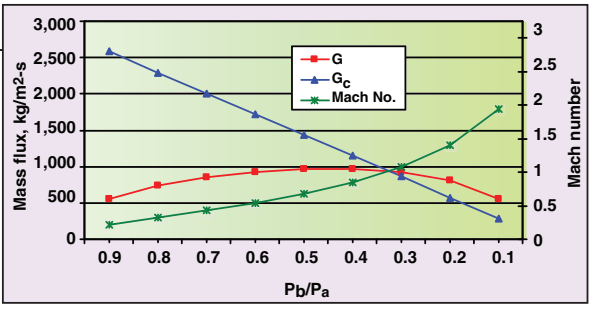

FIGURE 3. With the same piping system and inlet conditions as in Figure 2, the novel isothermal equation yields a smaller mass flux

pressure does not increase the mass flux. The choked mass flux is defined as Equation (2). Mach number is the ratio of the gas velocity to the velocity of sound in the gas under the given conditions and can be defined as Equation (3).

$$G^2 = \rho_{avg}\left(P_a - P_b\right)\frac{1}{\ln\frac{P_a}{P_b}+\frac{N}{2}} = \frac{M}{2RT}\left(P_a^{\,2} - P_b^{\,2}\right)\frac{1}{\ln\frac{P_a}{P_b}+\frac{N}{2}} \quad (1)$$

$$G_c = P_b\left[\frac{M}{RT}\right]^{0.5} \quad (2)$$

$$Ma_b = \frac{G}{G_c} \quad (3)$$

For the plot in Figure 2, an ideal gas of molecular weight 20 and specific heat ratio 1.0 is flowing through a constant-area piping system of $N = 5$. The gas pressure and temperature at the pipe inlet are 1,013,500 Pa and 300K, respectively. Figure 2 shows that the mass flux decreases slightly with a further decrease in outlet pressures after the flow chokes at the maximum mass flux. This means that the isothermal flow equation does not correctly account for the density changes in a pipe, and tends to overpredict the mass flux for the same pressure drop or underpredict the pressure drop for the same mass flux (see next section). But this has not been examined in the past because supersonic flow is not typically of interest to the piping system designer.

Novel isothermal equation

For the conventional isothermal flow equation, the calculation results have been found to overpredict mass flux, so there is a need to correct this deficiency. This fundamental drawback can be resolved by applying a physically real flow equation. A somewhat complicated Equation (4) represents the novel isothermal pipe flow equation developed based on the Bernoulli equation. The derivation of this equation is given in the box on p. 70.

$$G^2 = \frac{M}{RT}\frac{\left(P_a - P_b\right)}{\frac{\left(P_a - P_b\right)}{2P_b^{\,2}}\ln\left(\frac{P_a}{P_b}\right)^{-1}\left[1-\left(\frac{P_b}{P_a}\right)^2\right]+\frac{N}{P_a+P_b}} \quad (4)$$

Equation (4) is not perfect in the way it accounts for all the changes during flow in pipes. One of the pressure drop terms, expansion loss ($\Delta P_{expansion} = \Delta P_{total} - \Delta P_{kinetic} - \Delta P_{friction}$), can be accounted completely when the calculation is started from the stagnation pressure. However, Equation (4) provides conservative results because the changes in the expansion loss term will be smaller when the calculation is started from the stagnation pressure. The

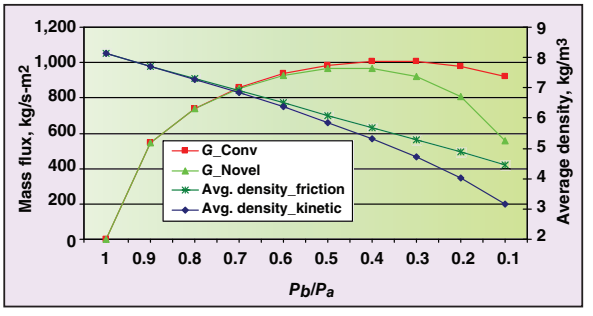

FIGURE 4. Mass flux and average density plots can help determine whether the novel or conventional isothermal flow equation should be used

plot in Figure 3 is created for the same inlet conditions and piping system as Figure 2. Figure 3 shows that choking occurs at a lower pressure ratio P_b/P_a (0.327 versus 0.352) than in the conventional isothermal flow equation.

The calculated choked mass flux (940 kg/s-m^2) is smaller than that calculated by the conventional isothermal flow equation (1,009 kg/s-m^2). It is interesting to note that Equation (4) does not achieve the maximum mass flux at choked conditions. On the other hand, the maximum mass flux is reached at choked conditions for the conventional isothermal pipe-flow Equation (6). As expected, the novel isothermal pipe-flow equation shows significant mass flux decrease after choking. Proper accounting for the variation in density at low pressure ratios is responsible for this difference.

Differences between models

The average density along the pipe can be determined by two different equations [Equations (5) and (6)]. One is based on arithmetic average density and the other is based on arithmetic average specific volume. An inappropriate selection of the equation affects the mass flux prediction. As shown in Figure 4, there are significant differences in mass flux at low pressure ratios (P_b/P_a). The difference in mass flux increases as the pressure ratio (P_b/P_a) decreases. From these results, it is considered unlikely that the conventional isothermal pipe flow equation predicts conservative mass flux calculations. However, for most operating conditions in industry, the two flow equations give similar mass flux results.

There are also apparent similarities between the two graphs of the mass flux and average density. Therefore, the mass flux difference between two equations is due to the different definition of average density along the pipe. The average density for the conventional isothermal flow equation is obtained using Equation (5) for both friction losses

and kinetic losses.

On the other hand, the novel isothermal flow equation is obtained using the average density for friction losses and the average density for kinetic losses using Equations (5) and (6), respectively. Applying the arithmetic average density for the friction losses is appropriate because the integration is based on N (pipe length), not on pressure. However, the arithmetic average density for the kinetic losses is not appropriate here because the integration is based on pressure, not on pipe length. The arithmetic average density is only a mathematically convenient solution that does not represent the actual average density for the kinetic loss term. Equation (6) is based on a density mixing rule to estimate the correct average density in pipe flows. The reciprocal of the arithmetic-average specific volume is both mathematically and physically satisfactory. This definition is much more representative of the average density for a kinetic loss term. In some cases, the arithmetic average density ends up with non-conservative calculation results.

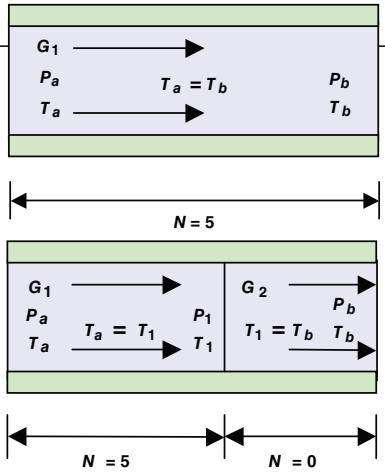

FIGURE 5. Splitting the pipe from one segment (top diagram) into two segments (two-step pipe flow; bottom diagram) can help determine which equation version is better for a particular case

$$\rho_{avg-friction} = \frac{\rho dP}{(P_a - P_b)} = \frac{M(P_a + P_b)}{2RT} \quad (5)$$

$$\rho_{avg-kinetic} = \frac{1}{v_{avg}} = \frac{P_a - P_b}{vdP} = \frac{M(P_a - P_b)}{RT \ln \frac{P_a}{P_b}} \quad (6)$$

Selecting the right model

The evaluation procedure outlined below examines the nature of the pipe flow for the assumed flow conditions. The mass flux calculation is extended to supersonic flow to maximize the effect of the arithmetic average density that results in the overprediction of mass flux. Therefore, the calculation results are supposed to provide a clue as to which flow equation is better or more applicable for cases involving short pipes with large pressure drops.

There are two different pipe outlet pressure locations for equivalent mass flux (Figure 4). The pipe outlet-pressure location, 101,350 Pa, is selected as one of them. Decreasing the pressure ratio (P_b/P_a) below choking conditions causes gas density to sig-

TABLE 1. EVALUATION RESULTS FOR DETERMINING THE BETTER ISOTHERMAL FLOW MODEL		
	Conventional (Equation 1)	**Novel (Equation 4)**
Mass Flux (G_1) with N = 5 for P_a to P_b	**921** kg/s-m^2	**557** kg/s-m^2
Irreversible Friction Losses (ΔP_1) at G_1 and N = 5 for P_a to P_b	474,871 Pa	173,527 Pa
Pressure (P_1)	630,206 Pa	908,450 Pa
Mass Flux with N = 5 for P_a to P_1	**921** kg/s-m^2	**557** kg/s-m^2
Irreversible Friction Losses (ΔP_2) at G_1 and N = 5 for P_a to P_1	322,083 Pa	100,628 Pa
$\Delta P_1 - \Delta P_2$	**152,788** Pa	**72,899** Pa
Mass Flux (G_2) with N = 0 for P_1 to P_b	**921** kg/s-m^2	**605** kg/s-m^2

nificantly decrease, which in turn increases the pressure drop. Using Equation (1) or Equation (4), the mass flux (G_1) for the one-step pipe flow path from P_a (1,013,500 Pa) to P_b (101,350 Pa) sketched in Figure 5 (top diagram) can be calculated. One can also calculate irreversible frictional losses (ΔP_1) for the one-step flow path using Equation (7).

$$\Delta P_{friction} = \frac{N}{2\rho_{avg-friction}} G^2 = \frac{NRT}{M(P_a + P_b)} G^2 \quad (7)$$

Another location for the equivalent mass flux shown in Figure 4 is located using Equation (1) or Equation (4) by changing P_b until the calculated mass flux equals G_1. For another flow-path case sketched in Figure 5 (bottom diagram), the pipeline is split into two pipe segments. The first pipe segment from P_a to P_1 is a frictional section. The second pipe segment from P_1 to P_b is a non-frictional section. Irreversible frictional losses (ΔP_2) for the two-step flow path can be calculated using Equation (7). The mass flux G_2 for the non-frictional pipe section is calculated using Equation (1) or (4) for N = 0. The calculated mass flux G_2 should be greater than G_1 if the flow equation is correct, because there is a net driving force — the difference of the friction losses ($\Delta P_1 - \Delta P_2$,) — that causes greater mass flux than G_1.

Table 1 exhibits the calculation results for the two pipe-flow equations. For the conventional isothermal flow equation, G_2 is not greater than G_1. This means that the one-step pipe flow path from 1,013,500 to 101,350 Pa results in same mass flux, even though the irreversible frictional losses are greater. The conventional isothermal equation overpredicts mass flux. Note that the direction of the arithmetic average density is to overpredict mass flux. In addition, two different irreversible frictional losses at the equivalent mass flux are contradictory. On the other hand, a novel isothermal flow equation gives a value of G_2 that is greater than G_1. This means that the novel isothermal pipe flow equation obeys the fundamental principles of flow in pipes. Therefore, it is evident that the novel isothermal equation represented by Equation (4) yields better results than the conventional isothermal equation.

DERIVATION OF THE NOVEL, ISOTHERMAL HORIZONTAL-PIPE-FLOW EQUATION

On the basis of the Bernoulli equation, if there is no friction, a general mechanical-energy equation for horizontal pipe flow can be written as:

$$\frac{dP}{\rho} + d\left(\frac{u^2}{2}\right) = 0 \quad \text{(A-1)}$$

Since $d\left(\frac{u^2}{2}\right) = u\ du$, Equation (A-1) can be written as:

$$\frac{dP}{\rho} + u\ du = 0 \quad \text{(A-2)}$$

Since $\rho = \frac{1}{v}$ and $u\ du = G^2 v dv$, Equation (A-2) can be written as:

$$vdP + G^2 v dv = 0 \quad \text{(A-3)}$$

Integrating Equation (A-3) between stations *a* and *b* gives:

$$(P_a - P_b) = -G^2 \frac{(v_a^{\ 2} - v_b^{\ 2})}{2v_{avg}} \quad \text{(A-4)}$$

For an isothermal flow of ideal gases $\left(v = \frac{RT}{MP}\right)$, Equation (A-4) becomes:

$$(P_a - P_b) = G^2 \frac{1}{2v_{avg}P_b^{\ 2}}\left(\frac{RT}{M}\right)^2\left[1 - \left(\frac{P_b}{P_a}\right)^2\right] \quad \text{(A-5)}$$

Equation (A-5) is defined as a kinetic loss term. However, the kinetic loss term includes an expansion loss term. For an actual pipe flow, a friction loss term is required to be included in Equation (A-5).

Since the friction loss term is $\frac{G^2}{2\rho_{avg-friction}}N$, Equation (A-5) can be written as:

$$(P_a - P_b) = G^2\left[\frac{1}{2v_{avg}P_b^{\ 2}}\left(\frac{RT}{M}\right)^2\left(1 - \left(\frac{P_b}{P_a}\right)^2\right) + \frac{1}{2\rho_{avg-friction}}N\right] \quad \text{(A-6)}$$

Since $v_{avg} = \frac{1}{\rho_{avg-kinetic}} = \frac{v\ dP}{P_a - P_b} = \frac{RT\ln\frac{P_a}{P_b}}{M(P_a - P_b)}$ and

$$\rho_{avg-friction} = \frac{\rho dP}{(P_a - P_b)} = \frac{M(P_a + P_b)}{2RT},$$

Equation (A-6) can be written as:

$$(P_a - P_b) = G^2\frac{RT}{M}\left[\frac{(P_a - P_b)}{2P_b^{\ 2}\ln\frac{P_a}{P_b}}\left(1 - \left(\frac{P_b}{P_a}\right)^2\right) + \frac{1}{(P_a + P_b)}N\right] \quad \text{(A-7)}$$

Rearranging Equation (A-7) for G^2 gives:

$$G^2 = \frac{M}{RT}\frac{(P_a - P_b)}{\frac{(P_a - P_b)}{2P_b^{\ 2}}\ln\left(\frac{P_a}{P_b}\right)^{-1}\left[1 - \left(\frac{P_b}{P_a}\right)^2\right] + \frac{N}{P_a + P_b}} \quad \text{(A-8)}$$

Concluding remarks

Conservative pipe design considerations favor the use of the isothermal flow equation over the adiabatic flow equation. However, the conservative results of conventional isothermal flow equation are no longer true because the arithmetic average density used in the conventional isothermal pipe-flow equation tends to overpredict the mass flux in pipes. Although the mass flux overprediction of vapor flow is not significant, the definition of average density in a pipe affects mass flux if the pipe pressure drop is greater than 40% of the inlet pressure.

It should also be noted that the arithmetic average density does not represent the flow behavior in a pipe, since the variation of density with pressure changes in a pipe is nonlinear. Unfortunately, the use of arithmetic average density in the conventional isothermal equation has not previously been identified in the literature. However, the novel isothermal pipe-flow equation employs the arithmetic-average specific volume for the kinetic loss term. This enables the novel isothermal flow equation to better represent the nature of flow in a pipe and to accurately predict mass flux results without any constraints. Therefore, conservative and safer design considerations favor the use of the novel isothermal pipe-flow equation. ■

Edited by Scott Jenkins

References

1. Kim, J.S. and Dunsheath, H.J., "A Homogeneous Equilibrium Model Improved for Pipe Flows," Proceedings of World Congress on Engineering and Computer Science 2010 Vol. II WCECS 2010, October 20–22, San Francisco, pp. 733–738, 2010.
2. Shapiro, A.H., "The Dynamics and Thermodynamics of Compressible Fluid Flow," Vol. 1, The Ronald Press Company, New York, 1953.
3. McCabe, W.L. and Smith, J.C., "Unit Operations of Chemical Engineering," McGraw-Hill, New York, 1976.
4. Crowl, D.A. and Louvar, J.F., "Chemical Process Safety: Fundamentals with Applications," Prentice-Hall, Englewood Cliffs, N.J., 1990.
5. Saad, M.A., "Compressible Fluid Flow," Prentice-Hall, Englewood Cliffs, N.J., 1985.
6. Holland, F.A. and Bragg, R., "Fluid Flow for Chemical Engineers," Elsevier Inc., Amsterdam, 1995.
7. Green, D. and Perry, R.H., "Perry's Chemical Engineers' Handbook," McGraw-Hill, 2008.
8. "Flow of Fluids through Valves, Fittings, and Pipe," Crane Technical Paper No. 410, 1988.
9. "Pressure-relieving and Depressuring Systems," ANSI/API Standard 521, pp. 104–110, January 2007.
10. Kern, R., How to Size Piping and Components as Gas Expands at Flow Conditions, *Chem. Eng.*, October, 1975, pp. 125–132.
11. Walters, T., Gas-Flow Calculations: Don't Choke, *Chem. Eng.*, January 2000, cover story.

Author

Jung Seob Kim is a senior process engineer at SK E&C USA Inc. (1401 Enclave Parkway Suite 100, Houston, TX 77077; Phone: 281-258-2619; Email: jkim3@sk.com) where he is responsible for designing petrochemical and refinery plants. He has more than 25 years of experience in different roles within the petrochemical process industry including with Bayer Technology Services, Samsung BP Chemicals and Samsung Engineering. He holds a B.S.Ch.E. from the University of Seoul, is a member of AIChE, and is a registered professional engineer in the State of Texas.

Navneet R. Singh is a Senior Process Engineer at Bayer CropScience LP (8400 Hawthorne Road, Kansas City, MO 64120; Phone : 816-242-2738; Email: navneet.singh@bayer.com) where he is responsible for process design, process modeling and emergency relief system design. He holds M.S. and Ph.D. degrees from Purdue University and a B.S.Ch.E. degree from the Institute of Chemical Technology, Mumbai. He is a Senior member of AIChE and an engineer intern in the State of West Virginia.

Take advantage of ChemInnovation's SHOW SPECIAL for ACHEMA participants.

Visit us at ACHEMA in Hall 9.0, Stand E2

Contact Carley Ziober,
+1-713-343-1884
or Petra Trautes,
+49 (69) 58604760

CHEMICAL ENGINEERING
presents the 3rd Annual

CHEM|NNOVATIONS 2012

CONFERENCE & EXPO

November 14 - 15, 2012

NEW ORLEANS, LA | ERNEST N. MORIAL CONVENTION CENTER

ChemInnovations, the leading process industries event in the Americas focused on Chemical, Petrochemical and Refining.

How can you maximize your time and money at ChemInnovations 2012?

- The Americas has a hotbed of activity! Over $10.3 billion is expected in Capital and Maintenance projects for 2012 in North America that is over 990 plants with in the Chemical Process Industries.
- Conference Content planned by the industry for the industry. Conference tracks focused on Chemical Process Industry challenges for Primer/Entry Level and Intermediate/ Management Level.
- See over 150 new technologies and solutions on the ChemInnovations show floor alone.

www.cpievent.com

CO-LOCATED WITH:

SHALE ENVIROSAFE
CONFERENCE & EXHIBITION

How is natural gas changing the CPI? The United States has become competitive for investments with the recent development from shale gas.

Find out at the co-located event Shale EnviroSafe the latest on regulatory issues, how costs are affecting feedstock, chemicals that are being provided to the oil & gas industry for fracking and much more.

A very confined space

Mike Resetarits is the technical director at Fractionation Research, Inc. (FRI; Stillwater, Okla.; www.fri.org), a distillation research consortium. Each month, Mike shares his first-hand experience with *CE* readers

Circa 1978, Reese and I visited a petrochemical plant in Corpus Christi, Texas. Primarily, our job was to inspect trays that had been installed in three columns. Each of those columns was about 10 ft in diameter and 100 ft tall.

Our first mistake: We tried inspecting all three columns on the same day. By the time we got to the third column we were physically drained. Nevertheless, with shaky legs and arms, we climbed up the outside of the third column. We entered the top of the column via a 24-in. dia. manhole.

Our second mistake: We told no member of the plant staff that we were entering the third column. Per our instructions, the deck manways on the 40 trays had been left open. This afforded us a path downward through the stack of trays, for our inspection. I went down first. Reese followed (above me). At each successive tray, I checked the installation and took a few measurements. Above me, Reese took notes. The trays were spaced 2 ft apart. The manway cross-section was only 17 in. by 17 in. This made descents, and ascents, difficult.

After about one hour, Trays 1 to 30 were sufficiently inspected, and there were just 10 more trays to go, but I began to feel light-headed and weak. Reese was just above me, but I could only see his feet. I said, "Hey Reese, how are you feeling." He called down, "I feel like stretching out on one of these trays and falling asleep." I said, "Me too. I can barely speak and think. Something's wrong! Let's get out of here!" Actually, at that moment, we were not sure that we could. It took all of our energy and our complete focus to muster the strength to climb up through the 30 trays that we had already inspected. We could not see each other's face but we spoke constantly. The sentences were different but each had the same inherent meaning: Keep going!

The next 20 minutes seemed like 20 hours. Reese reached the top tray and then exited the column. I was just inches and minutes behind him. The outside air smelled and felt good. After about 15 min we both felt well again — well enough to climb down the outside of the column. Before reaching the ground we stopped at Deck 1, about 20 ft up.

There it was, our third and biggest mistake: The lower column manhole was not open. Air was not circulating through the column while we were in it. Whatever we were breathing inside the column, down low in the column, was not air. It was possibly gasoline vapors. It was probably deficient in oxygen. Had we stayed in the column just a few more minutes, a rescue team would have been needed to pull our lifeless bodies out through the manways, assuming that the rescue team did not make the same mistakes that we did.

Back in the 1970s, safety training was too-often defined as "an annual PPE [personal protective equipment] transparency presentation." Back then, and now, confined spaces are very dangerous places. ■

Mike Resetarits
resetarits@fri.org

Intelligen Suite®

The Market-Leading Engineering Suite for Modeling, Evaluation, Scheduling, and Debottlenecking of Multi-Product Facilities

SuperPro®

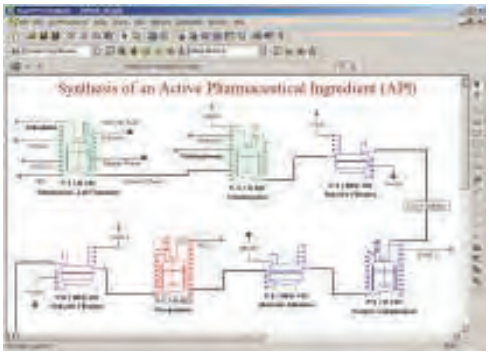

Use SuperPro Designer to model, evaluate, and optimize batch and continuous processes

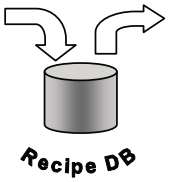

SchedulePro®

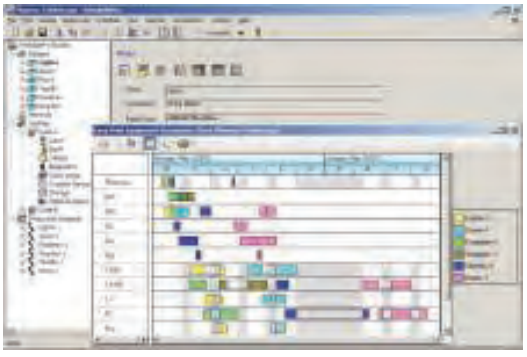

Migrate to SchedulePro to model, schedule, and debottleneck multi-product facilities

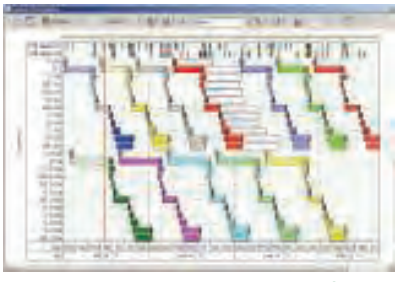

Easy production tracking, conflict resolution and rescheduling

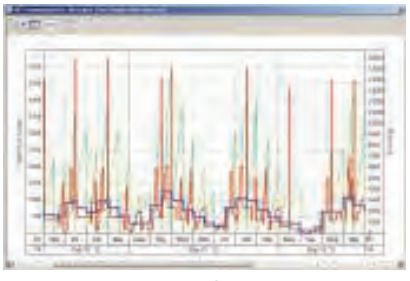

Tracking demand for resources (e.g., labor, materials, utilities, etc.)

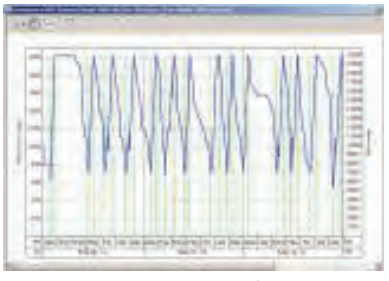

Managing inventories for input, intermediate, and output materials

SuperPro Designer is a comprehensive process simulator that facilitates modeling, cost analysis, debottlenecking, cycle time reduction, and environmental impact assessment of integrated biochemical, bio-fuel, fine chemical, pharmaceutical (bulk & fine), food, consumer product, mineral processing, water purification, wastewater treatment, and related processes. Its development was initiated at the Massachusetts Institute of Technology (MIT). SuperPro is already in use at more than 500 companies and 900 universities around the globe (including 18 of the top 20 pharmaceutical companies and 9 of the top 10 biopharmaceutical companies).

SchedulePro is a versatile production planning, scheduling, and resource management tool. It generates feasible production schedules for multi-product facilities that do not violate constraints related to the limited availability of equipment, labor, utilities, and inventories of materials. It can be used in conjunction with SuperPro (by importing its recipes) or independently (by creating recipes directly in SchedulePro). Any industry that manufactures multiple products by sharing production lines and resources can benefit from the use of SchedulePro. Engineering companies use it as a modeling tool to size shared utilities, determine equipment requirements, reduce cycle times, and debottleneck facilities.

Visit our website to download detailed product literature and functional evaluation versions of our tools

INTELLIGEN, INC. • 2326 Morse Avenue • Scotch Plains, NJ 07076 • USA
Tel: (908) 654-0088 • Fax: (908) 654-3866
Email: info@intelligen.com • Website: www.intelligen.com
Intelligen also has offices in Europe and representatives in countries around the world

Circle 240 on p. 76 or go to adlinks.che.com/40268-240

NEW & USED EQUIPMENT

JustFAXit! or go to www.che.com/adlinks

Fill out the form and circle or write in the number(s) below, cut it out, and fax it to 800-571-7730.

Go on the Web and fill out the online reader service card.

Name _____ Title _____

Company _____

Address _____

City _____ State/Province _____ Zip/Postal Code _____

Country\ _____ Telephone _____ Fax _____

Email _____

FREE PRODUCT INFO

(please answer all the questions)

YOUR INDUSTRY

01 Food & Beverages
02 Wood, Pulp & Paper
03 Inorganic Chemicals
04 Plastics, Synthetic Resins
05 Drugs & Cosmetics
06 Soaps & Detergents
07 Paints & Allied Products
08 Organic Chemicals
09 Agricultural Chemicals
10 Petroleum Refining, Coal Products
11 Rubber & Misc. Plastics
12 Stone, Clay, Glass, Ceramics
13 Metallurgical & Metal Products
14 Engineering, Design & Construction Firms
15 Engineering/Environmental Services
16 Equipment Manufacturer
17 Energy incl. Co-generation
18 Other_____

JOB FUNCTION

20 Corporate Management
21 Plant Operations incl. Maintenance
22 Engineering
23 Research & Development
24 Safety & Environmental
26 Other_____

EMPLOYEE SIZE

28 Less than 10 Employees
29 10 to 49 Employees
30 50 to 99 Employees
31 100 to 249 Employees
32 250 to 499 Employees
33 500 to 999 Employees
34 1,000 or more Employees

YOU RECOMMEND, SPECIFY, PURCHASE

(please circle all that apply)

40 Drying Equipment
41 Filtration/Separation Equipment
42 Heat Transfer/Energy Conservation Equipment
43 Instrumentation & Control Systems
44 Mixing, Blending Equipment
45 Motors, Motor Controls
46 Piping, Tubing, Fittings
47 Pollution Control Equipment & Systems
48 Pumps
49 Safety Equipment & Services
50 Size Reduction & Agglomeration Equipment
51 Solids Handling Equipment
52 Tanks, Vessels, Reactors
53 Valves
54 Engineering Computers/Software/Peripherals
55 Water Treatment Chemicals & Equipment
56 Hazardous Waste Management Systems
57 Chemicals & Raw Materials
58 Materials of Construction
59 Compressors

1	16	31	46	61	76	91	106	121	136	151	166	181	196	211	226	241	256	271	286	301	316	331	346	361	376	391	406	421	436	451	466	481	496	511	526	541	556	571	586
2	17	32	47	62	77	92	107	122	137	152	167	182	197	212	227	242	257	272	287	302	317	332	347	362	377	392	407	422	437	452	467	482	497	512	527	542	557	572	587
3	18	33	48	63	78	93	108	123	138	153	168	183	198	213	228	243	258	273	288	303	318	333	348	363	378	393	408	423	438	453	468	483	498	513	528	543	558	573	588
4	19	34	49	64	79	94	109	124	139	154	169	184	199	214	229	244	259	274	289	304	319	334	349	364	379	394	409	424	439	454	469	484	499	514	529	544	559	574	589
5	20	35	50	65	80	95	110	125	140	155	170	185	200	215	230	245	260	275	290	305	320	335	350	365	380	395	410	425	440	455	470	485	500	515	530	545	560	575	590
6	21	36	51	66	81	96	111	126	141	156	171	186	201	216	231	246	261	276	291	306	321	336	351	366	381	396	411	426	441	456	471	486	501	516	531	546	561	576	591
7	22	37	52	67	82	97	112	127	142	157	172	187	202	217	232	247	262	277	292	307	322	337	352	367	382	397	412	427	442	457	472	487	502	517	532	547	562	577	592
8	23	38	53	68	83	98	113	128	143	158	173	188	203	218	233	248	263	278	293	308	323	338	353	368	383	398	413	428	443	458	473	488	503	518	533	548	563	578	593
9	24	39	54	69	84	99	114	129	144	159	174	189	204	219	234	249	264	279	294	309	324	339	354	369	384	399	414	429	444	459	474	489	504	519	534	549	564	579	594
10	25	40	55	70	85	100	115	130	145	160	175	190	205	220	235	250	265	280	295	310	325	340	355	370	385	400	415	430	445	460	475	490	505	520	535	550	565	580	595
11	26	41	56	71	86	101	116	131	146	161	176	191	206	221	236	251	266	281	296	311	326	341	356	371	386	401	416	431	446	461	476	491	506	521	536	551	566	581	596
12	27	42	57	72	87	102	117	132	147	162	177	192	207	222	237	252	267	282	297	312	327	342	357	372	387	402	417	432	447	462	477	492	507	522	537	552	567	582	597
13	28	43	58	73	88	103	118	133	148	163	178	193	208	223	238	253	268	283	298	313	328	343	358	373	388	403	418	433	448	463	478	493	508	523	538	553	568	583	598
14	29	44	59	74	89	104	119	134	149	164	179	194	209	224	239	254	269	284	299	314	329	344	359	374	389	404	419	434	449	464	479	494	509	524	539	554	569	584	599
15	30	45	60	75	90	105	120	135	150	165	180	195	210	225	240	255	270	285	300	315	330	345	360	375	390	405	420	435	450	465	480	495	510	525	540	555	570	585	600

If number(s) do not appear above, please write them here and circle: _____

Fax this page back to 800-571-7730

ADVERTISING SALES REPRESENTATIVES

North America

Eric Freer, **District Sales Manager**
Chemical Engineering
11000 Richmond Ave, Suite 690, Houston, TX 77042
Tel: 713-343-1904 *E-mail:* efreer@che.com
Alabama, Alaska, Canada, Connecticut, Delaware, Florida, Hawaii, Idaho, Kentucky, Maine, Maryland, Massachusetts, Michigan, Mississippi, Montana, Nebraska, New Hampshire, New Jersey, New York, North & South Carolina, North & South Dakota, Ohio, Oregon, Pennsylvania, Rhode Island, Tennessee, Utah, Vermont, Virginia, Washington, D.C., West Virginia, Wyoming, Latin America

Jason Bullock,
District Sales Manager
Chemical Engineering
8325 Broadway, Ste. 202/PMB 261
Pearland, TX 77581
Tel: 281-485-4077; Fax: 281-485-1285
E-mail: jbullock@che.com;
Arkansas, Arizona, California, Colorado, Georgia, Kansas, Louisiana, Missouri, New Mexico, Nevada, Oklahoma, Texas, Washington

Dan Gentile
District Sales Manager
Tel: 512-918-8075
E-mail: dgentile@che.com
Indiana, Illinois, Iowa, Minnesota, Wisconsin

Diane Hammes
Inside Sales Manager
Chemical Engineering;
11000 Richmond Ave, Suite 690, Houston, TX 77042
Tel: 713-444-9939
E-mail: dhammes@che.com
Product Showcase, Literature Reviews, Classified Display Advertising

International

Petra Trautes
Chemical Engineering
Zeilweg 44
D-60439 Frankfurt am Main
Germany
Phone: +49-69-58604760
Fax: +49-69-5700-2484
Email: ptrautes@che.com
Austria, Czech Republic, Benelux, Eastern Europe, Germany, Scandinavia, Switzerland, United Kingdom

Dipali Dhar
Chemical Engineering
88 Pine Street, 5th floor, New York, NY 10005
Tel: 718-263-1162
E-mail: ddhar@accessintel.com
India

Katshuhiro Ishii
Chemical Engineering
Ace Media Service Inc., 12-6, 4-chome
Nishiiko, Adachi-ku, Tokyo 121, Japan
Tel: 81-3-5691-3335; Fax: 81-3-5691-3336
E-mail: amskatsu@dream.com
Japan

Ferruccio Silvera
Chemical Engineering
Silvera Pubblicita
Viale Monza, 24 Milano 20127, Italy
Tel: 39-02-284-6716;
Fax: 39-02-289-3849
E-mail: ferruccio@silvera.it/www.silvera.it
Andorra, France, Gibraltar, Greece, Israel, Italy, Portugal, Spain

Rudy Teng
Sales Represntative
Chemical Engineering;
Room 1102 #20 Aly 199 Baiyang Road
Pudong Shanghai 201204
China
Tel: +86 21 50592439
Fax: +86 21 50592442
MP: +86 13818181202
E-mail: rudy.teng@gmail.com
Asia-Pacific, Hong Kong, People's Republic of China, Taiwan

Advertisers' Index

Advertiser *Phone number*	Page number *Reader Service #*
A Box 4 U *1-877-522-6948* *adlinks.che.com/40268-01*	**59**
Abbe, Paul O. *1-800-524-2188* *adlinks.che.com/40268-02*	**32D-4**
* **Alfa Laval Copenhagen A/S** *adlinks.che.com/40268-03*	**32I-12**
Almatec Maschinenbau GmbH *1-714-396-1502* *adlinks.che.com/40268-04*	**29**
AUMA Riester GmbH & Co. KG *49 7631 809-0* *adlinks.che.com/40268-05*	**28**
Berndorf Band GmbH *43 2672 800-0* *adlinks.che.com/40268-06*	**17**
Beumer Group GmbH & Co. KG *adlinks.che.com/40268-07*	**7**
Bronkhorst - High Tech B.V. *adlinks.che.com/40268-09*	**8**
Buhler Aeroglide *1-919-851-2000* *adlinks.che.com/40268-08*	**55**
* **Buss-SMS-Canzler GmbH** *49 60 3385-0* *adlinks.che.com/40268-10*	**32I-14**
Cashco VCI *1-785-472-4461* *adlinks.che.com/40268-11*	**11**
Chemstations, Inc. *adlinks.che.com/40268-12*	**16**
Clean Harbors *1-800-422-8998* *adlinks.che.com/40268-13*	**56**
Collins Instrument Co. *1-979-849-8266* *adlinks.che.com/40268-14*	**57**
De Dietrich Process Systems GmbH *adlinks.che.com/40268-15*	**23**
Dupre Logistics *1-800-356-3658* *adlinks.che.com/40268-16*	**21**
Edwards Ltd. *adlinks.che.com/40268-17*	**58**
Ekato Rühr- und Mischtechnik GmbH *49 7622 29-0* *adlinks.che.com/40268-18*	**72**
EPI Engineering *1-800-551-9739* *adlinks.che.com/40268-19*	**FOURTH COVER**
Equipnet Direct *1-781-821-3482* *adlinks.che.com/40268-290*	**69**

Advertiser *Phone number*	Page number *Reader Service #*
Fike Corporation *1-866-758-6004* *adlinks.che.com/40268-20*	**14**
Flexicon Corporation *1-888-FLEXICON* *adlinks.che.com/40268-21*	**SECOND COVER**
* **GEA Niro** *45 39 54 54 54* *adlinks.che.com/40268-22*	**32I-3**
GEA Westfalia Separator Group GmbH *49 2522 77-0* *adlinks.che.com/40268-23*	**19**
* **GEA Wiegand GmbH** *49 7243 705-0* *adlinks.che.com/40268-24*	**32I-8**
GEMÜ Gebr. Müller Aparatebau GmbH & Co. KG *adlinks.che.com/40268-25*	**18**
GIG Karasek GmbH *adlinks.che.com/40268-26*	**27**
* **Haver & Boecker** *49 2522 30-271* *adlinks.che.com/40268-27*	**32I-11**
Heat Transfer Research, Inc. *adlinks.che.com/40268-28*	**65**
Hytorc *1-877GUN-2-GUN* *adlinks.che.com/40268-29*	**32a-32d**
* **Italvacuum** *39 011 470 4651* *adlinks.che.com/40268-30*	**32I-4**
* **KSB AG** *adlinks.che.com/40268-31*	**32I-5**

Advertiser *Phone number*	Page number *Reader Service #*
* **Lewa GmbH** *49 7152 14-0* *adlinks.che.com/40268-32*	**32I-6**
List AG *adlinks.che.com/40268-33*	**31**
Load Controls *1-888-600-3247* *adlinks.che.com/40268-34*	**32D-3**
Magnetrol *1-800-624-8765* *adlinks.che.com/40268-35*	**47**
Metso Corporation *adlinks.che.com/40268-36*	**13**
Müller GmbH *49 (0) 7623/969-0* *adlinks.che.com/40268-37*	**8**
MultiTherm LLC *1-800-339-7991* *adlinks.che.com/40268-38*	**45**
Orion Instruments *1-866-55-ORION* *adlinks.che.com/40268-39*	**10**
Outotec Oyj *adlinks.che.com/40268-40*	**6**
* **Phoenix Contact** *495 235 349494* *adlinks.che.com/40268-41*	**32I-7**
* **Pompetravaini** *39.0331.889000* *adlinks.che.com/40268-42*	**32I-10**
* **R. Stahl Schaltgeräte GmbH** *49 7942 943-0* *adlinks.che.com/40268-43*	**32I-15**
Saint Gobain Ceramics *1-716-278-6233* *adlinks.che.com/40268-44*	**25**

Advertiser *Phone number*	Page number *Reader Service #*
Samson AG *49 69 4009-0* *adlinks.che.com/40268-45*	**15**
Schmidt & Clemens GmbH & Co. KG *49 2266 92-0* *adlinks.che.com/40268-46*	**64**
Siemens AG I IA&DT CC *adlinks.che.com/40268-47*	**7**
Solutia, Inc. *1-800-426-2463* *adlinks.che.com/40268-48*	**2**
SoundPLAN International LLC *1-360-432-9840* *adlinks.che.com/40268-49*	**64**
Spencer Turbine *1-800-232-4321* *adlinks.che.com/40268-50*	**46**
Sulzer Chemtech AG *41 61 486 3737* *adlinks.che.com/40268-51*	**1**
Swagelok Company *adlinks.che.com/40268-52*	**4**
TLV Corporation *1-704-597-9070* *adlinks.che.com/40268-53*	**41**
* **Uhde GmbH** *adlinks.che.com/40268-54*	**32I-9**
WEFTEC *adlinks.che.com/40268-55*	**68**
Wood Group Mustang *adlinks.che.com/40268-56*	**32**
* **Zeppelin Silos & Systems GmbH** *adlinks.che.com/40268-57*	**32I-15**

* International Edition

Classified Index June 2012

Advertiser *Phone number*	Page number *Reader Service #*
Applied e-Simulators Software *adlinks.che.com/40268-241*	**75**
Equipnet Direct *1-781-821-3482* *adlinks.che.com/40268-242*	**75**
Eriez Manufacturing Co. *1-888-300-3743* *adlinks.che.com/40268-243*	**75**
Indeck Power Equipment Co. *1-847-541-8300* *adlinks.che.com/40268-244*	**75**
Intelligen Inc. *1-908-654-0088* *adlinks.che.com/40268-240*	**74**
NLB Corp. *1-248-624-5555* *adlinks.che.com/40268-201*	**73**
Plast-O-Matic Valves, Inc. *1-973-256-3000* *adlinks.che.com/40268-202*	**73**
Ross, Charles & Son Company *1-800-243-ROSS* *adlinks.che.com/40268-245*	**75**

Advertiser's Product Showcase 73
Computer Software 74–75
Equipment, New & Used 75

Advertiser *Phone number*	Page number *Reader Service #*
Shiv Shakti Process Equipments Pvt. Ltd. *91-22-2678-8480* *adlinks.che.com/40268-203*	**73**
Wabash Power Equipment Co. *1-800-704-2002* *adlinks.che.com/40268-246*	**75**
Xchanger, Inc. *1-952-933-2559* *adlinks.che.com/40268-247*	**75**

Send Advertisements and Box replies to: Diane Hammes

***Chemical Engineering*, 11000 Richmond Ave, Houston, TX 77042**

E-mail: dhammes@che.com Tel: 713-343-1885

See bottom of next page for advertising sales representatives' contact information

WHO'S WHO


Lindenhayn

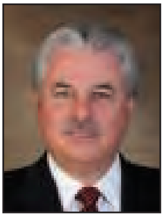
MacCleary

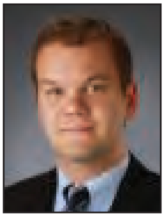
Goodrich


Little


Exton

Archer Daniels Midland Co. (Decatur, Ill.) names *Kyle James* general manager of glycols.

Christian Lindenhayn joins **Orion Engineered Carbons** (Kingwood, Tex.) as senior vice president of the rubber business line.

Jerry MacCleary becomes president for the NAFTA region of **Bayer MaterialScience LLC** (Pittsburgh, Pa.), succeeding *Greg Babe*, who is retiring. MacCleary will retain his leadership of the polyurethanes marketing and business development activities in the NAFTA region.

Jim Rowland joins **Watlow** (St. Louis, Mo.), a maker of thermal systems, as vice president of operations. Meanwhile, *Victoria Holt*, president and CEO of **Spartech** (Clayton, Mo.), joins Watlow's board of directors.

Toray Plastics (America), Inc. (North Kingstown, R.I.) names *Lauritz Goodrich* national sales manager for the company's Torayfan Polypropylene Film Div.

Steven Little becomes chair of the department of chemical and petroleum engineering at the **University of Pittsburgh's** (Pittsburgh, Pa.) Swanson School of Engineering.

Dow Polyurethanes (Midland, Mich.) names *Mark Bassett* global vice president.

Ralph Exton is named chief marketing officer of **GE Power & Water** (Trevose, Pa.). ■

Suzanne Shelley

BUSINESS NEWS

PLANT WATCH

Outotec's EOS process is selected for sinter project in India

May 14, 2012 — Outotec Oyj (Espoo, Finland; www.outotec.com) has been selected by Bhushan Power & Steel Ltd. (BPSL) to design and deliver technology for a new iron-ore sintering plant that will be built in Rengali in the state of Orissa. The contract value is approximately €20 million. The sintering facility is expected to produce 2.45 million metric tons (m.t.) per year of iron-ore sinter, which is used as a raw material in steel production.

Evonik plans to expand its L-threonine capacity in Europe

May 14, 2012 — Evonik Industries AG (Essen, Germany; www.evonik.com) plans to increase the capacity of L-threonine at Evonik Agroferm Zrt. (Kaba, Hungary), a 100% affiliated company of Evonik. The nameplate capacity is expected to be expanded to 30,000 m.t./yr of L-threonine (feed grade 98.5%), which represents an increase of 10,000 m.t./yr. The new capacity is scheduled to come on stream in the 3rd Q of 2013. L-threonine, which Evonik markets under the brand name ThreAmino, is an essential amino acid for animal feed.

Honeywell Green Diesel to be produced from biofeedstocks in U.S. facility

May 8, 2012 — UOP LLC (Des Plaines, Ill.; www.uop.com), a Honeywell company, has signed an agreement to license technology to Emerald Biofuels LLC to produce Honeywell Green Diesel at a facility in Louisiana. Emerald is expected to use UOP's Eni Ecofining process technology to produce 85-million gal/yr of Honeywell Green Diesel. For more on Green Diesel, see *Chem. Eng.*, May 2007; www.che.com/news/3251.html.

BASF to build formic acid plant in Louisiana

May 4, 2012 — BASF Corp. (Florham Park, N.J.; www.basf.us) has announced plans to build a state-of-the-art production plant for formic acid at its integrated facility in Geismar, La. Slated to start up in the 2nd Q of 2014, the new plant will have a capacity of more than 50,000 tons/yr.

Uhde supplies chlor-alkali electrolysis technology to AkzoNobel

May 2, 2012 — AkzoNobel (Amsterdam, the Netherlands; www.akzonobel.com) is converting an amalgam electrolysis plant to the modern membrane process in Frankfurt-Höchst, Germany, and has commissioned ThyssenKrupp Uhde GmbH (Dortmund, Germany; www.uhde.eu) to design and supply the membrane cells. The new plant will increase production capacity by around 50% to 250,000 m.t./yr of chlorine and 275,000 m.t./yr of caustic soda solution. Commissioning is scheduled for the 4th Q of 2013.

Chevron Phillips Chemical selects site for new polyethylene facilities

May 1, 2012 — Chevron Phillips Chemical Co. LP (The Woodlands, Tex.; www.cpchem.com) has announced that the two polyethylene facilities planned as part of the company's U.S. Gulf Coast (USGC) Petrochemicals Project, will be located on a site nearby the Chevron Phillips Chemical Sweeny facility in Old Ocean, Tex. The two facilities will each have a capacity of 500,000 m.t./yr and will utilize Chevron Phillips Chemical's proprietary Loop Slurry Technology. The estimated completion date for the USGC Petrochemicals Project is 2017.

Largest LNG plant in northeast China to feature B&V's patented technology

April 23, 2012 — Black & Veatch (B&V; Overland Park, Kan.; www.bv.com), in partnership with Chemtex, has been selected by Jilin Qianyuan Energy Development to deliver a liquefied natural gas (LNG) facility. Once completed in late 2013, the 500,000-Nm^3/d plant will be the largest of its kind in northeast China and will feature B&V's patented Prico LNG technology.

BASF to invest in new chemical production site in India

April 11, 2012 — BASF India Ltd. (Mumbai; www.basf.com) will invest €150 million in a chemical production site at the Dahej Petroleum, Chemicals and Petrochemicals Investment Region located in Gujarat. The site will be an integrated hub for polyurethane manufacturing and will also house production facilities for surfactants, largely for home and personal care applications, and polymer dispersions for coatings and paper. Production startup is planned for 2014.

MERGERS AND ACQUISITIONS

BASF acquires fatty-acid maker Equateq Ltd.

May 9, 2012 — BASF SE (Ludwigshafen, Germany; www.basf.com) has announced the acquisition of Equateq Ltd., a global leader in the manufacturing of highly concentrated omega-3 fatty acids. With the acquisition, BASF extends its portfolio of omega-3 products for the pharmaceutical and dietary supplement industries with a new offering of highly concentrated omega-3 fatty acids. The integration is expected to be completed by the end of 2012. The companies have agreed not to disclose financial details of the transaction.

Solazyme and Dow to accelerate commercialization of bio-based fluids

May 2, 2012 — Solazyme, Inc. (San Francisco, Calif.; www.solazyme.com) and The Dow Chemical Company (Midland, Mich.; www.dow.com) have entered into a contingent offtake agreement in which Dow has agreed to purchase from Solazyme all of its requirements of non-vegetable microbe-based oils for use in dielectric fluid applications through 2015, contingent upon Solazyme's ability to supply such oils. Concurrently, Solazyme and Dow have entered into a Phase 2 Joint Development Agreement (JDA2), a multi-year extension of the current joint-development agreement including accelerated commercialization timelines. JDA2 enables additional application development work to be conducted by Dow. Consumption of Solazyme's algal oil feedstocks is expected to significantly exceed the minimum estimated volumes of 8.5 million gallons (29,000 m.t.) starting in the 2nd half of 2013 and through 2015.

BASF acquires Novolyte Technologies

April 26, 2012 — BASF SE has purchased Novolyte Technologies (Cleveland, Ohio). from Arsenal Capital Partners (New York, N.Y.; www.arsenalcapital.com), a U.S.-based private equity firm. The companies have agreed not to disclose financial details of the transaction. The acquisition comprises Novolyte's energy storage activities focused on developing, producing and marketing performance electrolyte formulations for lithium-ion batteries. BASF has also purchased Novolyte's performance materials business. Additionally within the framework of the acquisition, BASF will continue a joint venture of Novolyte with Korean partner Foosung, a global producer of the high-purity specialty salt lithium hexafluorophosphate ($LiPF_6$), a key material for manufacturing lithium-ion battery electrolytes. ■

Dorothy Lozowski

FOR ADDITIONAL NEWS AS IT DEVELOPS, PLEASE VISIT WWW.CHE.COM

June 2012; VOL. 119; NO. 6
Chemical Engineering copyright @ 2012 (ISSN 0009-2460) is published monthly, with an additional issue in October, by Access Intelligence, LLC, 4 Choke Cherry Road, 2nd Floor, Rockville, MD, 20850. Chemical Engineering Executive, Editorial, Advertising and Publication Offices: 88 Pine Street, 5th Floor, New York, NY 10005; Phone: 212-621-4674, Fax: 212-621-4694. Subscription rates: $149.97 U.S. and U.S. possessions, $166.97 Canada, and $269 International. $20.00 Back issue & Single copy sales. Periodicals postage paid at Rockville, MD and additional mailing offices. Postmaster: Send address changes to Chemical Engineering, Fulfillment Manager, P.O. Box 3588, Northbrook, IL 60065-3588. Phone: 847-564-9290, Fax: 847-564-9453, email: clientservices@che.com. Change of address, two to eight week notice requested. For information regarding article reprints, please contact Wright's Media, 1-877-652-5295, sales@wrightsmedia.com. Canada Post 40612608. Return undeliverable Canadian Addresses to: PitneyBowes, P.O. BOX 25542, LONDON, ON N6C 6B2

FOR MORE ECONOMIC INDICATORS, SEE NEXT PAGE

DOWNLOAD THE *CEPCI* TWO WEEKS SOONER AT WWW.CHE.COM/PCI

CHEMICAL ENGINEERING PLANT COST INDEX (CEPCI)

(1957-59 = 100)	Mar.'12 Prelim.	Feb.'12 Final	Mar.'11 Final
***CE* Index**	596.1	596.3	575.9
Equipment	729.9	730.6	698.7
Heat exchangers & tanks	686.6	689.9	657.5
Process machinery	680.7	677.7	662.1
Pipe, valves & fittings	934.8	933.5	862.8
Process instruments	433.9	433.8	438.7
Pumps & compressors	922.2	919.6	898.5
Electrical equipment	513.6	514.2	499.4
Structural supports & misc	772.1	772.9	738.6
Construction labor	323.0	321.7	324.3
Buildings	526.3	524.4	514.2
Engineering & supervision	327.8	328.4	334.3

Annual Index:

2004 = 444.2
2005 = 468.2
2006 = 499.6
2007 = 525.4
2008 = 575.4
2009 = 521.9
2010 = 550.8
2011 = 585.7

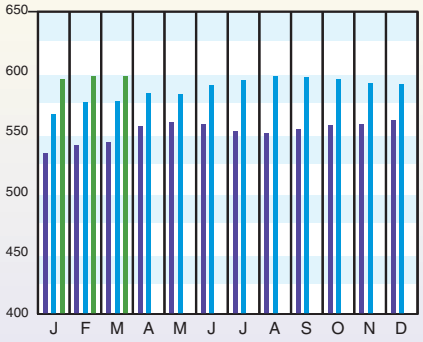

CURRENT BUSINESS INDICATORS

	LATEST		PREVIOUS		YEAR AGO	
CPI output index (2007 = 100)	Apr.'12 =	89.0	Mar.'12 =	89.0	Feb.'12 =	89.8	Apr.'11 =	87.3
CPI value of output, $ billions	Mar.'12 =	2,182.9	Feb.'12 =	2,180.4	Jan.'12 =	2,144.8	Mar.'11 =	2,072.8
CPI operating rate, %	Apr.'12 =	76.9	Mar.'12 =	76.9	Feb.'12 =	77.6	Apr.'11 =	75.3
Producer prices, industrial chemicals (1982 = 100)	Apr.'12 =	329.6	Mar.'12 =	329.5	Feb.'12 =	318.1	Apr.'11 =	332.0
Industrial Production in Manufacturing (2007=100)	Apr.'12 =	94.6	Mar.'12 =	94.1	Feb.'12 =	94.5	Apr.'11 =	89.5
Hourly earnings index, chemical & allied products (1992 = 100)	Apr.'12 =	159.2	Mar.'12 =	157.2	Feb.'12 =	157.3	Apr.'11 =	155.1
Productivity index, chemicals & allied products (1992 = 100)	Apr.'12 =	105.1	Mar.'12 =	105.4	Feb.'12 =	106.8	Apr.'11 =	107.3

CPI OUTPUT INDEX (2007 = 100)

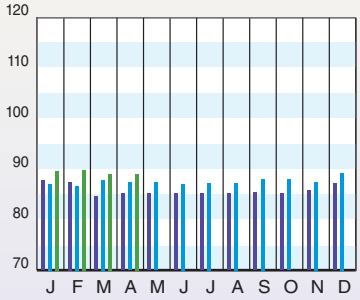

CPI OUTPUT VALUE ($ BILLIONS)

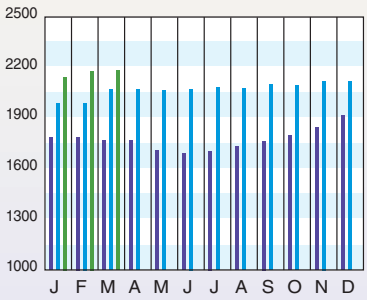

CPI OPERATING RATE (%)

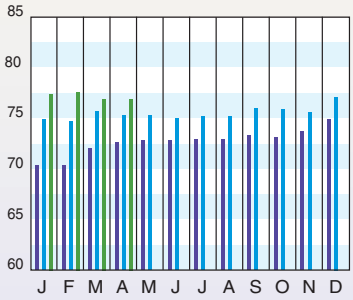

Current Business Indicators provided by IHS Global Insight, Inc., Lexington, Mass.

CURRENT TRENDS

Capital equipment prices, as reflected in the *CE* Plant Cost Index (CEPCI; top), were relatively flat from February to March (the most recent data).

Meanwhile, all of the Current Business Indicators from IHS Global Insight (middle), were relatively flat from March to April. According to the American Chemistry Council (ACC; Washington, D.C.; www.americanchemistry.com), the U.S. Chemical Production Regional Index (U.S. CPRI) rose by 0.1% in March, following a revised 1.0% gain in February, the fourth consecutive gain. Regionally, chemical production rose in the Gulf Coast, Midwest, Ohio Valley and Southeast regions. Production slipped in the Mid-Atlantic and West Coast and was flat in the Northeast.

Using a three month moving average, comparable to the U.S. CPRI, production gains were seen in nearly all chemical segments, except fertilizers, ACC says. Some of the largest gains were in man-made fibers, adhesives, industrial gases, inorganic chemicals, and pesticides. Compared to March 2011, total chemical production in all regions was up 1.3% and remained ahead year-over-year in all regions.

Visit www.che.com/pci for more information and other tips on capital cost trends and methodology. ■

Come visit *Chemical Engineering* in Frankfurt at ACHEMA – the leading international event for the chemical process industries!

CHEMICAL ENGINEERING
ChE.com

As a joint effort with Vogel Business Media, we will once again be the official show daily producers of the ACHEMA DAILY, highlighting the current news, trends, special programs, and events during the show.

Visit us in Hall 9.0, Stand E2

See you in Germany – June 18th-22nd!

Circle 19 on p. 76 or go to adlinks.che.com/40268-19